

**Anaerobic Co-digestion of Municipal Sewage Sludge with Selected
Commercial and Industrial Organic Wastes**

by

Vahid Razaviarani

A thesis submitted in partial fulfillment of requirement for degree of

Doctor of Philosophy

in

Environmental Engineering

Department of Civil and Environmental Engineering
University of Alberta

©Vahid Razaviarani, 2014

ABSTRACT

The overall goal of this research was to investigate the anaerobic co-digestion of municipal sewage sludge with selected organic wastes in three main areas: (1) to determine the maximum feasible loading of co-substrate, (2) to calibrate the ADM1 model for co-digestion system at steady state, and (3) to evaluate the linkage between microbial community dynamics and reactor performance and stability during steady state and overloading co-digestion.

In this study, restaurant grease waste (GTW) as a commercial waste and biodiesel glycerin waste (BGW) as an industrial waste were co-digested with municipal wastewater sludge (MWS) in separate trials. In the first part of this research, the maximum feasible loading of each of the organic wastes with MWS with respect to the reactor performance and stability were investigated in the separate pilot-scale experiments. In each run, two 1300L completely mixed reactors were operated under mesophilic temperature (37°C) and a solids retention time (SRT) of 20 days. Throughout the pilot experiment, one reactor served as control and received only MWS and the other was assigned as the test digester and fed with the mixture of MWS and the co-substrate (GTW or BGW) in various organic loadings. GTW co-digestion with MWS was found to be feasible up to a maximum loading of 23% VS or 58% COD relative to the total 1.6 kg VS/m³·d or 4.0 kg COD/m³·d loadings, respectively. At this loading, test digester biogas production was 67% greater than that of the control. The test digester biogas production declined markedly when the percentage of VS from GTW in its feed was increased to 30% of its total VS loading. Causes of the reduced biogas production were investigated and attributed to process inhibition due to long chain fatty acid accumulation. The maximum safe limit of BGW co-digested with MWS was found at 23% and 35% of the total 1.04 kg VS/ (m³·d) and 2.38 kg COD/ (m³·d) loadings, respectively. At this loading, the biogas and methane production rates in the test digester were 1.65 and 1.83 times greater than of those in the control digester which received only MWS, respectively. Process instability was

observed when the proportion of BGW in the test digester feed was 31% and 46% of the 1.18 kg VS/ (m³·d) and 2.88 kg COD/ (m³·d) loadings, respectively.

In the second part of the research, the ADM1 model was calibrated for co-digestion of MWS and GTW at steady state using anaerobic respirometric test with substrate characterizations. Initial biomass concentrations and distributions were estimated using methane production rate curves together with effluent values from full-scale anaerobic digesters. Two separate datasets obtained from steady state mesophilic bench-scale experiments were used to calibrate and validate the model. The modified model was able to predict reasonably well the steady-state results of biogas production, CH₄ and CO₂ contents, pH, alkalinity, COD and VSS observed within the evaluated GTW loading. The calibrated model predicted well the bench and pilot scale co-digesters performance.

The last part of the study was to investigate the relationships between microbial population (bacteria and archaea) dynamics and reactor performance and stability during the co-digestion of MWS with GTW or BGW in two separate trails. Pyrosequencing analysis revealed that *Methanosaeta* and *Methanomicrobium* were the dominant acetoclastic and hydrogenotrophic methanogen genera, respectively, during stable reactor operation. The roles of syntrophic bacteria such as *Candidatus Cloacamonas* and hydrogenotrophic methanogens were found to be substantial at overloading conditions in both experiments.

PREFACE

This thesis is an original work by Vahid Razaviarani under supervision of Dr. Ian D. Buchanan. The anaerobic digester pilot plant referred to in Chapters 3 and 6, owned by the King County Wastewater Treatment Division, was housed in a trailer and located at the Gold Bar WWTP. The test facility contained a grinder tank, a feed tank, pumps, two 1300 L digesters, effluent tanks and other required utilities were provided in the trailer during the pilot scale study. The data analyses during the entire research and sample analyses are my original work, as well as the literature review in Chapter 1.

Chapter 3 of this thesis has been published as an original research article of V. Razaviarani, I. Buchanan, S. Malik, H. Katalambula entitled “*Pilot-scale anaerobic co-digestion of municipal wastewater sludge with restaurant grease trap waste*”, Journal of Environmental Management, 123, 26-33. I was responsible for the lab measurements, data collection and analyses for the manuscript composition.

Chapter 6 of this thesis has been published as an original research article of V. Razaviarani, I. Buchanan, S. Malik, H. Katalambula entitled “*Pilot-scale anaerobic co-digestion of municipal wastewater sludge with biodiesel glycerin waste*”, Bioresource Technology, 133, 206-212. I was responsible for the lab measurements, data collection and analyses for the manuscript composition.

The bench-scale setup referred to in Chapters 4, 5 and 7 were designed by myself, with the assistance of Christine Heyregers. I was responsible for the reactor operation, data collection and analysis, and experimental measurements throughout the bench-scale study.

DEDICATION

This dissertation is dedicated to my beloved family for their love, endless support and encouragement. My mother who taught me that even the largest task can be accomplished if it is done one step at a time, and my father who taught me that the best kind of knowledge to have is that which is learned for its own sake. I also dedicate this thesis to my only brother, Farid, who has never left my side and is very special.

ACKNOWLEDGEMENTS

I would like to sincerely express my appreciation to my supervisor, Dr. Ian D. Buchanan for his continual support and guidance through my PhD study. His encouragement was essential to accomplish this work. My appreciation also goes to all my dissertation committee members: Dr. Ania Ulrich, Dr. Tong Yu, Dr. Lisa Stein and Dr. J. Patrick Hattiaratchi.

I would also like to thank the staff members in Edmonton Waste Management Center of Excellence. I could not have possibly completed the pilot-scale research section without the endless help from Dr. Shahid Malik, Ryan Litwinow and Radek Roznicki. Thank you for being unconditional co-workers and caring friends. I am very grateful to Dr. Hassan Katalambula for his helpful comments and sharing his knowledge and experiences during the pilot-scale research. I wish to thank to all operational members in the Gold Bar WWTP for helping me out with sample transportation throughout the pilot research.

I would like to give my thanks for the support I received from the labs crew in the department of civil and environmental engineering: Jela Burkus, Chen Liang and Elena Dlusskaya. Special thanks to Maria Demeter who was generously helpful during my research. Thanks to Christine Heyregers for helping me with the lab-scale reactor design. I also acknowledge the valuable help I received from the biological lab member, Dimitri Kits, in the Dr. Lisa Stein's lab for helping me with GC analysis during the pilot experiment.

I deeply thank to all my past and present friends who greatly supported and encouraged me during the course of my studies. Special thanks to Golnaz Arab for helping me with my bench-scale experiments.

Finally, a special thanks to my dearest family for their invaluable supports and sacrifices throughout the course of this journey.

Table of Contents

CHAPTER 1. INTRODUCTION AND RESEARCH OBJECTIVES	1
1.1 Introduction	1
1.1.2. Background.....	2
1.2. Objectives and Scope of the Research	4
1.2.1. Problem Statement.....	4
1.2.2. Research Objectives	6
1.2.3. Research Scope.....	6
1.3. Thesis Outline	8
CHAPTER 2. LITERATURE REVIEW	10
2.1. Introduction	10
2.2. Commercial Grease Trap Waste.....	10
2.3. Biodiesel Glycerin Waste.....	12
2.4. Modeling of Anaerobic Digestion	14
2.5. Microbial Community	17
CHAPTER 3. PILOT-SCALE ANAEROBIC CO-DIGESTION OF MUNICIPAL WASTEWATER SLUDGE WITH RESTAURANT GREASE TRAP WASTE*	
.....	20
3.1. Introduction	20
3.2. Materials and Methods.....	21
3.2.1. Substrates.....	21
3.2.2. Pilot Digesters.....	22
3.2.3. Digester Feed and Organic Loading Rate Protocols	23
3.2.4. Analytical Methods.....	25
3.3. Results and Discussion.....	26
3.3.1 Baseline Operation	26
3.3.2. Overall Digester Performance	27
3.3.3. Quasi Steady State Operation	32
3.3.4. Process Stability	33

3.4. Conclusions	39
CHAPTER 4. CALIBRATION OF THE ANAEROBIC DIGESTION MODEL	
NO.1 (ADM1) FOR STEADY-STATE ANAEROBIC CO-DIGESTION OF	
MUNICIPAL WASTEWATER SLUDGE WITH RESTAURANT GREASE	
TRAP WASTE*.....	41
4.1. Introduction	41
4.2. Materials and Methods.....	43
4.2.1. Analytical Methods.....	43
4.2.2. Substrates and Inoculum.....	44
4.2.3. Anaerobic Respirometry Test.....	47
4.2.4. Semi-Batch Reactors	48
4.3. Results and Discussion.....	49
4.3.1. Initial State of Inoculum in ADM1.....	49
4.3.2. Substrate Fractionations and Stoichiometric Coefficients.....	51
4.3.3. Model Calibration.....	53
4.3.4. Model Validation.....	58
4.4. Conclusions	64
CHAPTER 5. REACTOR PERFORMANCE AND MICROBIAL COMMUNITY	
DYNAMICS DURING ANAEROBIC CO-DIGESTION OF MUNICIPAL	
WASTEWATER SLUDGE WITH RESTAURANT GREASE WASTE AT	
STEADY-STATE AND OVERLOADING STAGES	
5.1. Introduction	65
5.2. Materials and methods	66
5.2.1. Inoculum and substrates	66
5.2.2. Reactor operation and loading protocol.....	68
5.2.3. Physico-chemical analysis.....	69
5.2.4. Microbial community analysis	70
5.2.5. Statistical analysis.....	72
5.3. Results and discussion.....	72
5.3.1. Process stability and reactor performance	72

5.3.2. Methanogenic community structure of the ACD	74
5.3.3. Bacterial community structure of the ACD	79
5.3.4. Correlation between environmental parameters and microbial dynamics	83
5.4. Conclusions	86
CHAPTER 6. PILOT-SCALE ANAEROBIC CO-DIGESTION OF MUNICIPAL WASTEWATER SLUDGE WITH BIODEISEL WASTE GLYCERIN*	88
6.1. Introduction	88
6.2. Materials and Methods	89
6.2.1. Substrates	89
6.2.2. Semi-continuous Pilot Digester	90
6.2.3. Digester Feed and Organic Loading Rate Protocols	91
6.2.4. Analytical Methods	93
6.3. Results and Discussions	94
6.3.1. Baseline Operation	94
6.3.2. Reactor Performance	95
6.3.2.3. Biogas and Methane Production Rates	98
6.3.3. BGW Loading and Specific Methane Production	99
6.3.4. Process Stability	100
6.3.5. Maximum Safe Loading Rate	103
6.4. Conclusions	103
CHAPTER 7. ANAEROBIC CO-DIGESTION OF BIODEISEL WASTE GLYCERIN WITH MUNICIPAL WASTEWATER SLUDGE: MICROBIAL COMMUNITY DYNAMICS AND REACTOR PERFORMANCE	104
7.1. Introduction	104
7.2. Materials and methods	106
7.2.1. Inoculum and wastes	106
7.2.2. Reactor setup and operation	107
7.2.3. Analytical methods	109
7.2.4. Microbial community analysis	110

7.2.5. Statistical analysis.....	111
7.3. Results and discussion.....	111
7.3.1. Reactors' stability	111
7.3.2. Reactors' performance.....	114
7.3.2. Methanogenic community dynamics.....	115
7.3.3. Bacterial community dynamics	120
7.3.4. Correlation between environmental variables and microbial dynamics	123
7.4. Conclusions	127
CHAPTER 8. GENERAL CONCLUSIONS AND RECOMMENDATIONS ..	128
8.1. Thesis Overview.....	128
8.2. Conclusions	130
8.3. Future Research and Recommendations	133
REFERENCES	135
APENDIX A: Pilot-Scale Supplementary Data.....	149
A.1. GTW Co-digestion	152
A.2. BGW Co-digestion	160
APENDIX B: GTW Modeling Supplementary Data.....	163
B.1. GTW Calibration Model.....	164
APENDIX C: Microbial Supplementary Data.....	167

LIST OF TABLES

Table 3.1. Characteristics of municipal wastewater sludge (MWS) and restaurant grease waste (GTW)	22
Table 3.2. Organic loading rate (OLR) at various increments	24
Table 3.3. Comparison of digester performance during baseline operation	27
Table 3.4. Description of similar previous studies of anaerobic co-digestion of MWS and GTW	31
Table 3.5. Characteristics of reactor effluents.....	35
Table 4.1. Characteristics of municipal wastewater sludge (MWS), grease trap waste (GTW) and inoculum.....	46
Table 4.2. Fractions of the composite stoichiometric coefficients in influents and ADM1 default values	52
Table 4.3. Default and calibrated kinetic parameters for biomass growth.....	54
Table 4.4. ADM1 Default and calibrated kinetic parameters used in anaerobic co-digestion of MWS and GTW.....	56
Table 4.5. Statistical comparison of observed and modeled values in calibrated model.....	57
Table 4.6. Comparison of observed and predicted values from modeling the steady state pilot-scale anaerobic co-digestion of MWS and GTW at a 190% GTW COD loading.....	63
Table 5.1. Characteristics of substrates and inoculum.....	67
Table 5.2. Reactor organic loading rates (OLR) and durations	69
Table 5.3. Reactors' stability and performance parameters at different loadings.....	73
Table 5.4. Relative abundance of phylogenetic groups of archaeal in reactors ...	75
Table 5.5. Relative abundance of phylogenetic groups of bacteria in reactors....	81
Table 6.1. Characteristics of municipal wastewater sludge (MWS) and biodiesel waste glycerin (BGW).....	90
Table 6.2. Organic loading rate (OLR) at various increments	92
Table 6.3. Comparison of digester performance during baseline operation	94
Table 6.4. Characteristics of reactor effluents and emissions	102
Table 7.1. Characteristics of substrates and inoculum.....	107

Table 7.2. Substrate loading characteristics	109
Table 7.3. Reactors' stability and performance parameters at different phases of organic loadings.	113
Table 7.4. Relative abundance of phylogenetic groups of archaeal in reactors .	117
Table 7.5. Relative abundance of phylogenetic groups of bacteria in reactors..	122

LIST OF FIGURES

Figure 3.1. Schematic of the pilot scale anaerobic digester setup.	25
Figure 3.2. Mean biogas production and GTW VS percentage at various loading rates	29
Figure 3.3. Biogas production, %VS and %COD removals at baseline and at quasi steady state.....	33
Figure 3.4. Effluent pH and IA/PA ratio at various organic loadings	37
Figure 3.5. Feed COD/TKN ratio at various organic loadings	38
Figure 4.1. Specific biomass concentrations of acclimated inoculum from steady state simulation of full-scale AD by ADM1	50
Figure 4.2. Comparison of measured and ADM1 predictions of; (a) biogas production, (b) biogas composition, (c) pH, (d) ammonia-N,(e) total alkalinity, (f) volatile suspended solids, (g) effluent COD, and (h) volatile fatty acids at steady-state anaerobic co-digestion of GTW and MWS.	61
Figure 5.1. Distribution of family level of archaeal community categorized in brackets for order level.....	76
Figure 5.2. Distribution of order level of bacterial community categorized in brackets for class level	80
Figure 5.3. Canonical correspondence analysis (CCA) triplot showing the relationship between the relative sequence abundance of the major bacterial and archaeal communities and the environmental variables pH, alkalinity and VFA concentration in the different stages of GTW COD loadings (●). The environmental variables are shown as vectors in the plot. The open triangle symbols (Δ) represent the genera of bacterial populations that include B1: <i>Anaerolinea</i> ; B2: <i>Esherichia</i> ; B3: <i>Dermatophilus</i> ; B4: <i>Candidatus Cloacamonas</i> . The open circle symbols (○) represent the genera of archaeal populations that include A1: <i>Methanomicrobium</i> ; A2: <i>Methanosarcina</i> ; A3: <i>Methanosaeta</i>	85
Figure 6.1. Schematic of the pilot scale anaerobic digester setup.....	93
Figure 6.2. COD removal efficiency and BGW COD percentage at various loadings.	95

Figure 6.3. VS removal efficiency and BGW VS percentage at various loadings.	98
Figure 6.4. Gas production rate and methane production rate at various loadings	99
Figure 6.5. SMP in terms of COD and VS added in various loadings.....	100
Figure 7.1. COD and VS removal percentages at different phases.....	115
Figure 7.2. Distribution of <i>family</i> level of archaeal community categorized in brackets for <i>order</i> level.	120
Figure 7.3. Distribution of <i>family</i> level of bacterial community categorized in brackets for <i>order</i> level.	123

LIST OF ABBREVIATIONS AND NOMENCLATURE

ADM1	Anaerobic Digestion Model No. 1
APE	Average Percentage Error
BGW	Biodiesel Glycerin Waste
CCA	Canonical Correspondence Analysis
COD	Chemical Oxygen Demand
FOG	Fat, Oil and Grease
GC	Gas Chromatography
GPR	Gas Production Rate
GTW	Grease Trap Waste
IA	Intermediate Alkalinity (TA-PA)
IC	Ion Chromatography
LCFA	Long Chain Fatty Acids
MPR	Methane Production Rate
MWS	Municipal Wastewater Sludge
OLR	Organic Loading Rate
PA	Partial Alkalinity
PCR	Polymerase Chain Reaction
PS	Primary Sludge
SCOD	Soluble Chemical Oxygen Demand
SMP	Specific Methane Production
SRT	Solids Retention Time

TA	Total Alkalinity
TAN	Total Ammonium Nitrogen
TKN	Total Kjeldahl Nitrogen
TS	Total Solids
TSS	Total Suspended Solids
VFA	Volatile Fatty Acids
VS	Volatile Solids
VSS	Volatile Suspended Solids
WAS	Waste Activated Sludge
WWTP	Wastewater Treatment Plant

CHAPTER 1. INTRODUCTION AND RESEARCH OBJECTIVES

1.1 Introduction

The demand for energy particularly from fossil fuels is rising globally. The use of renewable energy sources, as a reliable alternative, can reduce climate change and environmental issues. Organic waste is one of the widely dispersed and easily accessible renewable energy sources that can be used to reduce the fossil fuel usage and its environmental impacts.

Anaerobic digestion involves a series of microbiological reactions to convert organic matter (such as carbohydrates, proteins and lipids) into methane, carbon dioxide and cell mass in the absence of oxygen. It is a widely used technology which provides many substantial advantages, such as methane production as a source of energy, reduction of organic residues and reduction in greenhouse gas emissions (Li et al. 2011). In spite of these advantages, anaerobic digestion technology has a number of limitations including low reaction rate, sensitivity to various toxic materials and changes in operating conditions, and potentially high concentrations of heavy metals in the residual sludge depending on the feed material characteristics (Appels et al. 2008). Direct anaerobic treatment of organic wastes is not widely used by industry because many of the wastes do not have sufficient buffering capacity or nutrients to ensure stable operation (Davidsson et al. 2008). Conversely, digested sludge at municipal wastewater treatment facilities possesses an excess of micro-nutrients and many of these plants do not fully utilize the on-site anaerobic digestion capacity (Schwarzenbeck et al. 2008). Thus, co-digestion of industrial or commercial organic waste with municipal wastewater sludge provides sufficient buffering capacity, microbial populations that stimulate the digestion process, balanced nutrition, dilution of the inhibitor compounds, enhanced biogas yields, and leads to increased cost-efficiency due to the shared use of facilities at the municipal plants that do not employ all of their available anaerobic digestion capacity.

1.1.2. Background

Anaerobic digestion is a multistep process involving several species' metabolisms in order to degrade a single substrate. Substrates should be either water soluble or lipid soluble to be absorbed by microorganisms (bacteria and archaea) in order to be used in biochemical reactions (Geraldi 2006).

Generally, there are four principal biological steps that occur in an anaerobic process with respect to all bacterial metabolism interactions and syntrophy: (1) hydrolysis, (2) acidogenesis, (3) acetogenesis, and (4) methanogenesis.

Organic compounds are degraded in a multistep process by various types of microorganisms, which involve syntrophic interactions (Megini J. P. et al. 2003). Hydrolysis is adding water ('hydro') to complex molecules in bacteria to split ('lysis') their chemical bonds. Some organic compounds are easily decomposed by bacteria. Bacteria are unable to hydrolyze macromolecules larger than 600 Da, hence large molecules must be broken down into smaller ones in order to be utilized by bacteria (Weiss et al. 1991). Thus, a sufficient resident time is required for bacteria to produce exoenzymes for the solubilization of adsorbed substrates, so hydrolysis is often a limiting step in organic matter degradation (Wu et al. 2001). After substrate solubilization, it is absorbed by hydrolytic and non-hydrolytic bacteria, and the biodegradation of soluble substrates is completed by endoenzymes.

In an anaerobic environment, lipids are hydrolyzed to long chain fatty acids (LCFAs) and glycerol; they are then fermented into volatile fatty acids, CO₂ and H₂, meaning that acetogenesis converts glycerol to acetate and LCFAs are converted to fatty acids (acetate or propionate) and hydrogen. Hydrolysis is catalyzed by extracellular enzymes (lipases) and hydrogenotrophic methanogens, which play an important role in hydrogen utilization during fatty acid production (Cirne et al. 2007). The products of protein degradation under anaerobic conditions are peptides and amino acids, which are fermented to volatile fatty acids (propionate, butyrate, etc.) and finally are converted to CO₂ and CH₄ in an anaerobic environment (Tang Y. et al. 2005). The first hydrolysis products of carbohydrates are sugars. They are degraded by acidogenes to volatile fatty acids

and then converted to acetate, CO₂ and H₂ by acetogens. Finally, at the anaerobic conditions, methanogens convert the acetogenesis products into methane (Elbeshbishy and Nakhla 2012).

Fermentation is the second step of biodegradation of organic compounds in which organic compounds perform as both electron donors and acceptors. Also, fermentation is an intracellular degradation of organic compounds to release electrons from hydrogen atoms, which provide the energy that should be transferred by an electron transfer to molecules such as CO₂ and organic compounds. There are two predominant groups of fermentative bacteria in anaerobic degradation: acidogenic and acetogenic bacteria. In the primary fermentation the acidogenic bacteria convert the hydrolysis products, such as soluble carbohydrates, amino acids and fatty acids into volatile fatty acids (acetate, butyrate, formate, lactate, and succinate), ethanol, methanol, acetone, carbon dioxide and hydrogen. Acidogenesis products could be either directly utilized by methanogenic bacteria or after further conversions (secondary fermentation) to other simple compounds (Geraldi 2006). For instance, all fatty acids with chains more than two carbons, and all alcohols with more than one carbon need to be fermented by secondary fermentative bacteria to be available to methanogenic bacteria (Dworkin et al. 2006).

Methanogens are the largest specialized group of Archaea that utilize principally acetate, CO₂ and H₂ and produce CH₄ as a waste product (Meronigal et al. 2003). Methane-forming microorganisms are a diverse group with variety in shape (bacillus, coccus, and spirillum) and size (0.1 to 15µm) which are active within the pH range of 6.8 to 7.2. Reproduction and generation of methanogens are slow and sludge production from the substrate biodegradation is fairly low, approximately 0.02 kg per kg of substrate degraded. Under anaerobic conditions, methanogenic activities are performed through three fundamental groups of methane-forming bacteria, acetoclastic methanogens, hydrogenotrophic methanogens, and methyltrophic methanogens. Acetoclastic methanogens produce CH₄ by breaking acetate, while hydrogenotrophic methanogens produce CH₄ by association of CO₂ and H₂. Methyltrophic methanogens produce a small

amount of methane in contrast to the two other groups by removing methyl (-CH₃) groups from the substrates (Geraldi 2006).

1.2. Objectives and Scope of the Research

1.2.1. Problem Statement

Most previous anaerobic co-digestion studies, which are reviewed in the previous section, have been conducted in the bench-scale studies and have been implemented at several full-scale facilities. In addition, complexities in the waste characteristics due to the comingling of organic waste streams with the MWS may cause inhibition and process upsets. Such a process upset would not be acceptable in a study conducted at a full-scale facility. However, studies conducted at pilot-scale studies which more closely resemble the full scale operating conditions than do bench-scale testing can be undertaken to drive digesters to failure and collect valuable operational data. Therefore, pilot-scale studies are required to assess the reactor performance and operational parameters under both steady-state and upset conditions.

On the other hand, it is not economical and may not be possible to measure all the parameters concerning in the anaerobic co-digestion (ACD) process. Therefore, provision of a reasonable prediction of system behaviors is crucial through a reliable model to simulate optimal parameters for ACD process.

Anaerobic digestion is mediated by multiple biological sequential reactions in which deeper insight into the microbial dynamics and their activities can provide required knowledge and understanding of the process. This supportive microbial activities information would help to enhance understanding of the process performance and stability, reactor efficiency and process troubleshooting during the co-digestion.

Salerno and Parry (2009) analyzed and characterized six organic wastes including canola oil, restaurant grease waste, ethanol stillage, chicken waste, cheese whey, and biodiesel waste glycerin in terms of their values as co-substrates in anaerobic co-digestion with MWS. Restaurant grease trap waste (GTW) and

biodiesel waste glycerin (BGW) were shown to have the greatest potential to increase biogas production. Therefore, these two organic wastes are selected as co-substrates of municipal wastewater sludge in the present study.

If the ratio of an organic waste (GTW or BGW) to the MWS increases incrementally in pilot-scale reactor, it is hypothesized that the reactor performance and process stability will be productively improved to a maximum feasible loading level because of improvement in nutrition balance, buffer capacity, removal rates and methane yield. Therefore, pilot-scale studies are required to explore anaerobic co-digestion of organic wastes from restaurant grease traps and from biodiesel industry with municipal wastewater sludge (MWS).

Several models are available in the literature, but a very limited number of studies have focused on the modeling co-digestion systems and none has addressed modeling the co-digestion of municipal sludge with restaurant grease trap waste. Therefore, if the feed characteristics changes due to the addition of GTW to the MWS, it is hypothesized that the reactor performance of anaerobic co-digestion process will be predictable by the calibration of ADM1 under certain circumstances.

If the ratio of an organic waste (GTW or BGW) to the MWS increases, it is hypothesized that the microbial community dynamics (bacterial and archaeal) and reactor performance and stability will be effectively changed due to the changes in substrate compositions. To evaluate the involvement of microbial population dynamics throughout the ACD of these two wastes with MWS, separate bench-scale investigations were also conducted and the correlations between reactor performance and microbial activities were evaluated at different organic loadings of co-substrates.

1.2.2. Research Objectives

The objectives of this research were achieved through the investigation of the ACD of selected organic wastes (GTW & BGW) with the MWS in separate trials. These objectives were:

1. To evaluate reactor performance, process instability, and the maximum feasible organic loading rate of GTW to the MWS in the pilot-scale experiment (Chapter 3);
2. To develop a calibration method and apply it to the ADM1 model for ACD of GTW and MWS at steady state operation, using anaerobic respirometric analysis with substrate characterizations (Chapter 4),
3. To study the relationships between microbial community dynamics and reactor performance and stability during the mesophilic ACD of GTW and MWS (Chapter 5);
4. To assess reactor performance, process instability, and the upper loading limit of BGW during its co-digestion with MWS in pilot-scale mesophilic reactor (Chapter 6);
5. To investigate the linkage between reactor performance and microbial community dynamics during the mesophilic ACD of BGW and MWS (Chapter 7).

1.2.3. Research Scope

This research study will provide new complete and distinctive knowledge of anaerobic co-digestion of MWS with two selected commercial and industrial organic wastes in separate investigations. The study will reveal invaluable information regarding process performance and stability during the addition of co-substrate to the MWS at different organic loading rates. More importantly, the highest safe limit of comingling of these two organic wastes with the MWS will be determined in the pilot-scale study which better resembles the full-scale operation and the results could be applied for industrial purposes. The calibrated

ADM1 model will be a helpful tool to predict the reactor performance during the GTW co-digestion at steady-state condition and would be of particular interest to those who operate anaerobic digesters. Investigation of microbial community structures during the addition of co-substrate (GTW or BGW) to the MWS will provide unique information and knowledge of the microbial populations involved in the reactor performance and process stability. These inclusive findings will be novel and will provide a comprehensive knowledge and understanding of ACD of the organic wastes with MWS that can be applied to enhance the reactor efficiency and performance. Therefore the scope of this research is restricted to the following areas:

Phase I: Pilot-scale study – maximum safe loading: In two separate trials, GTW and BGW are co-digested with MWS to identify the maximum feasible loadings of these wastes. During the incremental addition of co-substrates at various COD loadings, reactors' performance and stability should be investigated. The biogas and methane productions, COD and VS removal rates, VFA, alkalinity, pH, ammonia and TKN are the most important parameters that should be quantified during this phase.

Phase II: Bench-scale study - model calibration: The GTW is co-digested with MWS at steady state mesophilic conditions and data obtain from this step are used to calibrate and validate the ADM1. Anaerobic respirometric analysis, as a useful tool, with substrate characteristics are used to calibrate the ADM1 model. Results from the GTW bench-scale and pilot-scale co-digestions are used to validate the calibrated model.

Phase III: Bench-scale study – microbial community dynamics: The role and influences of microbial (bacterial and archaeal) community dynamics on the reactors' performance and stability during the addition of co-substrates (GTW or BGW) to the MWS are investigated under mesophilic steady-state and overloading conditions. Pyrosequencing analysis is employed to determine the

bacterial and archaeal sequences. The canonical correspondence analysis is used to investigate the correlations between microbial community dynamics and reactors' performance and stability during the co-digestion of selected organic wastes with MWS.

1.3. Thesis Outline

This thesis consists of seven chapters focusing on the anaerobic co-digestion of MWS with selected organic wastes (GTW & BGW) in separate trials at pilot and bench scale. The general overview of GTW and BGW characteristics and global generations, anaerobic digestion process, ADM1 modeling and the benefits of co-digestion of organic wastes are presented in Chapters 1 and 2.

The maximum feasible loading of GTW comingled with the MWS in the mesophilic pilot-scale reactor is presented in Chapter 3. The reactor performance and stability were investigated at the various organic loadings.

In Chapter 4, the calibration of ADM1 model for simulation of the co-digestion of MWS and GTW at steady-state condition is investigated. A model calibration procedure based on anaerobic respirometry analysis, bench-scale and full-scale digesters and substrate characterizations is described and applied to identify the kinetic and stoichiometric parameters required by the ADM1 for mixed substrate digestion.

In Chapter 5, the relationships between the microbial population dynamics with the reactor performance and stability are investigated in mesophilic bench-scale reactors. The bacterial and archaeal community dynamics at the steady-state "safe" loadings as well as overloading of GTW are determined.

Chapter 6 includes an investigation of ACD of BGW with MWS to identify the safe limit loading of BGW to the mesophilic pilot-scale reactor. The effects of

BGW addition at the various loadings on the reactor performance and stability are evaluated in this part.

In Chapter 7, the correlations between reactor performance and microbial community dynamics at mesophilic steady-state conditions are investigated. The bench-scale reactors were run at different BGW loadings (safe & overloading) and the effects of bacterial and archaeal population dynamics on the reactor performance and stability were determined.

In Chapter 8, overall conclusions of the performed research and recommendations for future work are presented. Some of the supplementary graphs and tables to support the obtained results are presented in the Appendix sections attached at the end of the Thesis.

CHAPTER 2. LITERATURE REVIEW

2.1. Introduction

Organic waste disposal through the conventional treatment technologies (i.e. landfill and incineration) can cause severe environmental effects including soil and ground water pollution and greenhouse gas emissions (Kalloum et al. 2011; Liu et al. 2012). Anaerobic digestion technology, as a solution, is a well established process to convert organic matter into biogas as a renewable energy source and digestate as a soil conditioner (Iacovidou et al. 2012). However, anaerobic mono-digestion of industrial or commercial organic wastes is not practically feasible due to the lack of sufficient buffer capacity or nutrients. Conversely, municipal wastewater sludge possesses excess of nutrients and the disposal of MWS (primary sludge and waste activated sludge) has been being a major concern in terms of restricted disposal options and high disposal costs in the wastewater treatment plants (Knezevic et al. 1995; Schwarzenbeck et al. 2008). Therefore, there is a great interest in co-digesting of industrial, commercial or agricultural organic wastes with municipal wastewater sludge in order to increase the biogas production and decrease the sludge generation (Martínez et al. 2012).

Several researchers (Ağdağ and Sponza 2007; Bouallagui et al. 2009; Gomez et al. 2006; Hartmann and Ahring 2005; Macias-Corral et al. 2008; Ponsa' et al. 2011) have observed remarkable improvements in the reactor performance and biogas production when using co-substrate in the anaerobic digestion systems.

2.2. Commercial Grease Trap Waste

Grease trap waste (GTW) from restaurants, commercial kitchens, and food service providers has become a major stream of organic waste in urban areas. According to an estimation in 2010, based on surveys conducted in some US metropolitan areas, approximately 22 billion liters of GTW is generated annually in the United States with a population of 312 million (Long et al. 2011). These values represent an approximate generation of 70 L GTW/person/year. The GTW

characteristics are varied and highly depending on the source of collection and the type of the grease abatement device. As expected, the GTW is high in fat content, has a low pH value (acidic) with a total solids content ranging from 2% to 22% before dewatering. Theoretically, among the organic wastes, lipids (fats, oil, greases) have more biogas production potential (Neves et al. 2009). According to the previous studies (Bond et al. 2012; Davidsson et al. 2008; Luostarinen et al. 2009), the methane potential value of GTW was reported in a range of 0.9-1.4 m³/kg VS which is significantly higher than that of the primary sludge (0.47 m³/kg VS) and waste activated sludge (0.18 m³/kg VS). Dewatered GTW has a high biochemical oxygen demand with an approximate potential energy value of 4.5-6.5 kWh/kg. The portion of fat, oil and grease (FOG) in GTW was reported to be about 0-15% (v/v), and primarily contains of long chain fatty acids (LCFAs). The β -oxidation pathway mediates the anaerobic degradation of LCFAs where acetate and hydrogen are the final products.

Disposal of this waste to landfills is no longer permitted in many jurisdictions and incineration is not very encouraged due to the high moisture content and low energy recovery. Composting of GTW causes odor issues and requires a longer time to breakdown the compost raw materials because of the potential coating characteristic of greasy wastes. Thus, anaerobic digestion of GTW is an attractive option because lipid-rich materials have high energy content and methane production potential (Davidsson et al. 2008; Gregor D. et al. 2008; Kiepper et al. 2001). However, clogging, lack of sufficient buffer capacity, nutrient imbalance, low solubility due to the attachment of lipid-rich materials to the biomass surface and methanogens inhibition due to the LCFAs accumulation are the main limiting factors of mono-anaerobic digestion of GTW (Cirne et al. 2007). Therefore, co-digestion of GTW has become an interesting solution to overcome those challenges.

The feasibility of co-digesting grease trap sludge from a meat-processing plant with sewage sludge was investigated by Luostarinen et al. (2009) under semi-continuous feeding conditions at 35 °C. They observed that addition of 46% GTW from a meat-processing plant, based on VS, to the sewage sludge improved

methane yield by 66%. Wan et al. (2011) observed that co-digestion of fat, oil and grease (FOG) waste and waste activated sludge (WAS) enhanced methane production significantly. They reported a 137% increase in methane production with the addition of 64% FOG, based on VS, compared to digestion of WAS alone in a 4 L digester at mesophilic conditions. Recently, Zhu et al. (2011) reported a 65% enhancement in methane production by adding less than 4% (w/w) of GTW to the MWS in a 100 mL working-volume digester at 35°C. Silvestre et al. (2011) co-digested greasy sludge from a WWTP dissolved air flotation unit with blended WWTP sludge. Biogas production was reported to increase by 128% during co-digestion of a mixture in which VS from grease represented 23% of the total 1.6 kg VS/ (m³·d) loading.

Enhanced biogas production due to the commingling of GTW and MWS is in agreement with all aforementioned studies, however, may vary severely depending on the %GTW loading, reactor type and operational conditions. Additionally, physical and chemical characteristics of GTW can vary, mostly depending on the source of food service providers. Thus, a wide-range of published data is still needed to identify operating conditions in terms of the maximum safe limit GTW loading, SRT, temperature etc. that allow optimum reactor performance

2.3. Biodiesel Glycerin Waste

In recent decades, global fossil fuels crises have mounted concerning the non-sustained availability, escalating prices and impact on environment (Hansen et al. 2005). Biodiesel has drawn much attention in last two decades as an interesting renewable energy option that uses carbon already in the active carbon cycle (Siles López et al. 2009). Biodiesel is a liquid fuel derived from vegetable oil or animal fat through the esterification or transesterification process. In comparison to fossil fuel, biodiesel has a lower level of sulfur, burns cleaner with lower HC and CO emissions, and results in better engine performance (Quispe et al., 2013).

The biodiesel production industry generates a large amount of waste glycerin representing about 10% by mass of the initial raw materials (Chi et al. 2007). Annual waste glycerin generation increased rapidly after 2006 and is expected to reach 8.8 billion kg by 2015 which is double the 2009 production (Ayoub and Abdullah 2012). This significant growth rate is mainly in Asia, the European Union, and the United States, which in 2007 were responsible for 44%, 35% and 11%, respectively, of world glycerin production (Quispe et al., 2013). The same authors reported that in 2007, these three regions were also the three largest refined glycerin consumers in the world.

The lack of an economical purification process for waste glycerin (Slinn et al. 2008), together with the excess waste glycerin generating and the variability of its quality (Robra et al. 2010), have made the marketing of waste glycerin uneconomical. Therefore, beneficial disposal methods of waste glycerin have been investigated including combustion, composting, animal feeds and anaerobic digestion. However, glycerin is a readily digestible substrate that makes it an excellent co-substrate for anaerobic digestion process (Fountoulakis et al. 2010).

Several studies have evaluated the beneficial addition of waste glycerin to the anaerobic digestion of organic wastes such as municipal solid waste (Fountoulakis et al. 2010) manure and energy crops (Holm-Nielsen et al. 2008) and pig manure (Astals et al. 2012). To the author's knowledge, most of the aforementioned studies have been conducted in the lab-scale. Yet, pilot-scale studies which more closely resemble full scale operating conditions are required to assess several operational parameters. Fountoulakis and Manios (2010) demonstrated that addition of a maximum BGW concentration of 1% (v/v) in the feed enhanced biogas production by 112% compared to the digestion of sewage sludge alone. They conducted the experiment in a 3 L working volume reactor at mesophilic conditions. Astals et al. (2012), reported a 400% increase in biogas production under mesophilic conditions when 4% (w/w) of BGW was co-digested with pig manure compared to digestion of pig manure alone. Despite a number of studies on anaerobic co-digestion of BGW, there are very limited studies that have been conducted on the co-digestion of BGW and MWS.

2.4. Modeling of Anaerobic Digestion

Anaerobic digestion system is a complex biological process that generally receives complex organic chemicals and might suffer from inconstancy and imbalance of these compounds. Instability in such systems reduces process efficiency, imposes additional treatment cost in terms of chemical usage and labor, and can lead to process failure (Lyberatos and Skiadas 1999). Inhibitory substances, which have adverse effects on microbial population or bacterial growth rates, are the most likely reason of upset when they are present in high concentrations (Chen et al. 2008). Imbalance between acidogenic and methanogenic microorganisms due to the different in nutritional needs, growth kinetics and sensitivity to the environmental conditions, is the common instability in the anaerobic digesters (Demirel and Yenigun 2002). In order to be able to predict and operate anaerobic digestion systems efficiently to provide stabilized conditions, appropriate mathematical and kinetic models need to be developed. The first models were generally based on the rate limiting step, which is the slowest step of the multistep microbial process (Hill and Barth 1977). Lawrence and McCarty (1969) proposed one of the first models that considered the methanogenesis step as the limiting step of the process.

Some models only apply at the steady state conditions and generally consider a mass balance for the total substrates. Dynamic models are more complicated and generally consider the inhibitory factors of VFAs and ammonia, mass balance over several substrates and microbial cultures, methane production rate and predicting more parameters at the unstable operating conditions that could be more reliable to predict the anaerobic digestion process (Husain 1998).

Various dynamic models have been proven their productivity in the design and operation of anaerobic digestion systems. AM2 is a dynamic model which was developed cooperatively by INRIA of Sophia-Antipolis and INRA of Narbonne in 2001 based on acidogenesis and methanogenesis activities (Bernard et al. 2001). In 1987, Activated Sludge Model no.1 (ASM1) was developed by the International Association on Water Pollution Research and Control Task Group on Mathematical Modeling for ammonium nitrogen removal. Since 1987, more

complex models of ASM-based were introduced to the wastewater treatment plant. Models including, ASM2 for phosphorous removal, ASM2d for denitrifying and finally ASM3, in 1998, for the role of internal storage compound in the biological metabolism were developed (Henze et al. 2000).

2.4.1. Anaerobic Digestion Model No.1 (ADM1)

Recently, The International Water Association's Task Group for the Mathematical Modeling of Anaerobic Digestion Processes developed the Anaerobic Digestion Model No. 1 (ADM1) (Batstone et al. 2002). The ADM1 has a structure similar to ASM-based model which has been used over the last 10 years in the municipal wastewater treatment plants to design and operate the anaerobic digestion systems (Siegrist et al. 2002).

The ADM1 is a structured dynamic model with five biochemical conversion processes and eight bacterial groups including disintegration, hydrolysis, acidogenesis, acetogenesis and methanogenesis (Batstone et al. 2002). Disintegration is the first part of extracellular solubilization which converts composite particulate substrate to inert, carbohydrates, lipids, proteins and soluble inert substrate. The second part of extracellular solubilization is hydrolysis of hydrocarbons, lipids and proteins monomers to monosaccharides, long chain fatty acids (LCFA) and amino acids by three hydrolytic bacteria species (Batstone et al. 2002). The third step is the acidogenesis of monosaccharides, LCFA and amino acids to the mixed organic acids, hydrogen and carbon dioxide. The fourth step is acetogenesis which utilizes organic acids (butyrate, propionate and valerate) and LCFA to produce acetate, hydrogen and carbon dioxide. Finally, two groups of methanogens, acetoclastic methanogens and hydrogenotrophic methanogens, convert acetate and both hydrogen and carbon dioxide to methane, respectively (Boubaker and Ridha 2008). Monod-type kinetics is used for all the intracellular biological degradation and first order kinetics is used for the extracellular steps, which are disintegration and hydrolysis, and biomass decay process (Batstone et al. 2002). The composition of bacterial cells is represented by the imperial formula $C_5H_7O_2N$. All organic components and molecular hydrogen are

accounted for on the basis of the chemical oxygen demand (kgCODm^{-3}). Inorganic compounds, such as inorganic carbon (CO_2 and HCO_3^-) and inorganic nitrogen (NH_4^+ and NH_3), are described in terms of molar concentrations. The ADM1 model consists of 32 dynamic state variables with 19 biochemical process rates. A set of differential equations (DE) describes the dynamic state variables: 10 DE to model the soluble matter in the liquid phase, two DE to model inorganic carbon and nitrogen in the liquid phase, 12 DE interpret the behavior of particulate matter and biomass concentrations in the dynamic state, 2 DE illustrate cations and anions levels in the liquid phase and 6 DE of the acid-base reactions which describe the pH, carbon dioxide, free ammonia and VFAs levels in the model. The outputs from ADM1 are gas flow and compositions, pH, organic acids (VFAs) and ammonium. In the model, all the biological conversion processes are subject to the extremes of pH inhibition, so pH inhibition plus hydrogen and free ammonia inhibition are included in ADM. All the reactions in the model are categorized in the two main groups of conversion processes; biochemical and physico-chemical processes (Batstone et al. 2002).

Since the Task Group proposed the original ADM1 in 2002, many implementations and modifications have been completed by various researchers (Fezzani and Cheikh 2009; Mairet et al.; Ramirez et al. 2009b) who successfully used the model for various applications. These modifications were applied due to a number of key limitations in the original ADM1 model. The major drawbacks in the ADM1 are: (1) the incomplete glucose acidogenesis for the modeling of VFAs production; (2) the lack of stoichiometric and kinetic parameters for a number of related processes such as the sulfate reduction and precipitation; (3) the lack of long chain fatty acid (LCFA) inhibition kinetic parameters (Batstone et al. 2002).

The ADM1 structure applied some necessary simplifications in reactions for the substrate degradation rates. Yasui et al. (2008) indicated that the effect of using a combination of substrates originated from different sources with different degradation rates has not been fully considered in the original ADM1. Therefore, the differences in characteristics of input materials (substrates) are expected to affect their subsequent degradation parameter values in the ADM1. Ramirez et al.

(2009a) also indicated that some of these simplifications in reaction expressions may result in inaccurate simulation of some processes such as disintegration and hydrolysis. The effects of biomass concentration and activity on the hydrolysis rates have been demonstrated in previous study by Fernandez et al. (2001). Therefore, the biomass and substrate concentrations together with the effect of substrate accessibility and degradability contents should be considered during the modeling.

Since the ADM1 model has been established, the application of ADM1 model in the simulation of ACD systems has been rarely investigated. Derbal et al. (2009) proposed a calibrated ADM1 model to simulate the behavior of a reactor in the ACD of WAS with municipal solid waste. Boubaker and Ridha (2008) modified the ADM1 model and applied it to the mesophilic ACD of olive mill wastewater with olive mill solid waste. The results achieved from both aforementioned studies demonstrated the capabilities of ADM1 in the modeling of ACD systems. The implementation of ADM1 still continues to be applied to the various anaerobic digestion systems.

2.5. Microbial Community

Anaerobic degradation occurs in a mixed microbial community, in which microorganisms constantly interact with each other based on nutrient requirements. Mutualism and competition are two important mechanisms that affect the function of anaerobic microbial communities. Hence, thermodynamically, anaerobic microorganisms have syntrophic (which is a type of mutualism) interactions in the degradation of organic compounds. Syntrophic interactions are essential for the complete conversion of organic compounds, such as lipids, proteins, and polysaccharides, to CO₂ and CH₄ (Jackson and McInerney 2002). Competition is another important mechanism that is involved in anaerobic degradation. Competition for electron donors such as H₂ and acetate indicates the thermodynamic yield of anaerobic metabolic pathways which are strongly depend on their affinity for various substrates (Lovley et al., 1982).

Development of molecular techniques, such as DGGE, PCR, FISH, T-RFLP and more recently 454-pyrosequencing, have led to improve the investigation of microbial communities and their changes during anaerobic digestion.

Pyrosequencing is a sequencing-by-synthesis method that integrates the direct quantitative sequencing, reproducibility and speed for various applications in widely diverse research fields (Marsh 2007). In this method, the real-time incorporation of nucleotides (G, C, A and T) through the enzymatic conversion of released pyrophosphate (PPi) is quantitatively monitored by a proportional light signal. Four enzymatic reactions including polymerase, sulfurylase, luciferase and apyrase are involved to convert the incorporated nucleotides into a bioluminometric signal. At any time in the reaction vessel, only one of the nucleotides (G, C, A or T) is present in the biochemical reactions mediated by these four enzymes (Tost and Gut 2007). The pyrosequencing procedure entails multiple successive steps including DNA preparation, PCR amplification of target region, pyrosequencing reaction and data analysis.

Recently, pyrosequencing technology has been broadly applied in microbial ecology to determine the microbial structure in various environments. Although many investigations that using pyrosequencing technique were conducted, the influences of microbial community dynamics on the reactor performance are still unclear. As digester feedstock and operational conditions are two major factors which influence the reactor performance, substrate variety and nutritional balance leads to a versatile and dynamic microbial population (Mata-Alvarez et al., 2014). Several studies have been conducted to investigate the influences of substrate features and operational conditions on bacterial community dynamics (Wang et al., 2010; Ziganshin et al., 2013) and archaeal community dynamics (Karakashev et al., 2005; Martín-González et al., 2011). Therefore, it is well-known that alteration in the feed composition can alter the digester stability parameters such as VFA, alkalinity and ammonia which result in changes in the microbial community composition. For example, Lin et al. (2012) and Xia et al. (2012) found that adding co-substrate to digester feed changed the level of inhibitors, such as ammonia and VFA concentrations, which led to a shift in methanogenic

population between hydrogenotrophic and acetoclastic methanogens. Ziganshin et al., (2013) observed that dominance of some of the hydrogenotrophic methanogens under high concentrations of ammonia or VFA are accompanied with the presence of some syntrophic bacteria during the co-digestion of substrates. These findings suggest that co-digestion of mixed organic wastes can promote a superior diversity of nutrients which can result in a broader diversity of microbial populations and greater reactor stability and performance.

CHAPTER 3. PILOT-SCALE ANAEROBIC CO-DIGESTION OF MUNICIPAL WASTEWATER SLUDGE WITH RESTAURANT GREASE TRAP WASTE*

3.1. Introduction

The many advantages of anaerobic digestion make it an attractive alternative for organic waste management and treatment. The widespread application of anaerobic digestion by municipalities is in part due to its environmental and energy benefits (Chen et al. 2008; Li et al. 2011; Nuchdang and Phalakornkule 2012). It is a reliable and mature technology to stabilize sewage sludge and many organic wastes effectively and economically (Iacovidou et al. 2012). However, anaerobic treatment of organic wastes is not widely used by industry because many of the wastes do not have the proper nutrient balance to ensure stable operation or the wastes are not produced in quantities that could sustain continuous anaerobic digester operation. Conversely, digested sludge at municipal wastewater treatment facilities possesses an excess of nutrients and many of these plants do not fully utilize the on-site anaerobic digestion capacity (Schwarzenbeck et al. 2008). Therefore, there is great interest in co-digesting industrial, commercial and agricultural organic wastes with municipal wastewater sludge. The bioenergy production potential of organic waste anaerobic co-digestion as well as the related research trends and requirements are reviewed in Appels et al. (2011). Additional advantages of co-digestion as a biomass valorization technology are reported by DeMeester et al. (2012).

Fats, oils and grease (FOG) wasted from restaurants, commercial kitchens, and food service providers has become a major stream of organic waste in urban areas. Disposal of this waste to landfills is no longer permitted in many jurisdictions and of the alternative disposal methods, anaerobic digestion is an attractive option because greasy wastes have high energy content and methane production potential (Davidsson et al. 2008). Although individual digestion of

* A version of this chapter has been published. Razaviarani et al. *Journal of Environmental Management*, 123 (2013) 26-33.

greasy waste is not viable because of long-chain fatty acid inhibition (Luostarinen et al. 2009) its co-digestion with municipal wastewater sludge has been demonstrated in a number of bench-scale studies and has been implemented at several full-scale facilities. Nevertheless, pilot-scale studies are required to assess several operational parameters.

In this study, pilot-scale anaerobic co-digestion of municipal wastewater sludge (MWS) and grease trap waste (GTW) was investigated to determine the maximum safe GTW loading rate. The effect of GTW addition on volatile solids and total chemical oxygen demand (COD) reduction rates and on biogas production were also determined.

3.2. Materials and Methods

3.2.1. Substrates

Municipal wastewater sludge consisting of a 3:1 (v/v) mixture of primary treatment scum and sludge (PS) and thickened waste activated sludge (WAS) was obtained daily from the Gold Bar Wastewater Treatment plant (WWTP) in Edmonton, Alberta. GTW was obtained from a local waste collection company in Edmonton, Alberta. Effluent from full scale mesophilic anaerobic digesters at the Gold Bar WWTP was used as the inoculum (seed) during digester start-up.

The characteristics of the MWS and GTW varied somewhat during the investigation and are shown in Table 3.1, which also indicates the nominal COD loadings to the test digester relative to the control digester loadings. The characteristics of the GTW varied primarily because of differing water contents from one batch to another. The COD and VS content of GTW ranged from approximately 737 to 1510 kg/m³ and 127.6 to 256.9 kg/m³, respectively. The MWS had COD and VS values between 31.2 to 34.3 kg/m³ and 18.8 to 24.3kg/m³, respectively.

Table 3.1. Characteristics of municipal wastewater sludge (MWS) and restaurant grease waste (GTW)

Nominal	MWS			GTW		
	COD	TS	VS	COD	TS	VS
loading (%)	(kg/m ³)	(kg/m ³)	(kg/m ³)	(kg/m ³)	(kg/m ³)	(kg/m ³)
100	34.1±4.5 ^a	26.5±1.4	20.5±1.3	N/A ^b	N/A	N/A
120	32.6±5.7	26.3±4.0	19.0±2.4	1510.0±55.8	258.4±4.6	256.9±4.3
170	31.2±3.7	30.7±3.8	22.3±1.8	737.0±196	129.0±7.1	127.6±7.2
190	32.5±1.9	31.5±3.3	18.8±2.5	860.0±21.6	155.4±8.7	154.7±8.4
240	33.1±5.8	33.8±4.6	24.3±2.5	1026.0±65.2	179.7±5.5	178.4±6.7
280	34.3±6.2	32.0±3.5	22.3±1.1	1150.0±24.2	178.4±4.0	176.3±4.6

^a Standard deviation

^b Not applicable

3.2.2. Pilot Digesters

Two identical 1300 L (1200 L active volume) complete mix digesters housed in a trailer were received from the King County Wastewater Treatment Division in Washington USA., and modified as required to conduct anaerobic co-digestion testing at the Gold Bar WWTP in Edmonton. Each digester was approximately 91 cm in diameter and 214 cm tall, with a sloped bottom. The digesters were operated in the mesophilic temperature range ($36 \pm 1^\circ\text{C}$), with a solids retention time (SRT) of 20 days. Start-up involved placing 1200 L of full-scale digester effluent sludge in each digester and purging the headspace with nitrogen gas. Each day, 60 L of digested sludge were withdrawn and replaced with an equal volume of MWS (or a mixture of MWS and GTW) to provide a 20 day SRT. Digester internal temperature was monitored by Type J thermocouples whose output to a programmable logic controller allowed the temperature to be controlled by an external thermal jacket. A top-mounted three bladed digester mixer was operated at a nominal shaft speed of 100 rpm in each digester. Biogas

flow rate from each digester was measured by a mass flow meter (Kurz Instruments Model 502FT-6A, Monterey, CA). Each flow meter was provided with a transmitter wired to a digital panel meter (Precision Digital Model # PD690, Natick, MA) which produced an analog output wired to the data collection system. A data collection system logged the digesters' biogas flow rates as well as their internal temperatures and active volumes every 5 minutes.

3.2.3. Digester Feed and Organic Loading Rate Protocols

The loading to the test digester was based on the control digester loading and expressed as a percentage of the control digester COD loading. The study was divided into three stages in terms of the COD loading of the test digester: baseline performance without a co-digestate; quasi steady state co-digestion; and ultimate co-digestate loading determination. The digesters initially received the same amount and type of feed (MWS only) in order to establish the baseline performance of each reactor. This operating mode was continued for a 30-day period. When the equivalence of the digesters' performance was established, the COD loading of the test digester was increased with the addition of a known volume of GTW in addition to the MWS to achieve the desired COD loading. Digester loading rates and their durations of application are shown in Table 3.2. Because, the MWS was collected daily from the WWTP, the operational changes and variations in plant flow rates and influent quality resulted in variations in MWS feed characteristics throughout the study.

The COD loading to the test digester was increased until it reached 190% relative to the control digester. This 190% loading was maintained for 30 days to allow the system to stabilize. Subsequently, the test digester loading was increased incrementally until the biogas production rate reduced and process instability was observed.

Table 3.2. Organic loading rate (OLR) at various increments

COD loading (%)	Day	OLR (kg COD/m ³ d)		OLR (kg VS/m ³ d)	
		Control	Test	Control	Test
100	1-30	1.71±0.2 ^a	1.71±0.2	1.03±0.1	1.03±0.1
120	31-55	1.63±0.2	2.00±0.2	0.95±0.4	1.01±0.4
170	56-80	1.56±0.2	2.62±0.2	1.12±0.1	1.26±0.1
190	81-110	1.62±0.1	3.01±0.2	0.94±0.1	1.16±0.1
240	111-135	1.66±0.3	3.99±0.4	1.22±0.1	1.58±0.1
280	136-155	1.72±0.3	4.87±0.3	1.12±0.2	1.60±0.2

^a Standard deviation

Each day, a volume of MWS sufficient to meet the line flushing and feed requirements for both digesters (approximately 150 L) was obtained from the WWTP sludge blending tank and transferred to the grinder tank to be mixed thoroughly (see Figure 3.1). 75 L of the MWS were then transferred to the feed tank. Before feeding, 60 L of digested sludge was drained from each digester to its effluent tank. Samples were collected from the feed and the effluent tanks for subsequent analysis. The control digester feed line was flushed with the MWS and the digester was fed a sufficient amount of MWS (60 L) to return its active volume to 1200 L. Then, feed tank and control digester feed lines were emptied and flushed with clean water. The volume of MWS in the grinder tank was determined, and a quantity of GTW was added to the grinder tank in order to achieve the required total COD target (120%, 170%, 190%, 240% and 280% of the control feed). After thorough mixing, the feed was transferred to the feeding tank. 60 L of the feed mixture was then pumped to the test digester to return its active volume to the 1200 L level. Finally, the test digester feed line and all tanks were emptied and flushed with clean water.

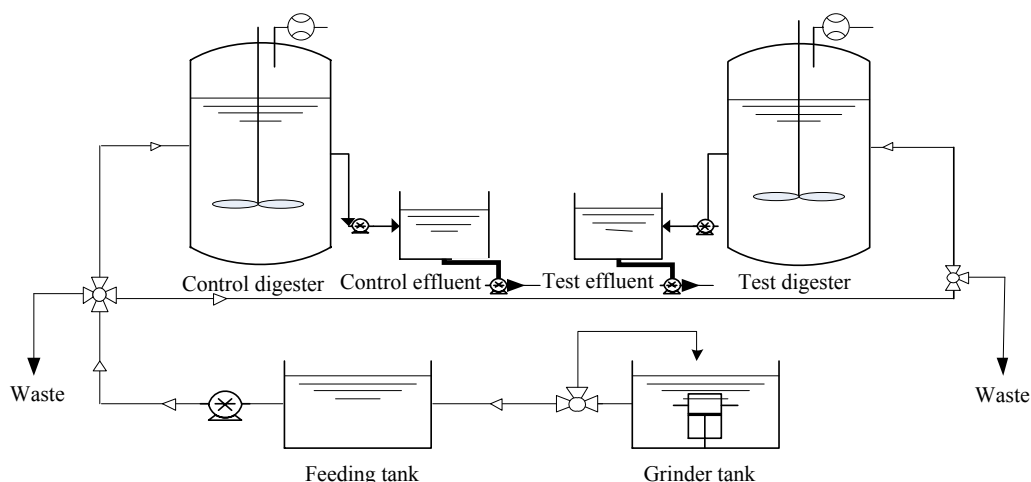


Figure 3.1. Schematic of the pilot scale anaerobic digester setup.

3.2.4. Analytical Methods

The percentage of carbon dioxide in biogas was measured using a Fyrite[®] gas analyzer according to the method specified by the manufacturer (Bacharach Inc., 2010). Total chemical oxygen demand of influents and effluents were measured with the closed reflux (5220C) method (APHA 2005). Because GTW is a lipid-rich material with no affinity to dissolve in distilled (DI) water, GTW samples were saponified using a known volume of 19 mmol/L NaOH solution. This dilution of the GTW sample was taken into account when calculating its COD. Total solids and volatile solids also were quantified using methods 2540C and 2540E, respectively (APHA 2005).

Samples were centrifuged at 1018×g for 10 minutes and the supernatants were analysed according to Standard Method 2320B (APHA 2005) to determine alkalinity. The titration end point for partial alkalinity was pH 5.75 and that for total alkalinity was pH 4.30. All the above measurements were performed in triplicate. Intermediate alkalinity was calculated as the difference between total and partial alkalinity values.

Volatile fatty acids (VFAs) in the effluents were analyzed by the on-site laboratory staff using a Metrohm Peak ion chromatograph by an internally developed method based on the Metrohm Peak Method, Application Note #0-15.

Total Kjeldahl nitrogen (TKN) and total ammonia nitrogen (TAN) were measured by the EPCOR laboratory staff at Gold Bar WWTP according to the Alberta Research Council (1996) Code 235 (Semi-automated block digestion, phenate colorimetric method).

3.3. Results and Discussion

The daily biogas production per unit digester active volume is shown in Figure A1 of the Supplementary Data in Appendix A. The evaluation of reactor performance parameters was based on sampling performed during the final 10 days of each test digester loading level, and the mean performance of the test digester was compared to that of the control during each period.

The variability of the test and control digester effluents is shown graphically and statistically in terms of COD and VS in Appendix A. True steady state conditions could not be achieved in the digesters because of day-to-day variability in the blended MWS used as feed. Unlike bench-scale studies, which involve smaller feed volumes that can be stored under conditions that preserve their characteristics, the larger volumes of sludge used in the pilot-scale study (approximately 150 L per day including the piping hold-up) required that fresh feed be obtained daily from the on-site sludge blend tank. The control digester was operated throughout the 155 day study at a constant volumetric loading rate and with the same source of feed (sludge from the full-scale plant blend tank). Because of the varying characteristics of the blended sludge, comparisons are made between the test and control digester on an on-going basis. Quasi steady state was deemed to prevail when coefficients of variation of effluent COD and VS daily measurements over a 10 day period were less than 5%.

3.3.1 Baseline Operation

Baseline operation was conducted to assess the equivalence of the performance of the two digesters. The mean values of the six parameters monitored during this stage are listed in Table 3.3. Paired two tailed t-tests performed on the data indicated that the parameter means were not significantly

different for the two digesters as shown by the p-values given in Table 3.3. This indicates that equivalent performance had been established in the digesters.

As shown in Table 3.3, volatile solids destruction in the two digesters was not significantly different during the baseline loading when the control and test digesters achieved 47% and 45% VS removals, respectively. These values represent VS removal rates of 0.49 and 0.46 kg VS/(m³·d) in control and test digesters, respectively. The digesters' behaviours in terms of COD removal also did not differ significantly during this period. Percent COD removals of 60% and 58% corresponding to COD removal rates of 1.03 and 1.00 kg COD/(m³·d) were achieved in the control and test digesters, respectively.

Table 3.3. Comparison of digester performance during baseline operation

Parameter	Mean value ± standard deviation			<i>p</i> -value
	Feed	Control	Test	
COD (g/L)	34.1±4.5 ^a	13.4±1.7	14.1±1.1	0.40
VS (g/L)	20.5±1.3	10.8±0.4	11.3±0.4	0.44
Biogas production (m ³ /d)	N/A ^b	1.1±0.2	1.0±0.1	0.39
pH	6.0±0.2	7.2±0.1	7.2±0.1	0.34
PA (mgCaCO ₃ /L)	N/A	2577±92	2535±85	0.27
TA (mg CaCO ₃ /L)	1520±8.5	3656±139	3599±95	0.30

^a Standard deviation

^b Not applicable

3.3.2. Overall Digester Performance

When equivalence of digester performance had been established, increasing proportions of GTW were added to the test digester MWS feed to progressively increase its COD loading rate relative to that of the control digester. The control

digester continued to receive only MWS as before. The mean digester loading levels and their durations are shown in Table 3.2.

Biogas production declined in the control digester from the 190% test digester COD loading period onward (data not shown). This was due to a leak in the gas collection system that was not located until the end of the testing period. The control digester biogas production per unit COD removal ($\text{m}^3\text{biogas/kg COD}_{\text{removed}}$) was calculated for the 100% to 170% test digester loading periods. An ANOVA test performed on the resulting mean values indicated no significant difference (p -value = 0.33). The overall mean control digester biogas production rate per unit mass of COD removed was calculated to be $1.02 \text{ m}^3 \text{ biogas/kg COD removed}$ for the period up to and including the 170% test digester loading. This value was applied to control digester COD removals measured during the 190% to 280% test digester loading periods in order to estimate control digester biogas production during this period. Biogas production by the two digesters is shown in Figure 3.2. This figure also indicates the percentage of the volatile solids in the test digester feed that was due to GTW. As shown in Figure 3.2, test digester biogas production increased with increasing loading. GTW additions amounting to 19% and 23% of the total 1.16 and $1.58 \text{ kg VS/ (m}^3\cdot\text{d)}$ loadings resulted in 63% and 67% increases in biogas generation relative to the control, respectively. The maximum test digester biogas production rate of $1.84 \text{ m}^3/\text{d}$ ($1.53 \text{ m}^3/\text{m}^3\cdot\text{d}$) was attained at the 240% COD loading (23% GTW VS). Increasing the test digester COD loading to 280% relative to the control resulted in a rapid reduction of biogas generation.

Enhanced biogas production during GTW co-digestion has been reported in a number of bench-scale studies. A comparison of the results from other studies to those obtained from the present study is shown in Table 3.4. Silvestre et al. (2011) co-digested greasy sludge from a WWTP dissolved air flotation unit with blended WWTP sludge. Biogas production was reported to increase by 128% during co-digestion of a mixture in which VS from grease represented 23% of the total $1.6 \text{ kg VS/ (m}^3\cdot\text{d)}$ loading. Luostarinen et al. (2009) co-digested grease trap sludge from a meat processing facility with sewage sludge. These researchers reported

the biogas production rate to increase by 164% compared to the baseline value when VS from grease represented 46% of the total 3.46 kg VS/ (m³·d) loading. Process instability was observed when the proportion of VS from grease reached 55%.

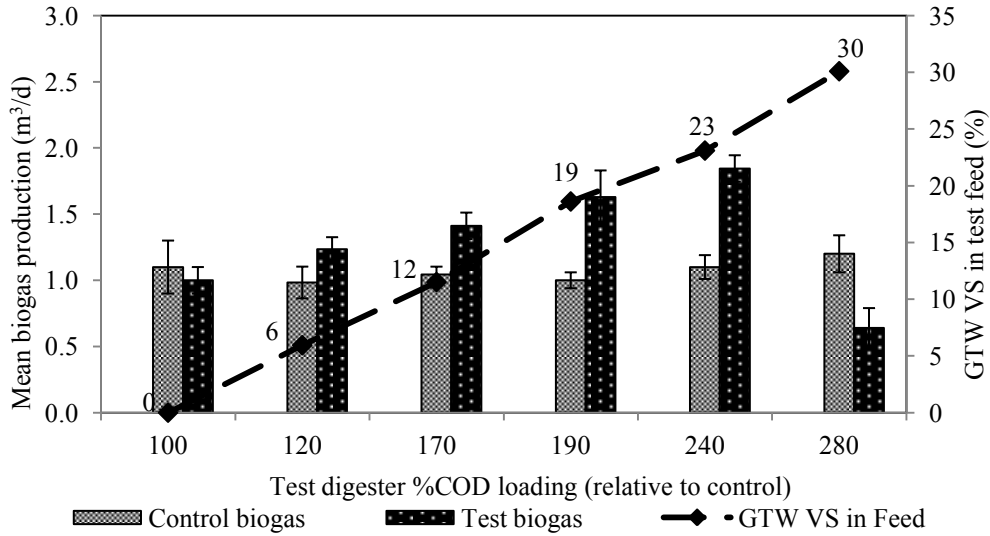


Figure 3.2. Mean biogas production and GTW VS percentage at various loading rates

Enhanced biogas production has been reported to be due to the increased methane potential of the VS in the feedstock as well as the increased VS loading rate. The methane potential of GTW has been reported to range from 0.9 to 1.4 m³/kg VS_{removed} in previous studies (Davidsson et al. 2008; Luostarinen et al. 2009; Bond et al. 2012). These values are significantly higher than those of the primary sludge (0.47 m³/kg VS) and waste activated sludge (0.18 m³/kg VS). Increased methane potential of grease-MWS has been demonstrated by Wan et al. (2011) who studied co-digestion of thickened WAS and GTW. In this work, the organic loading in terms of kg VS/(m³·d) was held constant, but the proportion of VS from grease was increased to 64% of the total 2.34 kg VS/(m³·d) loading resulting in a 125% increase in biogas production. Process instability was noted when the proportion of VS from grease reached 74%. Girault et al. (2012) studied the co-digestion of thickened WAS and greasy sludge from a pork processing plant dissolved air flotation unit. In that study, the OLR was held relatively constant at 3.0 kg COD/(m³·d) but the OLR in terms of VS decreased from 1.9 kg

VS/(m³·d) to 1.0 kg VS/(m³·d) as the proportion of greasy sludge VS in the feed was increased. Biogas production was reported to increase by 55% during co-digestion of a mixture in which the VS from greasy sludge represented 52% of the total 1.2 kg VS/(m³·d) loading. Process instability was noted when the proportion of VS from grease reached 74%.

As shown in Figure 3.2, test digester biogas production decreased remarkably when the percentage of VS from grease was increased to 30% of the total 1.60 kg VS/ (m³·d) loading. This indicates that a process upset had occurred at considerably lower proportions or loadings of grease VS than reported by Girault et al. (2012), Wan et al. (2011) or Luostarinen et al. (2009). This may be due in part to the greater process control that is possible at bench scale and to differences in the waste grease origins and mixture characteristics.

Table 3.4. Description of similar previous studies of anaerobic co-digestion of MWS and GTW

References	Substrate sources (MWS + GTW)	Operational conditions (mesophilic) ^a	Optimum OLR (kgVS/m ³ d)	Initial biogas generation (m ³ /m ³ .d)	GTW added at optimum loading (%VS)	GTW added at failure loading (%VS)	Biogas increase (at optimum loading) (%)
Present study	25% WAS & 75% PS from WWTP + GTW from restaurant waste	1200L-pilot scale 20days SRT	1.58	0.83	23	30	67
Girault et al. (2012)	100% WAS from WWTP + GTW from meat industry	200 L-batch 25days SRT	1.2	0.74	52	> 60	55
Silvestre et al. (2011)	30% WAS & 70% PS from a WWTP + GTW from DAF ^b unit	5.5 L-lab scale 20days SRT	1.5	0.35	23	NA	128
Wan et al. (2011)	100%TWAS from WWTP +Un-dewatered FOG	4L-lab scale 15days SRT	2.34	0.46	64	74	125
Luostarinen et al. (2009)	Sewage sludge from WWTP +GTW from meat processing facility	4L-lab scale 16days SRT	3.46	0.70	46	71	164

^a All the studies operated at the mesophilic (35-37°C) condition in the continuous mixed reactor

^b Dissolved air floatation

3.3.3. Quasi Steady State Operation

Volatile solids removal is a major anaerobic digestion performance indicator as it relates to the mass of biosolids that must be disposed ultimately. Typical VS destruction in anaerobically digested thickened waste activated sludge (TWAS) has been reported to be in the range of 30% to 45% (Wan et al. 2011). During the 190% test digester COD loading period, VS removal reached 44% in the control digester, and 56% in the test digester. This represents VS removal rates of 0.42 and 0.64 kg VS/ (m³·d) in the control and test digesters, respectively. Improved VS removal has been commonly reported by other researchers as a benefit of co-digestion of GTW and MWS (Luostarinen et al. 2009; Silvestre et al. 2011; Wan et al. 2011).

The degree of COD removal is a measure of organic waste stabilization. The percent COD removals are shown in Figure 3.3 for the baseline and quasi steady state 190% loading periods. COD removal in the test digester reached 76% during the period of 190% COD loading, while 54% COD removal was observed in the control digester during this same period. These values represent COD removal rates of 2.28 kg COD/(m³·d) and 0.89 kg COD/(m³·d) in test and control digesters, respectively. The effluent COD concentrations were approximately the same from each digester during the 190% test digester COD loading period despite the 90% greater COD loading to the test digester (data not shown).

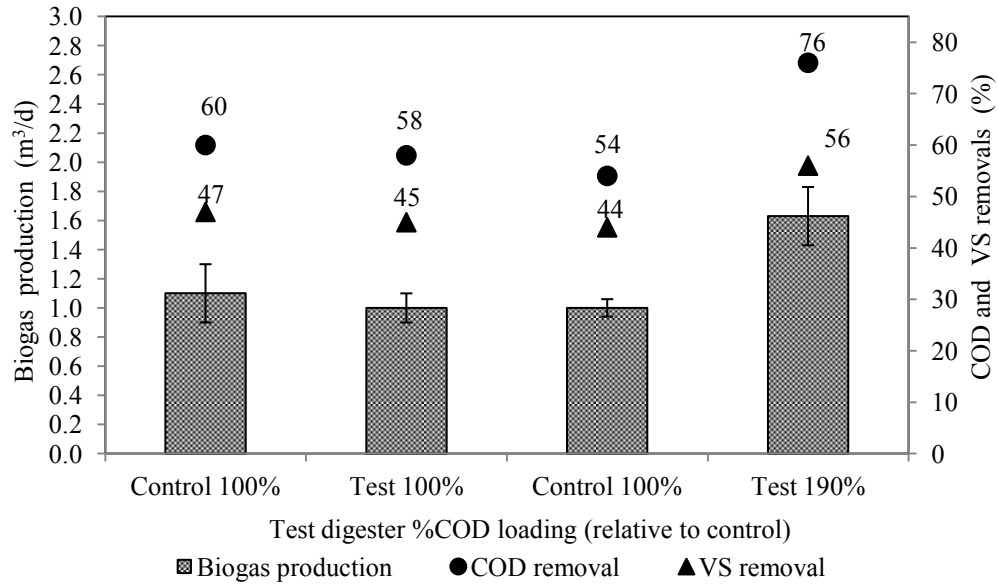


Figure 3.3. Biogas production, %VS and %COD removals at baseline and at quasi steady state

As indicated in Table 3.5 and shown in Figure 3.3, biogas production was similar in each digester during the baseline loading period. During the 190% test digester COD loading period, test digester biogas production of 1.63 (m³/d) (1.36 m³/m³·d) was estimated to be 63% greater than that of the control. The VS and COD percentage removals in the test digester were 12% and 22% greater in test digester relative to the control, respectively (Figure 3.3). Other researchers have also reported enhancements in biogas production and VS and COD removals during the co-digestion of MWS and GTW (Girault et al. 2012; Kabouris et al. 2008; Silvestre et al. 2011). In a similar study using lab-scale reactors, Kabouris et al. (2009) conducted mesophilic co-digestion of MWS and FOG. These researchers reported 79% and 98% increase in the VS and COD removals, respectively when the feed consisted of 44% FOG VS and 59% FOG COD compared to the feeding of only municipal sewage sludge.

3.3.4. Process Stability

Biogas generation in the test digester increased with increasing COD loading until a large reduction in its production was observed at the 280% COD loading

(see Figure 3.2). At this point volatile solids from GTW represented 30% of the total 1.6 kg VS/(m³·d) loading to the test digester. The cause of this reduction in biogas generation was investigated by reviewing parameters including pH, partial and total alkalinity, VFA, TAN, TKN and %CO₂. The values of these parameters are shown in Table 3.5. A comparison between the values of these parameters measured for the test and control digesters shows little difference. During co-digestion, the test digester TAN concentration remained well below the range of 1.7 to 14 g/L reported to cause upset (Chen et al. 2008). Based on the pH of 7 and a temperature of 36°C, the free ammonia concentration was approximately 10 mg NH₃/L which is well below the inhibitory level of approximately 90 mg/L reported by Gallert et al. (1998).

Table 3.5. Characteristics of reactor effluents

parameters		Nominal COD loading (%)					
		100	120	170	190	240	280
<i>Effluent</i>							
Control	TAN(mg/L)	889±40	897±22	957±94	1085±29	906±27	858±43
	TKN(mg/L)	1766±49	1919±112	1993±41	2157±80	2097±211	1905±70
	PA(mg/L)	2970±224	2857±195	3094±148	3228±143	2982±137	2717±120
	TA(mg/L)	3607±263	3483±178	3829±173	4334±273	4186±191	3869±75
	IA (mg/L)	637±152	626±102	735±124	1106±287	1204±111	1152±111
	VFA(mg/L)	3.9±1.1	5.8±2.8	7.6±4.1	15.9±6.4	16.9±2.3	13.3±2.1
Test	TAN(mg/L)	879±37	836±7	943±53	1096±41	815±36	690±47
	TKN(mg/L)	1700±62	1945±150	1929±49	2289±64	2225±85	1966±110
	^a PA(mg/L)	2965±182	2729±196	2755±144	3020±253	2492±248	1852±133
	^a TA(mg/L)	3634±130	3313±197	3465±155	3945±375	3677±334	2967±130
	^a IA(mg/L)	669±130	584±160	710±106	925±276	1185±136	1115±55
	^b VFA(mg/L)	3.7±0.9	7.2±2.6	6.5±0.9	23.6±3.0	27.9±2.5	38.2±5.6
<i>Biogas</i>							
Control	Biogas(m ³ /d)	1.1±0.2	0.98±0.1	1.04±0.1	1.0±0.1	1.1±0.1	1.2±0.1
Test	%CO ₂	31.4±2.0	35.1±1.7	34.3±2.8	34.8±3.5	33.8±4.0	30.4±3.5
	Biogas(m ³ /d)	1.0±0.1	1.24±0.1	1.41±0.1	1.63±0.2	1.83±0.1	0.64±0.1
	%CO ₂	29.7±3.0	33.5±1.7	32.1±3.5	33.6±3.4	34.4±3.2	34.5±3.9

^a Partial alkalinity (PA), total alkalinity (TA) and intermediate alkalinity (IA) represented as mg/L CaCO₃, ^bVFA represented as mg/L acetic acid

The test digester partial and total alkalinities were lower than those of the control and the total VFA was greater. A reduction in alkalinity is typically caused by an increase in VFA and CO₂ generation. However, the biogas %CO₂ had remained at an acceptable level and the total VFA remained low (38.2 mg/L as acetic acid). The ratio of partial alkalinity (due primarily to bicarbonate ion) to total VFA was 29:1 (mol/mol), which is well above the minimum safe value of 1.4:1 reported by Appels et al. (2008). Other researchers have used the ratio of intermediate alkalinity (IA) to partial alkalinity (PA) as a measure of process stability (Astals et al. 2012; Ferrer et al. 2010). Astals (2012) reported that the IA/PA ratio should remain below 0.4 for stable operation. Fernandez (2001) indicated that the IA/TA ratio should remain below 0.3. Figure 3.4 shows that the IA/PA ratio increased in both the control and test digester beginning from the period of 190% test digester loading. The increase in the control digester IA/PA may be due to changing MWS characteristics. The accelerated increase of IA/PA in the test digester is due to the increasing proportion of GTW in its feed. The IA/PA ratio of the test digester effluent reached 0.6 at the 280% loading, which is well above the reported safe level of 0.4. The IA/TA ratio reached 0.30 and 0.38 in the control and test digesters, respectively (data not shown). This indicates that the test digester's buffering capacity was declining and the system was exhibiting signs of instability. System instability is also indicated by the decline in the test digester pH which had remained relatively constant until the 280% COD loading.

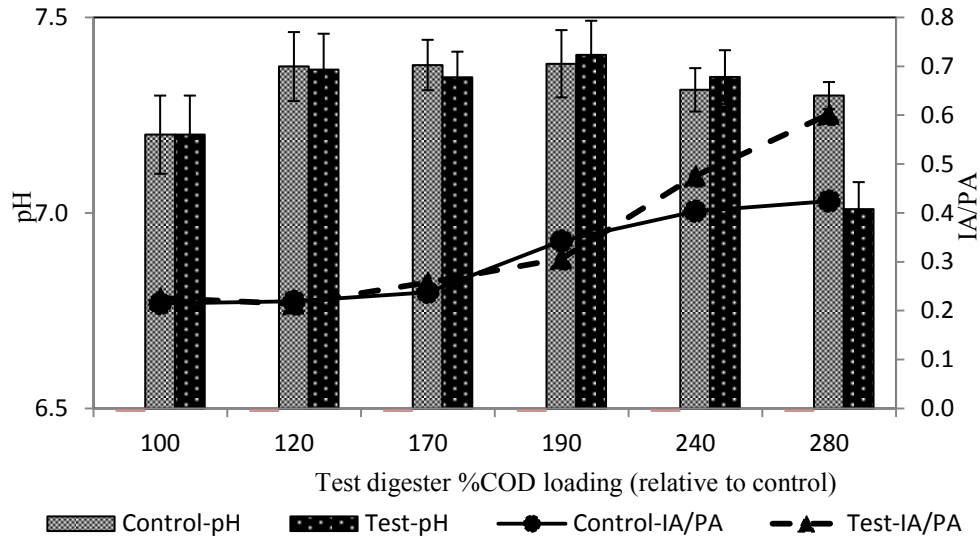


Figure 3.4. Effluent pH and IA/PA ratio at various organic loadings

A COD/TKN ratio less than 70 is cited by Álvarez et al. (2010) to avoid nitrogen limitations. The COD/TKN ratio in the feeds to the test and control digesters is shown in Figure 3.5. The COD/TKN ratio in control digester remained between 10 and 20 throughout the study, whereas that of the test digester increased with increasing proportions of GTW in its feed, to reach a value of 50 at the 280% COD loading. Therefore an excess of nitrogen was available in both the control and test digesters throughout the study.

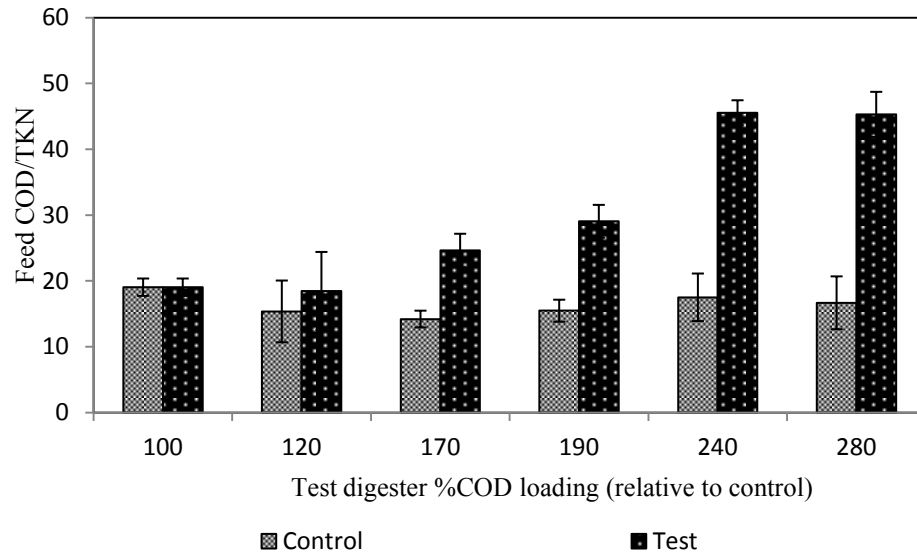


Figure 3.5. Feed COD/TKN ratio at various organic loadings

The relatively low VFA concentrations in the test digester and steady %CO₂ in its biogas suggest that methanogens inhibition was not the cause of the observed decline in biogas production. Therefore, inhibition of other microbial populations must be considered.

None of the measures of process stability that have been examined would indicate a process upset that could account for the observed reduction in biogas production. The sole indication of a process upset was the reduced biogas production in the test digester shown in Figures 3.2 and A1 (in Appendix A). Following the conclusion of the test runs, the test digester was drained, cleaned and re-started with blended municipal wastewater treatment plant sludge. Good gas production was obtained, indicating that the equipment was functioning properly. Thus, test digester equipment failure was also ruled out.

Other researchers have reported either a similar rapid reduction in biogas production as the proportion of grease in co-digestate was increased or a lag in biogas production when the initial feed contained a high proportion of lipid. Cirne et al. (2007) reported a lag time in the initiation of biogas generation when the proportion of lipid in an anaerobic digester feed exceeded 31% on a COD basis. This lag period lasted approximately 25 days when the proportion of lipid initially

fed was 47%. A rapid increase in VFA concentration was observed during this period. This is somewhat contrary to results reported by Girault et al. (2012) who observed a decline in biogas generation when grease VS was increased to greater than or equal to 74% of the total feed VS. However, during the reduced biogas production, these researchers observed no accumulation of VFAs and the pH values were reported to remain relatively steady within the range of 7.2 to 6.9. Results similar to those reported by Girault et al. (2012) have also been reported by Pereira et al. (2005) and Silvestre et al. (2011). Silvestre et al. (2011) reported long chain fatty acid concentration to increase by more than two-fold during the period of low biogas production, while VFA concentration remained relatively low. These researchers attributed the reduction in methane production to mass transfer limitation caused by an accumulation of long chain fatty acids (LCFA). This inhibition can occur without an increase in VFA, presumably due to inhibition of acidogenesis and acetogenesis (Girault et al. 2012).

The effect of LCFA inhibition has been shown to be reversible (Cirne et al 2007, Pereira et al. 2004) and so the reactor in the present study may have recovered. Nevertheless, such a process upset would not be acceptable at a full-scale facility. Therefore, a safe upper limit on GTW loading may be identified based on the results of the present study. These results indicate that a GTW loading in excess of 23% VS or 58% COD relative to the total feed VS or COD loading were detrimental to the process stability (see Figure 3.2). These values are lower than some reported from bench-scale studies. This may be due to the lower mixing efficiency and greater difficulty in controlling other operational variables at pilot- or full-scale facilities as well as differences in the waste grease characteristics.

3.4. Conclusions

Mesophilic co-digestion of MWS and GTW was found to be feasible up to a maximum GTW amounting to 23% of the 1.58 kg VS/(m³·d) loading to a pilot-scale CSTR digester, operating at 35°C and a 20 day SRT. Biogas production at this maximum feasible loading of GTW was enhanced 67% relative to the control

digester. COD and VS removals in the test digester at the 190% relative COD loading were 2.56 and 1.53 fold those of in the control digester, respectively. This resulted in essentially equivalent VS and COD concentrations in the reactors' effluents despite the higher loading to the test digester.

Increasing the GTW addition to 30% of the 1.6 kg VS/ (m³·d) test digester loading resulted in a marked decline in biogas generation. No sign of conditions that would cause methanogens inhibition was observed and the reduction in biogas production was attributed to an accumulation of long chain fatty acids as has been reported in other studies.

CHAPTER 4. CALIBRATION OF THE ANAEROBIC DIGESTION MODEL NO.1 (ADM1) FOR STEADY-STATE ANAEROBIC CO-DIGESTION OF MUNICIPAL WASTEWATER SLUDGE WITH RESTAURANT GREASE TRAP WASTE*

4.1. Introduction

The generation of lipid-rich materials from food service establishment waste streams has increased over the past decades. According to a survey sponsored by the US Department of National Renewable Energy Laboratory, approximately 70 liters/person of grease trap waste (GTW) are generated annually in the United States, which amounts to an annual US GTW production of 22 billion liters (Long et al., 2012). This GTW typically has a volatile solids content ranging from 17% to 97% (w/w) and represents a valuable potential source of energy (Zhu et al., 2011).

Anaerobic digestion is a widely applied technology for the treatment of several organic wastes to simultaneously benefit from its environmental effects and energy production. This technology has been used at municipal wastewater treatment plants (WWTPs) for decades to stabilize sewage sludge, and the benefits of co-digestion of sewage sludge with industrial, commercial and agricultural organic wastes have been demonstrated in previous studies (Álvarez et al., 2010; Razaviarani et al., 2013a). The feasibility of co-digesting of GTW has been investigated in several bench-scale (Luostarinen et al., 2009; Silvestre et al., 2011), pilot-scale (Davidsson et al., 2008; Razaviarani et al., 2013b), and full-scale studies (Johnson et al., 2011) with resulting enhanced biogas production being unanimously reported.

Achieving stable operation in a co-digestion process is not trivial and requires adequate knowledge of the interconnected biochemical reactions that result in the conversion of blended substrates into biogas. Therefore, due to the complexity and importance of the anaerobic digestion process, several mathematical models

* A version of this chapter has been submitted for publication. Razaviarani and Buchanan, *Chemical Engineering Journal* (August 2014).

have been developed to simulate process behavior and operational management over the last three decades (Fezzani and Cheikh, 2009). Notably, the International Water Association's Task Group for the Mathematical Modeling of Anaerobic Digestion Processes developed the Anaerobic Digestion Model No. 1 (ADM1) (Batstone et al., 2002a). Since the ADM1 was developed, many implementations and calibrations have been undertaken successfully (Fezzani and Cheikh, 2009; Mairet et al., 2011; Ramirez et al., 2009b). However, only a few studies have focused on the application of the ADM1 model to the simulation of co-digestion systems (Boubaker and Ridha, 2008; Derbal et al., 2009).

Calibration of the large number of model parameters and the requirement of full substrate characterization are the main drawbacks of ADM1. Evaluation of all model parameters and fractionation of all individual components in substrate are not practical in many cases (Kleerebezem and Van Loosdrecht, 2006). To overcome this issue, some studies have used the default ADM1 values of the kinetic and stoichiometric parameters (Derbal et al., 2009; Galí et al., 2009). However, some of the default values, including the kinetic coefficients, initial biomass concentrations and distribution, and fractionation of soluble and particulate compounds are critical input parameters which can substantially influence the final modeling results. The ADM1 default values were determined for the digestion of municipal wastewater sludge alone, and may not be suitable for co-digestion applications. The anaerobic respirometry test is a useful tool to estimate kinetic parameter values during the degradation of a substrate based on the methane production profile. This test is appropriate for a broad range of substrates, but has rarely been applied in previous studies (Girault et al., 2012). A review of the literature reveals that this methodology has yet to be applied to the determination of the kinetic parameters for the anaerobic co-digestion of mixed substrates such as municipal wastewater sludge (MWS) and GTW.

The objective of this study was to calibrate the ADM1 for anaerobic co-digestion of MWS and GTW. To achieve this goal, anaerobic respirometry, together with substrate characterizations were used to evaluate the important kinetic and stoichiometric parameters for the mixed substrates. The initial

biomass concentrations and distributions were also calibrated according to the method described by Girault et al. (2011) based on data obtained from MPR curves and the effluent values from full-scale anaerobic digesters. One experimental run of GTW and MWS co-digestion was conducted at steady-state in order to provide the data set for model calibration. A second co-digestion of GTW and MWS with a different proportion of GTW and a new batch of sludge was carried out to obtain steady state data to check the accuracy of the calibrated model. The calibrated model was also tested to determine its ability to predict the performance of pilot-scale co-digestion of MWS and GTW using a data set compiled previously by the authors.

4.2. Materials and Methods

4.2.1. Analytical Methods

Analyses of the feed substrates and digester effluents were performed on the regular basis. The soluble fractions were obtained by centrifuging samples at 5000 x g for 10 min and then the supernatants were filtered through 0.45 μ m and 0.2 μ m nylon syringe filters. Total and soluble chemical oxygen demands (tCOD and sCOD) of samples were measured according to the closed reflux (5220C) method using a HACH COD reactor and GENESYS20 spectrophotometer. Total solids (TS), volatile solids (VS), total suspended solids (TSS) and volatile suspended solids (VSS) were quantified using methods 2540G and 2540D, respectively. Total alkalinity (TA), partial alkalinity (PA) and pH were determined using Thermix stirrer 120S and ACCUMET AB15 Plus pH meter. The titration endpoint for PA and TA were pH 5.75 and 4.3, respectively according to Standard Method 2320B. All of the above analyses were performed according to the standard methods in triplicate (APHA, 2005). Particulate COD was calculated as the difference between total and soluble COD. Individual volatile fatty acids (acetate, propionate, iso-butyrate, n-butyrate, iso-valerate and n-valerate) in the samples were analyzed using a Varian 430 gas chromatograph (GC) equipped by Stabilwax-DA capillary column and a flame ionization detector (FID). Total ammonia-N (TAN) and TKN were measured by the Biochemical Analytical

Service Laboratory staff at the University of Alberta according to standard methods.

Protein in the substrates was estimated by multiplying the organic nitrogen (TKN-TAN) by 6.25 (Girault et al., 2012). Lipids in substrates were extracted with chloroform-methanol mixture 2:1 (v/v) according to the methodology described by Folch et al. (1957). The biodegradable COD values of protein and lipids were initially calculated using the theoretical oxygen demands values reported by Liu et al. (2008). Then, the carbohydrate content of substrates was estimated by subtracting the proteins and lipids from the particulate COD in samples.

The biogas flow rate from each reactor was quantified by a digital gas flow meter and logged to a lab computer. An Agilent 7890A gas chromatograph (GC) was used to measure the CH₄ content in the biogas. The GC was equipped by Agilent GS-Q column and a flame ionization detector (FID). The CO₂ percentage in biogas was measured using a Fyrite gas analyzer according to the method specified by the manufacturer (Bacharach Inc., 2010).

4.2.2. Substrates and Inoculum

Municipal wastewater sludge, consisting of a 4:1 (v/v) blend of primary sludge (PS) and waste activated sludge (WAS), was obtained from a municipal wastewater treatment plant (WWTP) in Edmonton, Alberta, Canada and stored at 4°C until its utilization. GTW was obtained from a local waste collection company in Edmonton, Alberta. The GTW from restaurants and food services typically has some settleable solids which are not degraded during anaerobic digestion and accumulate at the bottom of the reactor. These solids can account for up to 22% of total GTW volume (Long et al., 2012). Accumulation of the settleable solids contents in GTW over the time will reduce the working volume of the reactor and consequently reduce the process efficiency. Therefore, the GTW was brought to room temperature to allow solids to settle and FOG to form a surface layer. This surface layer of FOG was then separated from the lower layers of water and settled solids before being blended with MWS. The inoculum (seed)

used in this study was obtained from full-scale mesophilic anaerobic digesters at an Edmonton municipal WWTP operated at a 17 day solids retention time. The characteristics of substrates and inoculum used during the study are shown in Table 4.1.

Table 4.1. Characteristics of municipal wastewater sludge (MWS), grease trap waste (GTW) and inoculum.

Parameter	Unit	^a MWS _r	^b MWS ₁	^c MWS ₂	GTW	Inoculum
Density	kg L ⁻¹	0.9	0.92	0.96	0.9	0.98
TS	g L ⁻¹	40.37	63.92	22.92	776.79	22.29
VS	g L ⁻¹	31.15	35.75	18.28	776.23	12.17
TSS	g L ⁻¹	38.3	61.47	19.2	47.73	20.90
VSS	g L ⁻¹	29.17	34.80	15.6	47.58	11.30
tCOD	g L ⁻¹	57.96	75.3	40.89	2697.78	22.87
sCOD	g L ⁻¹	3.87	5.3	2.5	197	nm
pH		5.51	5.8	5.75	5.0	7.27
VFAs	mg L ⁻¹	720.09	2982.76	1639.87	^e nm	7.98
Acetic acid	mg L ⁻¹	233.26	853.2	659.17	nm	5.2
Propionic acid	mg L ⁻¹	298.28	874.53	389.93	nm	0.61
<i>iso</i> -Butyric acid	mg L ⁻¹	15.54	107.83	61.07	nm	2.17
<i>n</i> -Butyric acid	mg L ⁻¹	98.69	611.22	324.46	nm	0.00
<i>iso</i> -Valeric acid	mg L ⁻¹	23	207.94	121.95	nm	0.00
<i>n</i> -Valeric acid	mg L ⁻¹	51.32	328.04	83.29	nm	0.00
TKN	mg N L ⁻¹	980	804	794	nm	2140
TAN	mg N L ⁻¹	382.5	346	332	nm	755
Total alkalinity	mgL ⁻¹ CaCO ₃	1800	1850	2000	nm	nm
Partial alkalinity	mgL ⁻¹ CaCO ₃	^d NA	670	525	nm	nm
Proteins	mg L ⁻¹	3477	2008	1635	nm	nm
Carbohydrates	mg L ⁻¹	13247	16853	5867	nm	nm
Lipids	mg L ⁻¹	5395	7011	3525	nm	nm

^a Municipal wastewater sludge used in respirometric test; ^b Municipal wastewater sludge used in Run 1; ^c Municipal wastewater sludge used in Run 2, ^d Not applicable, ^e Non – measured.

4.2.3. Anaerobic Respirometry Test

Substrate characterization is a most critical step in modeling calibration. Chemical analyses provide the basic composition of the substrate but no information about substrate degradability. Anaerobic respirometry is a valuable experimental tool to evaluate the substrate fractions and hydrolysis kinetic parameters in forms suitable for use as inputs to ADM1.

Three identical 10 L (8 L working volume) batch reactors were used in this test. The reactors were mixed by magnetic stirrers and maintained at 37°C using heating tape wrapped around the reactors. An insulating jacket was also applied around each reactor to minimize heat loss. A thermocouple and a temperature controller were used to measure and control the reactors' temperatures, which were recorded in a data logger. Each reactor was connected to a digital gas flow meter to allow continuous measurement of biogas production. The biogas methane content was measured using an Agilent 7890A gas chromatograph.

The anaerobic respirometry procedure involves injecting a pulse of substrate into a batch anaerobic digester that contains a volume of biomass and recording the resultant methane production (Girault et al., 2010). This methodology has been used in several studies to characterize complex substrates (Girault et al., 2012; Yasui et al., 2008). The quantity of substrate to be added to a reactor, in terms of substrate to biomass ratio, must be determined beforehand. The influence of the substrate to biomass ratio on parameter estimation was investigated by Girault et al. (2012). These researchers cautioned that too low a substrate to biomass ratio hampers differentiation between methane produced from substrate degradation and that produced from inoculum degradation, whereas too high a substrate to biomass ratio could cause inhibition phenomena. The loading limit that did not cause inhibition during GTW co-digestion with MWS was identified in Razaviarani et al. (2013b) to be at a level where the COD loading from GTW represented approximately 90% of the COD loading from MWS. Therefore, this proportion was set as the upper limit for GTW+MWS addition.

Before the anaerobic respirometry test was initiated, each reactor was filled to its 8 L working volume with inoculum collected from a full-scale anaerobic

digester at an Edmonton municipal WWTP and incubated until to reach the stabilized biogas and methane production. Reactor 1 (AR1) was assigned as a control in order to obtain baseline inoculum anaerobic respirometry information. Following this incubation period, Reactors 2 and 3 (AR2 and AR3, respectively) each received a 400 mL slug of substrate. The methane production rates of each reactor were then monitored for 10 days. AR2 received 400 mL of municipal wastewater sludge (MWS_r), while AR3 received a 400 mL mixture of MWS_r and GTW in which the COD loading due to the GTW was 90% of that due to the MWS_r . After each addition to a reactor, its headspace was purged with nitrogen gas for 5 min.

In terms of COD loading, AR2 received $2.90 \text{ g COD}_{\text{substrate}}/L_{\text{inoculum}}$ and AR3 received $5.43 \text{ g COD}_{\text{substrate}}/L_{\text{inoculum}}$. The resultant MPR curves for each reactor are shown in Figure B1 of the Supplementary Data (Appendix B).

4.2.4. Semi-Batch Reactors

Two separate semi-batch experiments were run; one for the purpose of model calibration and the other for model validation. Two identical 10 L (8 L working volume) reactors were used in each run. The reactors were operated at 37°C , with a solids retention time (SRT) of 20 days. Start-up involved placing 8 L of full-scale digester effluent in each reactor as inoculum. Thereafter, each reactor's headspace was purged with nitrogen gas for 5 min.

The study was conducted in two stages based on the different GTW loadings and different samples of MWS (MWS_1 and MWS_2), shown in Table 4.1, to provide two identifiable datasets: steady-state co-digestion of MWS_1 with 50% GTW COD loading relative to MWS_1 COD loading; and steady-state co-digestion of MWS_2 with 90% GTW COD loading relative to MWS_2 COD loading. In each stage, 400 mL/d of digested effluent were withdrawn daily from each reactor and replaced with an equal volume of thoroughly-mixed substrate (a mixture of GTW with MWS_1 or MWS_2) to provide a 20-day SRT.

Initially, Reactor 1 (BR1) and Reactor 2 (BR2) received only the same amount of MWS_1 and MWS_2 for 1.5 SRT (30 days), respectively in order to

establish consistent performance. When stable reactor performance was established, the COD loading was increased with the addition of a known volume of GTW in addition to the MWS_1 or MWS_2 to achieve the desired COD loading in the reactors. From this point onward, BR1 received a mixture of MSW_1 and 50% GTW COD loading relative to the MWS_1 COD loading, and BR2 was fed with a mixture of MWS_2 and 90% GTW COD loading relative to the MWS_2 COD loading. This operating mode was continued for 60 days (3 SRT) to reach steady-state conditions in each reactor. Then, samples were collected daily for subsequent analyses during a 10 day period. The data from BR1 were used to calibrate the ADM1 parameters while those from BR2 were applied to check the model validity.

4.3. Results and Discussion

4.3.1. Initial State of Inoculum in ADM1

The inoculum used in this study was taken from a full scale anaerobic digester at an Edmonton municipal WWTP. The inoculum was characterized as required for input to ADM1 to evaluate the initial composite concentration (iX_C) and its component microbial distributions iX_{su} (sugar degraders), iX_{fa} (fatty acid degraders), iX_{aa} (amino acid degraders), etc. These parameters' values were estimated through a multi-step procedure. Firstly, the initial biomass concentration and its component microbial distributions were estimated from the results obtained from a steady-state ADM1 simulation of the full-scale anaerobic digester from which the inoculum was sampled. Then, the estimated component microbial distributions were optimized through a series of simulations of the full-scale anaerobic reactor operated over a period of four times the SRT of the full-scale digester and the modeled methane production results were compared to those obtained from the AR2 according to the method described by Girault et al. (2011). The initial composite concentration and its microbial proportions differed from the default values in the ADM1. The optimized and default values of initial microbial distributions are shown in Figure 4.1. The ADM1 initial concentrations

values along with the adjusted initial concentrations values are listed in Table B1 of Supplementary Data, Appendix B. The results for the distribution of microbial populations obtained in this study were in the range of results obtained by Astals et al. (2013) from the seven different blended sludge samples. The distribution of methanogens obtained in this study is similar to those reported in previous studies and to the ADM1 model default values due to the fact that these populations are involved at the end of the anaerobic degradation chain reactions where they are not strongly dependent on the influent characteristics.

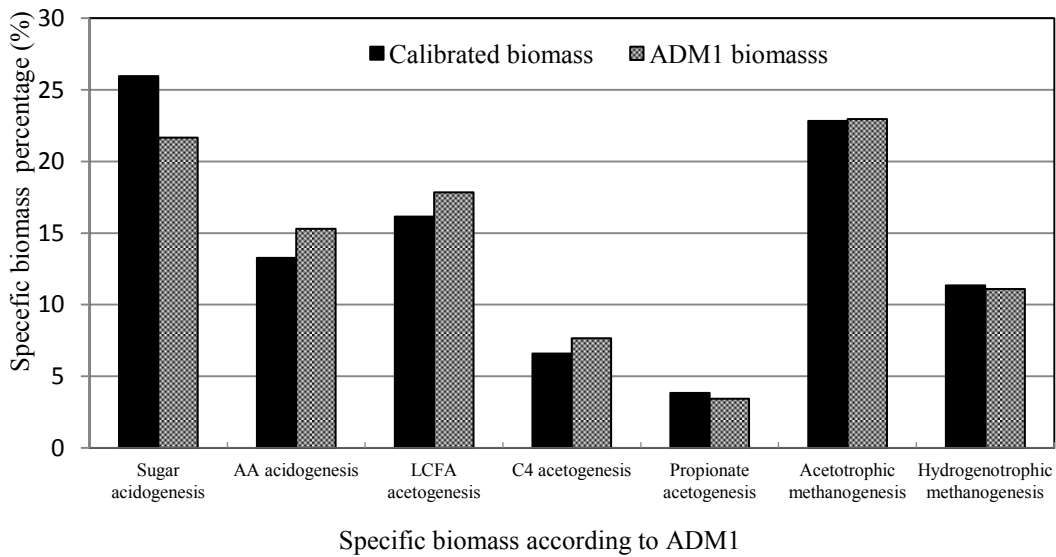


Figure 4.1. Specific biomass concentrations of acclimated inoculum from steady state simulation of full-scale AD by ADM1.

Before being used to model the semi-batch experiments, the initial composite concentration (iX_C) and inoculum disintegration rate (k_{dis, iX_C}) were optimized using simulation to fit the MPR results obtained from the control reactor (AR1). This MPR curve is shown in Figure B1 of the Supplementary Data in Appendix B. The value of k_{dis, iX_C} has been reported to be between 0.15 d^{-1} (Galí et al. 2009) and 0.7 d^{-1} (De Gracia et al., 2009). The optimization procedure yielded a disintegration rate (k_{dis, iX_C}) value of 0.47 and increased the initial composite concentration (iX_C) by 1% compared to its initially estimated value. These results

demonstrated that, unlike the initial microbial distributions, the initial composite concentration and its disintegration rate do not strongly influence the inoculum methane production. Also, the results showed that iX_C was about 13.4% of the inoculum COD used in this study which is in agreement with other studies (de Gracia et al., 2011; Galí et al., 2009) that reported iX_C values between 10% and 15% of the inoculum COD. The parameter values obtained from the foregoing procedures were applied in the subsequent ADM1 modeling of semi-batch reactors.

4.3.2. Substrate Fractionations and Stoichiometric Coefficients

Based on the 4:1 proportion of PS to WAS in the MWS samples, it was expected that the MWS would have a high proportion of particulate organic matter. This was verified by the high VSS to VS ratio and the low sCOD to tCOD ratio calculated from information in Table 4.1. To determine the ADM1-COD fractions, the following assumptions were applied:

- a) The input COD includes soluble COD composed of the soluble readily biodegradable COD (COD_{ss}) and soluble inert COD (COD_{si}) fractions, and particulate COD comprising the COD due to carbohydrates (COD_{xch}), proteins (COD_{xpr}), lipids (COD_{xli}) and inert particulate material (COD_{xi}) fractions. All other COD fractions are negligible and can be set to zero in ADM1.
- b) The soluble inert COD fraction in the influent (f_{si}) can be quantified directly from COD measurements as

$$f_{si} = \frac{\text{effluent sCOD}}{\text{influent tCOD}}$$

The latter assumption neglects any soluble inert COD generated within the system and implies that the soluble inert COD fraction in influent samples

comprises all soluble COD unaffected by biological reactions during the degradation.

The readily biodegradable COD (COD_{ss}) was evaluated by subtracting the soluble inert COD from the influent soluble COD. The VFA-COD fractions were calculated using the VFA results shown in Table 4.1 and their theoretical oxygen demands.

Slowly biodegradable COD fractions of proteins, lipids, and carbohydrates (X_{pr} , X_{li} and X_{ch} , respectively) were calculated using the data from Table 4.1 and theoretical oxygen demands cited in Liu et al. (2008). The GTW sample used in this study was initially dewatered and its settleable solids were removed. Therefore, it was considered to have a 100% lipid content. This was included in the overall lipid COD fraction of the mixed substrate. Finally, the particulate inert COD fraction was evaluated by a mass balance on the total COD. The composite stoichiometric coefficients used in this study are shown in Table 4.2.

Table 4.2. Fractions of the composite stoichiometric coefficients in influents and ADM1 default values

Fraction	MWS_r	MWS_1+GTW	MWS_2+GTW	ADM1
X_{ch}	0.240	0.155	0.117	0.20
X_{pr}	0.090	0.040	0.060	0.20
X_{li}	0.270	0.510	0.607	0.25
X_i	0.032	0.011	0.005	0.25
S_i	0.368	0.284	0.211	0.10

Nitrogen fractions were determined through a combination of direct measurements and a nitrogen mass balance over the substrate. It was assumed that

the total soluble fractions of TKN were in the forms of total free and ionized ammonia. This assumption eliminates the need for the direct measurement of initial amino acid concentration in the samples. The inorganic carbon and inorganic nitrogen in the substrates were calculated as their alkalinity and total free and ionized ammonia concentrations, respectively. Astals et al. (2013) reported that in MWS samples almost 90% of the inorganic carbon is present as $S_{\text{HCO}_3^-}$ and more than 95% of inorganic nitrogen is present as $S_{\text{NH}_4^+}$. These considerations were applied in this study to simplify model calibration.

4.3.3. Model Calibration

The visualization of the MPR curves (Appendix B) showed unique double-peak curves where the first instantaneous peak was followed by a distinct second peak. After the second peak, the curve gradually declined in a steady manner. The first peak was attributed to the fractions for which hydrolysis is not rate limiting and the second peak was ascribed to the slowly biodegradable fractions, including proteins (X_{pr}), lipids (X_{li}) and carbohydrates (X_{ch}), for which hydrolysis is rate limiting. This methane production profile has been reported in previous studies. Yasui et al. (2008) and Girault et al. (2012) suggested that the initial peak was due to very rapid conversion of soluble readily biodegradable compounds and readily hydrolysable substrates with the second peak being ascribed to the degradation of more complex substrates for which hydrolysis was rate limiting.

The results of MPR curves and batch experiments were used to calibrate the ADM1 model (Batstone et al., 2002a) using the GPS-X® computational process simulator (Hydromantis Inc., Canada). Kinetic parameters in ADM1 were adjusted by performing a best fit between the experimental and the simulated MPRs. The calibrated biomass concentration and microbial distributions were used as the initial ADM1 conditions during this process. The calibrated kinetic parameters for biomass growth are listed in Table 4.3.

Table 4.3. Default and calibrated kinetic parameters for biomass growth

Parameter	Unit	ADM1 Default	Calibrated
k_{m-su}	d^{-1}	30	18.11
K_{s-su}	mg COD L ⁻¹	500	683.34
k_{m-pro}	d^{-1}	13	11.99
K_{s-pro}	mg COD L ⁻¹	100	407.6
k_{m-ac}	d^{-1}	8	7.37
K_{s-ac}	mg COD L ⁻¹	150	232.8

In the ADM1, many parameters related to several biological groups are involved in simulating the anaerobic digestion process where precise and reliable quantifications of key variables are extremely vital. Yet, in the case of complex models as ADM1, quantifying all the parameters and coefficients is not practical. Only those stoichiometric parameters with a high level of variability reported by Batstone et al. (2002b) were calibrated in this study, as shown in Table 4.2. Other stoichiometric parameters retained their default values.

Principally, the direct link between kinetic parameters and degradation rate can be interpreted through the MPR curves. Only some of the kinetic parameters have considerable impact on the model fit to the MPR curves. Several parameters including Monod specific uptake rates (k_m), half saturation coefficients (K_s) and decay rates (k_d) influence the output variables of such processes. However, some of these parameters are mathematically correlated and cannot be adjusted simultaneously. The decay rates and Monod coefficients are mathematically linked and as a result the decay rates, due to the lower sensitivity, were not adjusted in this study. This is because the decay rate values are sensitive mostly

under dynamic conditions. Thus, only specific growth rates and half saturation coefficients were calibrated.

In addition, in systems fed with a heterogeneous mixture of particulate materials, disintegration and hydrolysis rates are critical parameters and estimation of such parameters is an important step (Meta-Alvarez, 2003). The methane production is essentially limited by these kinetic parameters. The breakdown and solubilization of organic matter are considered the limiting substrate degradation processes and are modeled by disintegration and hydrolysis rates, respectively (Batstone et al., 2002b). In this study, the hydrolysis rates for carbohydrates, proteins and lipids were initially set to 1.017, 0.384 and 0.999 d⁻¹ respectively, as determined previously by Derbal et al. (2009) who used ADM1 to simulate the anaerobic co-digestion of organic waste with waste activated sludge under mesophilic conditions. The hydrolysis rates were held constant while the disintegration rate was adjusted during a series of simulations over the methane gas production obtained from the semi-batch experiment (BR1) at steady state. To calibrate hydrolysis rates, the latter part of the MPR results obtained from AR3 (MWS_r+GTW) were used. According to the method described by Girault et al. (2012), hydrolysis rates were optimized by simulating over the last five days of the AR3 MPR curve, where hydrolysis was assumed to be rate limiting.

Other kinetic parameters for acidogenesis of sugars and fatty acids, acetogenesis of propionate and of acetate were adjusted using VFA experimental data obtained from BR1 at steady state. The maximum specific uptake rate and half saturation coefficients for sugars, fatty acids, acetate, propionate, butyrate and valerate were calibrated through fitting the ADM1 predicted VFAs values to the measured VFAs. The calibrated parameters are shown in Table 4.4.

Table 4.4. ADM1 Default and calibrated kinetic parameters used in anaerobic co-digestion of MWS and GTW.

Parameter	Unit	ADM1(default)	Calibrated
k_{dis}	d^{-1}	0.5	0.2
k_{hy-ch}	d^{-1}	10	0.75
k_{hy-pr}	d^{-1}	10	0.7
k_{hy-li}	d^{-1}	10	2.1
k_{m-su}	d^{-1}	30	37.4
K_{s-su}	mg COD L ⁻¹	500	496
k_{m-c4}	d^{-1}	20	14.1
K_{s-c4}	mg COD L ⁻¹	200	193
k_{m-fa}	d^{-1}	6.0	5.9
K_{s-fa}	mg COD L ⁻¹	400	381.5
k_{m-pro}	d^{-1}	13.0	17.11
K_{s-pro}	mg COD L ⁻¹	100	63.5
k_{m-ac}	d^{-1}	8.0	10.9
K_{s-ac}	mg COD L ⁻¹	150	96.1

Table 4.5 presents a comparison between measured and simulated biogas, methane, COD, pH and VFAs values. The calibrated ADM1 model led to an acceptable representation of the effluent parameters of the anaerobic co-digestion of GTW and MWS. The average percentage error (APE) is defined as the

normalized summation of the absolute differences between the observed and modeled values divided by observed values. The APE values for the seven parameters are given in Table 4.5. In order to evaluate the significance of agreement between the observed and modeled values, a one sample mean t-test was applied for each dependent parameter presented in Table 4.5. The calibrated model shows significant agreement with *p*-values well above 0.05 for all parameters, except the results of valeric acids. This is because the same kinetic equations are used in ADM1 for butyric and valeric acids degradations and ADM1 cannot differentiate the proportionality of these compounds.

Table 4.5. Statistical comparison of observed and modeled values in calibrated model

Parameter	Unit	Observed	Modelled	%APE	<i>p</i> -value
Methane	Ld ⁻¹	9.00	8.6	7.82	0.44
Biogas	Ld ⁻¹	13.5	12.85	9.67	0.34
COD	gL ⁻¹	58.1	60.7	8.50	0.12
pH	---	7.20	7.15	1.20	0.26
Acetic acid	mg COD L ⁻¹	18.56	21.76	0.21	0.49
Propionic acid	mg COD L ⁻¹	5.63	7.78	0.44	0.29
Butyric acid	mg COD L ⁻¹	18.82	22.14	0.20	0.50
Valeric acid	mg COD L ⁻¹	2.50	13.04	----	<0.05

4.3.4. Model Validation

4.3.4.1. Semi-Batch Experiment

The second semi-batch experiment (BR2) was conducted with the aim of acquiring data to evaluate the calibrated steady-state model. The BR2 was operated at 37°C throughout 60 days (3 SRT), after 30 days of baseline establishment, with a constant volumetric loading rate of a mixture of MWS₂ and GTW containing 90% GTW COD loading relative to MWS₂ COD loading. After 3 SRT, steady state operation was attained when coefficients of variation of effluent COD, VS, pH and alkalinity were less than 5%. The modeling was carried out by applying the calibrated kinetic parameters obtained from the first semi-batch experiment run. The stoichiometric coefficients and input variables were determined from the substrates characterization according to the values presented in Table 4.1. Because the sole source of the inoculum used during the entire study was from a full scale anaerobic digester at an Edmonton municipal WWTP, the initial biomass distributions determined previously were applied as initial values of microbial concentrations in BR2.

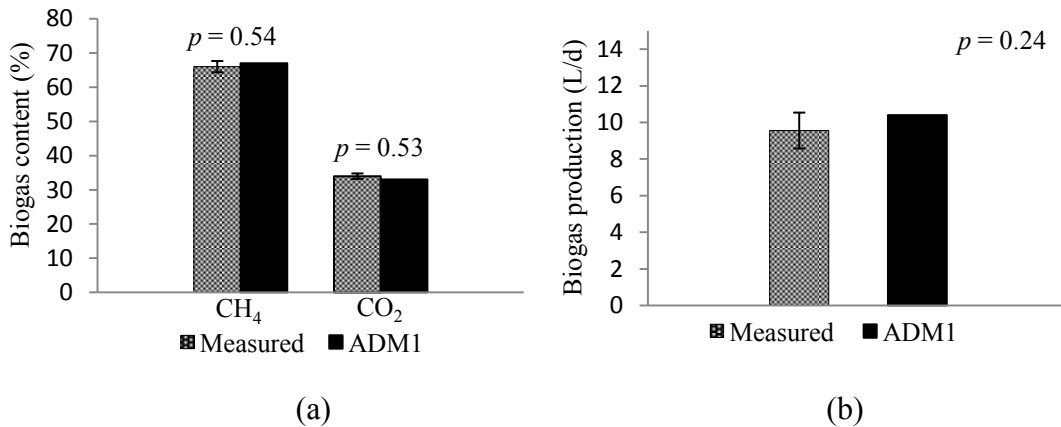
The comparison between measured and modeled parameters of biogas production, biogas composition, pH, total ammonia-N, total alkalinity, VSS, COD and VFA are shown in Figure 4.2. There was no significant difference between the observed and modeled values of biogas production, and the biogas content (CH₄ & CO₂) were also predicted well by the model when compared to the observed values (Figures 4.2 a and b, respectively). As can be seen from Figures 4.2 (c, d and e) the model was able to well predict the pH, total ammonium nitrogen and alkalinity of the reactor.

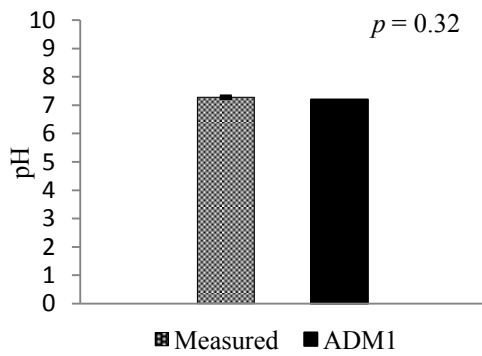
Figures 4.2 (f and g) show that the model also predicted the effluent VSS and COD values well. One sample mean t-tests performed on the data indicated that the measured and modeled parameters were in good agreement as shown by the *p*-values.

The predicted total VFA value was much higher than the experimental measurements. However, the measured acetate, propionate and butyrate were close to the modeled values, while the measured valerate was much lower than

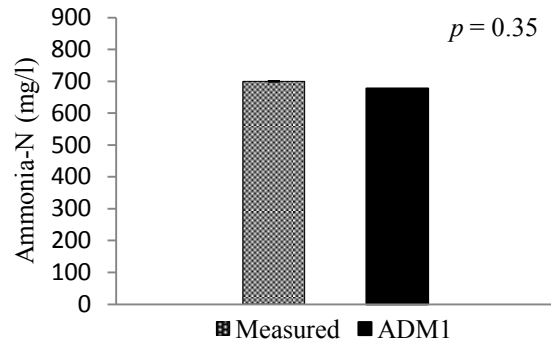
predicted. This inconsistency in measured and predicted VFAs has been noted in previous studies and attributed to the difficulty to accurately predict the VFAs concentrations with ADM1 because of the complex behavior of acidogenesis processes (Blumensaat and Keller, 2005; Chen et al., 2009). This ADM1 limitation can be accentuated when a large portion of lipids is introduced to the system. During anaerobic degradation, lipids are first hydrolyzed to long chain fatty acids (LCFA) at a rapid rate compared to LCFA conversion to acetate and hydrogen (Batstone et al., 2002b). The effects of LCFA accumulation were not included in the ADM1 model because of the complexity of the inhibition phenomena. Owing to the fact that the reactor did not operate truly as a CSTR, the lack of thorough mixing could also have contributed to the lower VFA values observed during the experiment (BR2). Thorough mixing keeps organic materials evenly distributed and improves the mass transfer of substrate to microorganisms.

The low rates of VFA production in the absence of complete mixing was reported by Yuan et al. (2011). Page et al. (2008) also reported the importance of the mixing in biogas and VFA production during anaerobic digestion. The higher predicted valerate concentration may be also because of model overestimation due to the lack of separate kinetic rates for butyric and valeric acids in ADM1. Consequently, these limitations in the model and experiment have led to the observed discrepancy between measured and predicted VFAs results.

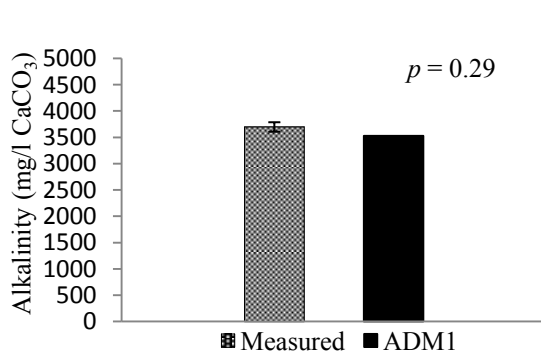




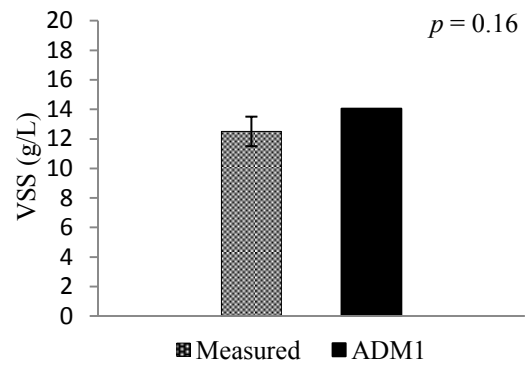
(c)



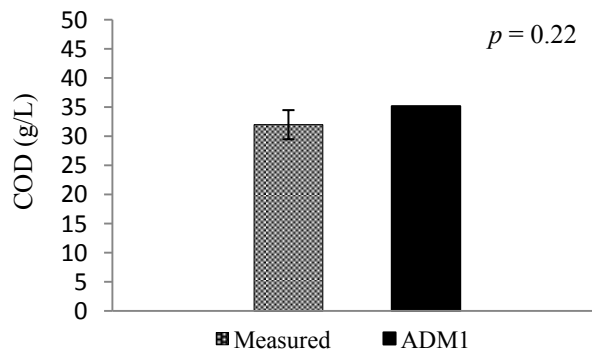
(d)



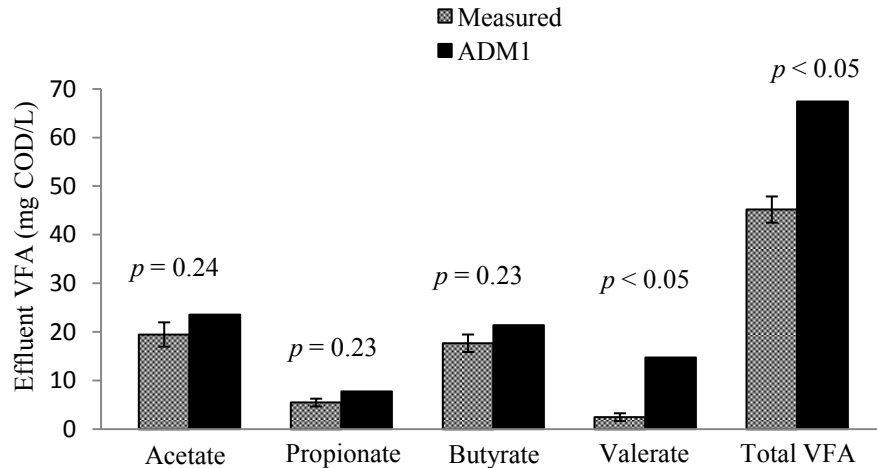
(e)



(f)



(g)



(h)

Figure 4.2. Comparison of measured and ADM1 predictions of; (a) biogas production, (b) biogas composition, (c) pH, (d) ammonia-N, (e) total alkalinity, (f) volatile suspended solids, (g) effluent COD, and (h) volatile fatty acids at steady-state anaerobic co-digestion of GTW and MWS.

4.3.4.2. Pilot-Scale Experiment

A data set collected from a previous pilot-scale study (Razaviarani et al. 2013b) was used to evaluate the model validity. This 1200 L working volume digester was operated in the mesophilic temperature range at a 20 day SRT. The proportion of GTW in its feed was increased in steps throughout the 155 days of operation. The data set used for modeling was collected over the final 10 days of the “190% COD loading” step during which the COD loading due to GTW was 90% of that due to MWS in the feed mixture. It is important to note that the substrates (MWS and GTW) and inoculum used in the pilot-scale study were obtained from the same sources but at different times from those used in the current study.

The optimized initial biomass compositions along with the adjusted kinetic parameters obtained above were implemented without change. The stoichiometric parameters were calculated based on the influent substrate characteristics reported by Razaviarani et al. (2013b) at the “190% COD loading”. Because the substrate

distribution between carbohydrates, lipids and proteins was not directly quantified during the pilot-scale study, the model parameters were estimated accordingly. As reported in the literature, the fractions of composite biodegradable of MWS vary in a limited range of 0.53 to 0.66 (Astals et al. 2013; De Gracia et al. 2011).

Therefore, considering the proportionality of a 3:1 (v/v) blend of primary sludge to waste activated sludge in the MWS used at the pilot-scale experiment and the similarity of the MWS characteristics to the composite degradable fraction ($X_{ch}+X_{pr}+X_{li}$) used at lab-scale in this study (Table 4.2), a composite biodegradable fraction of 0.6 was used for the purpose of modeling. This is also in agreement with results reported by Astals et al. (2013) for a similar sludge. The protein fraction of MWS was estimated by multiplying the organic nitrogen (TKN-TAN) by 6.25 according to the method applied by Girault et al. (2012) and calculated its COD value as described before. The fractions of lipids and carbohydrates were split according to the default ratio ($X_{li} = 1.25 X_{ch}$) in the original ADM1 model. The GTW used in the pilot scale study was assumed to be 100% lipids as added to the MWS.

The results shown in Table 4.6 indicate that the calibrated model can reasonably well represent the overall steady-state behavior of the pilot-scale anaerobic co-digestion of MWS and GTW. The one mean t-test conducted on data indicated significant agreement between the measured and predicted parameters as shown by *p*-values given in Table 4.6. The biogas and methane productions were predicted well by the calibrated model; although the COD removal value showed the weakest agreement among the parameters, there is not a significant difference between measured and calibrated values ($p>0.05$). This can be explained simply since this parameter is strongly dependent on the nature, composition and biodegradability of the substrates.

The agreement between measured and predicted values reveals considerable robustness in the model's predictive ability. Factors that differed between the calibration basis and the model's application to pilot-scale co-digestion included the substrate characteristics (biodegradable fractions were estimated due to the lack of measured values from the pilot scale experiment) and the method of

reactor loading. Although the sources of the substrates were the same at pilot- and bench-scale, fresh MWS was collected daily during the pilot-scale study and variation in MWS characteristics can affect reactor performance. In addition, the adjusted kinetic parameters all came from the batch experiment without further optimization concerning the variability in the MWS quality during the pilot-scale experiment. The loading to the pilot-scale reactor was increased in several steps with the addition of GTW COD to the MWS until it reached the “190% loading” level where it was maintained for 30 days. Whereas, the bench-scale reactor (BR2) was operated with a single step from a constant feed of MWS to the “190% loading”. It has been reported in other studies that when biomass is exposed to gradually increasing concentrations of substrate, the microorganisms can adapt more efficiently and perform more actively (Kim and Oh 2011). The ADM1 is inherently unable to predict and consider the effects of biomass adaptation to the substrate loadings. The ability of the model to predict both BR2 and pilot-scale reactor performance quite well suggests that the 60 day period after the single step increase to the “190% loading” allowed the biomass in BR2 to adapt to the changed feed characteristics to the same extent as did the biomass in the pilot-scale digester during the more gradual loading increments.

Table 4.6. Comparison of observed and predicted values from modeling the steady state pilot-scale anaerobic co-digestion of MWS and GTW at a 190% GTW COD loading

Parameter	Unit	Observed	Predicted	<i>p</i> -value
Biogas	m ³ d ⁻¹	1.63	1.57	0.46
CH ₄	m ³ d ⁻¹	1.08	1.06	0.51
pH	---	7.32	7.30	0.66
Alkalinity	mg L ⁻¹ CaCO ₃	3945	3865	0.47
COD _{removal}	%	76	67	0.13

It must be noted that very high GTW loadings can cause LCFA inhibition which is not considered in the original ADM1. Additional work is required to model reactor performance as GTW loadings approach inhibitory levels.

4.4. Conclusions

Anaerobic respirometric analysis along with substrate characterizations was used to calibrate the kinetic parameters of the ADM1 in order to simulate and predict the steady-state anaerobic co-digestion of MWS and GTW. Two separate batch experiments with the different GTW COD loadings and batches of MWS were run at steady-state to calibrate and validate the model. The model predictions regarding biogas production, pH, alkalinity, CH₄ and CO₂ contents, ammonia, VSS and COD were in good agreement with the experimental data. The overall VFA value was overestimated by the model due to the model limitations. Pilot scale co-digestion data obtained from a previous study were also used to investigate range of the model's applicability. The overall results showed good agreement between measured and modeled parameters. Small deviations were observed between predicted and measured biogas and COD values could be attributed to the lack of comprehensive substrate characterization, the difference in the loading mode and biomass acclimatization. The present calibrated model can predict reasonably well the behavior of the similar anaerobic co-digestion systems operating at the steady-state within the examined of GTW COD loadings.

CHAPTER 5. REACTOR PERFORMANCE AND MICROBIAL COMMUNITY DYNAMICS DURING ANAEROBIC CO-DIGESTION OF MUNICIPAL WASTEWATER SLUDGE WITH RESTAURANT GREASE WASTE AT STEADY-STATE AND OVERLOADING STAGES*

5.1. Introduction

Disposal and sustainable management of grease trap waste (GTW) have been a challenge for years due to a variety of operational issues and municipal disposal limitations. GTW is a lipid-rich organic material collected from the waste streams of restaurant and food service establishments. Direct disposal of this waste into the environment is no longer permitted by most municipalities (Long et al., 2012). Anaerobic digestion as a robust alternative technology is widely applied to stabilize municipal wastewater sludge (MWS) and many organic wastes economically and effectively. However, due to some intrinsic limitations of using this technology for the treatment of MWS, various pre-treatments are required to improve its efficiency. GTW anaerobic co-digestion (ACD) with MWS has become a valuable alternative to improve nutrient balance in mixed substrates and enhance buffer capacity, biogas production and reactor performance (Zhu et al., 2011).

Despite all the reported benefits of ACD systems, previous studies have indicated that the performance and stability of such systems are dependent on reactor design as well as many operational and physico-chemical parameters such as substrate characteristics, organic loading rates, temperature, and pH among others (Razaviarani et al., 2013a and 2013b; Zhu et al., 2011). Anaerobic digestion, as a syntrophic biological process, also is reliant on microorganisms' activities via the four major stages of hydrolysis, acidogenesis, acetogenesis and methanogenesis. A deeper understanding and resolution of the linkage between microbial community dynamics and process stability can provide invaluable information to predict the reactor performance. Yet, the microbial dynamics and

* A version of this chapter has been accepted for publication. Razaviarani and Buchanan, *Bioresource Technology* (September 2014).

their interactions still remained uncertain primarily due to the complexity of the microbial activities within the inter-related biological reactions in these systems (Supaphol et al., 2011). Several studies were conducted over the last decade to investigate the microbial population structure in anaerobic digestion of lipid-rich waste (Palatsi et al., 2010; Pereira et al., 2002) with a focus mostly on the LCFA inhibition effects. Nevertheless, to the authors' knowledge, microbial studies linked to reactor performance of the anaerobic co-digestion of GTW with MWS have not yet been conducted.

Among the available microbial fingerprinting techniques, denaturing gradient gel electrophoresis (DGGE) and clone library are the most popular methods used to evaluate the microbial populations (Lee et al., 2010). However, using the DGGE method for investigation of complex microbial populations is intricate due to drawbacks which include the identification of limited bands and co-migration of sequences. Also, the cloning technique and its data analysis are laborious and uneconomical. The development of 454 Pyrosequencing, as a new generation of sequencing techniques, facilitates the investigation of microbial community dynamics in various environments by identifying a larger number of sequences more quickly (Guo et al., 2014).

The objective of this study was to investigate the reactor performance linked the microbial community dynamics of mesophilic ACD of GTW and MWS at (1) steady-state conditions conducted at two different runs with different organic loadings and (2) during reactor overload conditions. For this purpose, physico-chemical analysis along with the Pyrosequencing microbial technique was performed and reactors' stabilities and performance were monitored accordingly with the associated microbial population dynamics.

5.2. Materials and methods

5.2.1. Inoculum and substrates

Municipal wastewater sludge (MWS) consisting of a 4:1 (v/v) mixture of primary sludge (PS) and waste activated sludge (WAS), was collected from Gold

Bar Wastewater Treatment Plant (WWTP) in Edmonton, Alberta, Canada. GTW was received from a local waste collection company in Edmonton, Alberta. During the study, substrates were stored at 4°C until its utilization. The GTW from restaurants and food services has typically some settleable solids which are not degraded during the anaerobic digestion and are remained at the bottom of the reactor. Therefore, before adding the GTW to the MWS, it was kept at the room temperature for few hours and then the top layer was separated from the settleable solids and water layers. Digested effluent from a full-scale mesophilic anaerobic reactor at the Gold Bar WWTP was used as the inoculum (biomass) for the start-up of the reactors. The characteristics of substrates and inoculum were shown in Table 5.1.

Table 5.1. Characteristics of substrates and inoculum

Parameter	^b MWS ₁	^c MWS ₂	GTW	Inoculum
COD (g/L)	75.3	40.9	2697.8	22.9
TS (g/L)	63.9	22.9	776.8	22.3
VS (g/L)	35.7	18.3	776.2	12.2
TSS (g/L)	61.5	19.2	47.7	20.9
VSS (g/L)	34.8	15.6	47.6	11.3
VFA (mg/L)	2982.8	1639.9	^d nm	7.9
TKN (mgN/L)	804	794	nm	2140
TAN (mgN/L)	346	332	nm	755
^a Alkalinity (mg/L)	1850	2000	nm	nm
pH	5.8	5.7	5.0	7.3

^a Alkalinity represented as mg/L CaCO₃; ^b Municipal wastewater sludge used in Stage 1;

^c Municipal wastewater sludge used in Stage 2; ^d Non-measured.

5.2.2. Reactor operation and loading protocol

The experiment was conducted at two separate stages, as shown in Table 5.2, with respect to the collection of MWS at different times from Gold Bar WWTP. At each stage, two identical 10 L (8 L working volume) reactors were mixed by magnetic stirrers and operated at mesophilic temperature range ($37 \pm 0.5^\circ\text{C}$) with solids retention time (SRT) of 20 days. The reactors were sustained at desired temperature (37°C) using heating tapes wrapped around the reactors and the temperatures were controlled and monitored by Type K thermocouples and digital temperature controllers. An insulating jacket was also applied around each reactor to minimize heat loss.

Each reactor was initially filled with 8 L of inoculum and then the reactors' headspace was purged with nitrogen gas. Each day, 0.4 L of digested material was withdrawn from each reactor and replaced with the same volume of substrate to provide a 20 day SRT. Reactor 1 served as a control (C-1) and received only MWS, while reactor 2 was operated as the test digester (T-1) and was fed a mixture of MWS and GTW based on a percentage of the control reactor COD loading. Initially, for the first run of the experiment, C-1 and T-1 received an equal amount of MWS_1 to establish their baseline performance for a period of 30 days (1.5 SRT). When the equivalence of the reactors' performance was established, the COD loading of T-1 reactor was increased with the addition of a known volume of GTW to the MWS_1 to obtain the desired COD loading of 150% relative to the control reactor (C-1). This operating mode was continued for 3 SRT (60 days) to reach the steady-state conditions and then for another 10 day period during which daily sampling was conducted. Similarly, for the second stage, the control (C-2) and test (T-2) reactors were fed with same volume of MWS_2 for 30 days to establish the baseline performance. Then the test reactor (T-2) was fed with a mixture of GTW and MWS_2 to reach 190% of the control reactor (C-2) COD loading. Steady state conditions were achieved after 3 SRTs when coefficients of variation of effluent COD, VSS and methane daily measurements were less than 5%. Thereafter, for a period of 10 days, samples were collected for the subsequent analyses. In order to investigate the reactor's

performance and microbial community response to reactor overloading, GTW addition to T-2 was increased to achieve a COD loading approximately four-fold that of C-2. This operating mode was continued for 3 weeks in the T-2 reactor which hereafter is termed the overload condition. Reactor T-2 is indicated as T-2' when operated under this overload condition. Reactors loading rates during the experiment are shown in Table 5.2.

Table 5.2. Reactor organic loading rates (OLR) and durations

Stage	Reactor	Substrate	Duration (d)	OLR (g COD/L·d)	Relative Loading (%)
1	C-1	MWS ₁	100	3.77	100
	T-1	MWS ₁	30	3.77	100
	T-1	GTW + MWS ₁	70	5.57	150
2	C-2	MWS ₂	121	2.05	100
	T-2	MWS ₂	30	2.05	100
	T-2	GTW + MWS ₂	70	3.84	190
	T-2'	GTW + MWS ₂	21	8.00	400

5.2.3. Physico-chemical analysis

The biogas flow rate from each reactor was quantified by a digital gas flow meter and logged to a lab computer. Agilent 7890A gas chromatograph (GC) was used to measure the CH₄ content in the biogas. The GC was equipped by Agilent GS-Q column and a flame ionization detector (FID). The CO₂ percentage in biogas was intermittently measured using a Fyrite gas analyzer according to the method specified by the manufacturer (Bacharach Inc., 2010).

Chemical oxygen demands (tCOD and sCOD) of substrates and effluents were measured with the close reflux (5220C) method using HACH COD reactor and GENESYS20 spectrophotometer. Total solids (TS), volatile solids (VS), total

suspended solids (TSS) and volatile suspended solids (VSS) were quantified using methods 2540G and 2540D, respectively. Total alkalinity (TA), partial alkalinity (PA) and pH were determined using Thermix stirrer 120S and ACCUMET AB15 Plus pH meter. The titration end points for PA and TA were pH 5.75 and 4.3, respectively according to Standard Method 2320B. All the above analyses were performed according to the standard methods in triplicate (APHA, 2005). For the VFA measurement, the samples were centrifuged at 5000 g for 10 min and then the supernatants were filtered through the 0.45 μ m and 0.2 μ m nylon syringes. Individual volatile fatty acids (acetate, propionate, iso-butyrate, n-butyrate, iso-valerate and n-valerate) in the substrates and digested effluents were analyzed by a Varian 430 gas chromatograph (GC) equipped by Stabilwax-DA capillary column and a flame ionization detector (FID). Total ammonia and TKN were measured by the Biochemical Analytical Service Laboratory staff in the University of Alberta according to the standard methods.

5.2.4. Microbial community analysis

5.2.4.1. Sludge sampling and DNA extraction

The effluent sludge samples were collected from the reactors during the last 10 days of steady-state period operation at each COD loading. Total genomic DNA was extracted from approximately 500 μ L of well-homogenized sample using Fast DNA[®] Spin kit for soil (Biomedical, USA) according to the manufacturer's instructions. The effluent sludge samples were initially centrifuged at 10,000g for 20min, and the supernatant was decanted carefully to obtain the settled biomass for DNA extraction. NanoDrop[®] 2000C spectrophotometer was used to determine the concentrations, quality and integrity of the extracted DNA. Extracted DNAs were stored at -20°C until submitted to the microbiology lab for the pyrosequencing analysis.

5.2.4.2. Pyrosequencing analysis

The 16S rRNA genes were amplified using bar-coded universal bacterial and archaeal primers for each sample. The primer sequences are as follows; bacterial universal (27F: AGR GTT TGA TCM TGG CTC AG, 519r: GTN TTA CNG CGG CKG CTG) and archaeal universal (349F: GYG CAS CAG KCG MGA AW, 806r: GGA CTA CVS GGG TAT CTA AT). The PCR reactions were conducted in a single step 30 cycle PCR using HotStarTaq Plus Master Mix Kit (Qiagen, Valencia, CA) under following conditions: initial denaturation at 94°C for 3 min, followed by 28 cycles of 94°C for 30s; annealing at 53°C for 40s and elongation at 72°C for 1 min; after which a final elongation step at 72°C for 5 min was performed. All the amplified 16S rRNA from different samples was mixed in equal concentrations and purified using Agencourt Ampure beads (Agencourt Bioscience Corporation, MA, USA). All samples were subjected to pyrosequencing using Roche 454 FLX Titanium instruments and reagents according to the manufacture's guidelines. The nucleotide sequence reads were sorted out using a proprietary analysis pipeline. Initially, the barcode sequences shorter than 200bp, non-16S rRNA sequences and sequences with homo-polymer runs exceeding 6bp were removed from barcode sorted sequences. Then, sequences were de-noised and chimera sequences of selected reads were also removed. Operational taxonomic units (OTUs) of each sequence were identified after removal of singleton sequences, clustering at 3% divergence (97% similarity). Final OTUs were taxonomically classified using BLAST and database derived from GreenGenes, RDP11 and NCBI (DeSantis et al., 2006) and compiled into each taxonomic level into both "count" and "percentage" datasets. The count dataset contains the actual number of sequences while the percentage dataset defined as the ratio of number of assigned sequence reads of specific taxon divided by the number of total sequence reads.

5.2.5. Statistical analysis

The correlation between microbial communities (bacteria and archaea) and reactors' performance and stability parameters were determined by the canonical correspondence analysis (CCA) using the XLSTAT software version 2014.

5.3. Results and discussion

5.3.1. Process stability and reactor performance

The reactors operated in two stages were carried out in different OLRs (Table 5.2) and the obtained experimental results are shown in Table 5.3. The methane yield per unit VS applied increased with increasing the GTW COD addition to the test reactors T-1 and T-2 relative to the control reactors C-1 and C-2, respectively until a reduction in methane yield was observed in T-2 at the 8.0 gCOD/L.d loading (the overloaded condition). The cause of this reduction was investigated by monitoring the critical parameters including pH, VFA and alkalinity. As shown in Table 5.3, during the experiment, the pH remained practically constant with values ranging between 7.25 and 7.33 in the reactors. Yet at the overloaded condition, a reduction in the pH value was observed. In the same way, the VFA remained low during the experiment until a sudden increase was observed during the overloaded condition. The pH reduction and VFA accumulation was associated with a marked reduction in biogas production and methane yield as well as decreased COD and VS removals.

The VFA/alkalinity ratio is a reliable indicator of process stability with the process being stable when this ratio is less than 0.3 to 0.4 (Rincón et al., 2008). As can be easily calculated from Table 5.3, this ratio was well below the limit range during the experiment until the overloaded condition in reactor T-2. At this loading, a substantial increase in the VFA/alkalinity ratio to the value of 0.6 was observed. Furthermore, acetate and propionate were the major fermentation products consisting of 56% and 27% of the total VFA, respectively at this loading. However, low concentrations of acetate in reactors T-1 and T-2 coincided with increased biogas production and methane yield compared to the control reactors prior to the T-2 overloaded condition. This could be possibly as a

result of good acclimation of microbial populations, particularly acetoclastic methanogens, to the addition of GTW to the reactors. GTW addition at the 150% and 190% COD relative loadings to T-1 and T-2 resulted in 65% and 120% increases in biogas production relative to C-1 and C-2, respectively. The relative loadings also resulted in 47% and 85% increases in the methane yield relative to the C-1 and C-2 reactors, respectively. Yet, as shown in Table 5.3, when the relative loading was increased to 400% in T-2, its biogas production and methane yield decreased by 48% and 80%, respectively compared to that observed during the previous 190% relative loading. It is noted that under this overloaded condition the non-acetate VFAs also increased considerably compared to the other loading levels which may suggest a reduction in the syntrophic acetogenic populations.

Table 5.3. Reactors' stability and performance parameters at different loadings

Parameters	Stage 1		Stage 2		
	C-1	T-1	C-2	T-2	T-2'
Reactor	C-1	T-1	C-2	T-2	T-2'
Loading (g COD/L·d)	3.77	5.57	2.05	3.84	8.00
pH	7.30	7.28	7.33	7.25	6.2
VFA (mg/L)	39.5	26.7	54	9.5	1200
Acetic ac.(mg/L)	21.7	15.2	33.8	8.5	677
Propionic ac.(mg/L)	7.0	3.1	4.4	1.0	324
Butyric ac.(mg/L)	22.2	10.4	6.4	¹ nd	90.4
Valeric ac.(mg/L)	4.5	1.9	9.5	nd	108.6
Alkalinity (mg/L)	4060	3930	4180	3780	2590
COD (g/L)	43.5	58.0	24.0	30.0	110.0
VS (g/L)	17.5	17.0	9.7	10.0	35.0
Biogas production (L/d)	8.2	13.5	4.5	10.0	5.2
Methane yield (LCH ₄ /gVS _{added})	0.34	0.50	0.33	0.61	0.12

¹ Not detected

5.3.2. Methanogenic community structure of the ACD

The methanogenic community is generally less diverse than that of the bacterial community and can occupy a limited ecological niche in anaerobic reactors. The type and origin of inoculum and substrate along with the environmental conditions can have considerable effects on the archaeal distribution (Leclerc et al., 2004). As shown in Table 5.4, the majority of archaeal 16S rRNA gene sequences are assigned to the orders *Methanomicrobiales*, *Methanosarcinales* and *Methanobacteriales*. The sequence distributions at the family and class levels are shown in Figure 5.1. Typically, methanogens are categorized as either acetoclastic or hydrogenotrophic according to the substrate they utilize. Acetoclastic methanogens utilize acetate to produce methane while hydrogenotrophic methanogens consume CO₂ and H₂ to produce methane.

Start-up is a critical step in the operation of an anaerobic digester and is highly dependent on the microbial source, the size of the inoculum and the initial operation mode (Griffin et al., 1998). The archaeal populations in the inoculum used as seed throughout the experiment were found to be predominantly of the *Methanosarcinales* order. Genus *Methanosaeta* sequences were present in the greatest relative abundance (2619 sequences, 78% of total archaeal sequences), followed by *Methanomicrobium* (262, 8%), *Methanosarcina* (190, 6%), *Methanospirillum* (168, 5%) and *Methanobacterium* (105, 3%). Therefore, 84% of the sequences obtained from the inoculum were of acetoclastic methanogens of genera *Methanosaeta* and *Methanosarcina*. McMahon et al. (2004) observed that anaerobic digesters with high levels of archaea of which *Methanosaeta* was the dominant acetoclastic methanogen started up well, whereas those having low levels of archaea in which the dominant methanogens were *Methanosarcina* and *Methanobacteriaceae* experienced problems at start-up. The spectrum of sequence abundance in the inoculum used in the current study indicates that the seed was collected from a stable anaerobic digester where the sequences belonging to acetoclastic methanogens were over 5-fold more abundant than those of hydrogenotrophic methanogens.

Table 5.4. Relative abundance of phylogenetic groups of archaeal in reactors

Reactor		C-1	T-1	C-2	T-2	T-2'	
% Loading		100	150	100	190	400	
^a % of total archaeal sequence reads							
Class	Genus (similarity %)	Stage 1		Stage 2		^b PF	
<i>Methanomicrobia</i>	<i>Methanomicrobium (97)</i>	42.0	24.4	41.1	18.0	28.3	^c H
	<i>Methanospirillum (99)</i>	2.1	1.5	1.4	4.3	5.3	H
	<i>Methanoculleus (99)</i>	3.5	0.0	3.2	2.9	1.0	H
	<i>Methanosarcina (99)</i>	4.7	7.6	3.7	2.9	22.1	^d A/H
	<i>Methanosaeta (99)</i>	43.9	59.6	47.8	68.5	34.8	A
<i>Methanobacteria</i>	<i>Methanobacterium (97)</i>	1.5	2.5	1.4	1.8	2.2	H
	<i>Methanosphaera (99)</i>	2.1	1.3	0.0	1.5	2.6	H
	<i>Methanobrevibacter(99)</i>	0.2	2.9	1.4	0.0	2.4	H
<i>Other</i>		0.0	0.2	0.0	0.1	1.3	

Phylum; *Euryarchaeota*; ^a The relative abundance of taxon defined as the number of sequences divided by the total number of sequence per sample; ^b Putative function; ^c Hydrogenotrophic methanogens, ^d Acetoclastic methanogens.

As shown in Figure 5.1, regardless of the different batches of MWS (Table 5.1) fed into the control reactors (C-1) and (C-2) during Stages 1 and 2, the proportion of acetoclastic (*Methanosarcinales*) sequences was approximately the same as that of hydrogenotrophic (*Methanomicrobiales* and *Methanobacteriales*) methanogens in these reactors. The sequence numbers of archaeal phylogenetic groups during each operating condition are shown in Table C-1.2. The proportion of acetoclastic methanogens increased when COD loading was increased to the test reactors (T-1 and T-2). Acetoclastic methanogens have been found to predominate under stable operating conditions where the molecular hydrogen

concentration is low (Kim et al., 2014). *Methanosaeta* is the dominant acetoclastic methanogen at low acetate concentrations under stable operating conditions. This is in agreement with the parameter values listed in Table 5.3 for the T-1 and T-2 operating conditions.

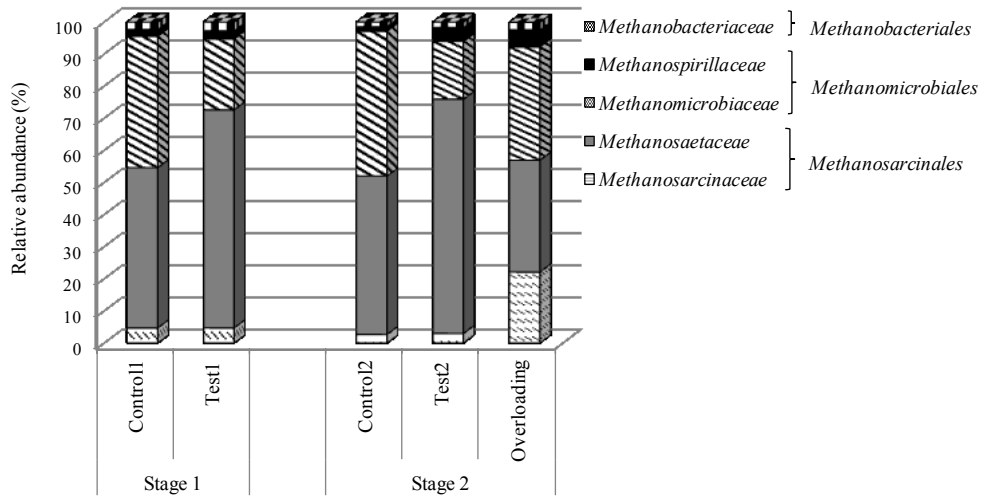


Figure 5.1. Distribution of family level of archaeal community categorized in brackets for order level

During Stage 1, the 150% relative COD loading to reactor T-1 resulted in only a 3% decrease in the total number of archaeal sequences compared to the C-1 reactor (see Table C-1.1). Although the archaeal community in reactor C-1 was distributed equally between hydrogenotrophic and acetoclastic methanogens, 67% of the archaeal sequences in T-1 consisted of acetoclastic methanogens, predominantly of the family *Methanosaetaceae* (Figure 5.1). Therefore, the 47% increase in methane yield in T-1 compared to the C-1 (see Table 5.3) was accompanied by a 35% increase in the relative abundance of acetoclastic methanogens and a 30% decrease in acetate concentration. Typically, over 70% of methane production is carried out by this group of archaea under stable reactor conditions (Kundu et al., 2014). The genus *Methanosaeta* has a lower half saturation coefficient than does the genus *Methanosarcina* (Conklin et al., 2006;

McMahon et al., 2004; among others). Therefore, *Methanosaeta* is dominant in the presence of a low acetate concentration. Hori et al. (2006) reported that the genus *Methanosaeta* grows more rapidly than *Methanosarcina* at acetate concentrations lower than 1mM while the genus *Methanosarcina* are the predominant acetoclastic methanogens at acetate concentrations higher than 1mM. As shown in Table 5.3, the acetate concentration in the T-1 reactor was well below the 1 mM threshold where the genus *Methanosaeta* would predominate over the genus *Methanosarcina*.

During Stage 2, 3592 archaeal sequences were obtained for reactor T-1 during its 190% relative COD loading, whereas the control C-2 reactor yielded 2330 archaeal sequences. This represents a 54% increase in T-2 archaeal sequences relative to C-2. Approximately 76% of the archaeal sequences from T-2 belonged to acetoclastic methanogens with relative abundances of 69% and 3% for *Methanosaeta* and *Methanosarcina*, respectively. This is consistent with *Methanosaeta* outcompeting *Methanosarcina* in the presence of a low acetate concentration (see Table 5.3). The increase in the relative abundance of acetoclastic methanogens was accompanied by 120% and 85% increases in biogas production and methane yield in the T-2 reactor relative to C-2, respectively (see Table 5.3). The predominance of this genus also represents a stable reactor as indicated in previous studies (Ariesyady et al., 2007; Raskin et al., 1994).

The distribution and dynamics of methanogens in the anaerobic co-digestion of lipid-rich materials under mesophilic conditions have not been documented. Martín-González et al. (2011) investigated the thermophilic anaerobic co-digestion of FOG with the organic fraction of municipal solid wastes and observed the genus *Methanosarcina* to be the predominant acetoclastic methanogens in their samples. It should be noted that they did not detect the genus *Methanosaeta* during their investigation. In contrast, the genus *Methanosaeta* represented the largest number of acetoclastic populations in the present study, whereas the relative abundance of *Methanosarcina* sequences remained low during all steady state sampling periods and were only observed to increase in number during the overloading period (Figure 5.1).

As shown in Figure 5.1, the hydrogenotrophic pathway was primarily associated with the family *Methanomicrobiaceae* within the order *Methanomicrobiales* at all loadings. Members of the order *Methanobacteriales* were present throughout the study in all reactors, but their numbers of sequences accounted for only 1.4 to 3% of the total methanogen population. The increase of GTW loading at the 400% relative COD loading (overload condition) resulted in changes in both the acetoclastic and hydrogenotrophic communities as shown in Figure 5.1. The total number of archaeal sequences obtained during the overload condition (reactor T-2') decreased by 7% compared to those obtained from reactor T-2 (the same reactor) during the 190% relative COD loading. Thus, the total number of archaeal sequences changed little despite signs of instability in the reactor such as low pH, high VFA concentrations and reduced biogas production (Table 5.3), among others. The major change was in the distribution of the archaeal community. As shown in Figure 5.1, the relative abundance of hydrogenotrophic methanogens increased considerably compared to that at the previous 190% relative COD loading. The relative sequence abundance *Methanomicrobium* within the family *Methanomicrobiaceae* and the order *Methanomicrobiales* increased from 18.0% to 28.3%. This indicates that the community response to the GTW overloading that caused a reduction in the reactor performance was an increase in the activity of hydrogenotrophic methanogens due presumably to an increase in the H₂ partial pressure. Padmasiri et al. (2007) also observed similar behavior of hydrogenotrophic methanogens during decreased reactor performance. Kim et al. (2014) reported *Methanoculleus bourgensis* of the order *Methanomicrobiales* to become the predominant methanogen as the reactor used in their study approached unstable conditions.

High H₂ partial pressure in an anaerobic digester can hamper the syntrophic relationship between its microbial communities (Kundu et al., 2014). This can cause the dominance of hydrogenotrophic populations such as *Methanobacteriales* and *Methanomicrobiales* over acetoclastic methanogens. Although the hydrogenotrophic communities did not become predominant at the 400% relative COD loading in terms of sequence abundance, the proportion of

hydrogenotrophic methanogens did increase to approximately 42% of the total archaeal sequences. If *Methanosarcina* which can produce methane using either H₂/CO₂, acetate or methyl are included

The *Methanosarcina* sequences increased to 22% of the total number of archaeal sequences during the overloading condition from 2.9% at the previous 190% relative COD loading (Table 5.4). In contrast, the relative abundance of *Methanosaeta* sequences decreased by approximately 50% under the overloading conditions. This can be attributed primarily to their growth kinetics as discussed previously, which allows *Methanosarcina* to outcompete *Methanosaeta* in the presence of high acetate concentrations.

5.3.3. Bacterial community structure of the ACD

The bacterial 16S rRNA gene sequence at different taxonomic levels and loading percentages are summarized in Figure 5.2 and Table 5.5. The total sequence abundance of bacteria in the inoculum sample was 9,139 (see Table C-1.1). This is almost three times the total sequence abundance of the archaeal population in the inoculum sample. The genus *Candidatus Cloacamonas* was the dominant bacterial community in the inoculum as well as in the reactors at all loading rates (Tables C-1.3 and C-1.4). *Candidatus Cloacamonas ssp.* are syntrophic fermentation bacteria found in a number of anaerobic digesters and were recently categorized under the phylum *Spirochaetes* (Pelletier et al., 2008). *Spirochaetes* are gram-negative bacteria with a distinctive spiral shape and are able to ferment carbohydrates and amino acids into mainly acetate, H₂ and CO₂ in anaerobic digesters (Lee et al. 2013).

During the two 100% MWS loadings stages, as shown in Figure 5.2, the bacterial distributions remained almost constant in the control reactors regardless of the different batches of sludge used. However, compared to the inoculum, the total number of bacterial sequences was reduced by 10% and 41% in control reactors C-1 and C-2, respectively (Table C-1.1). These changes could be attributed to several factors including alteration and availability of substrates. In these reactors the bacterial sequences were predominantly affiliated with the

genus *Candidatus Cloacamonas* within the phylum *Spirochaetes* with the relative abundance of 82.0% and 82.2% in C-1 and C-2, respectively. The number of sequences in the phylum *Actinobacteria* in inoculum was very low, but was slightly increased in the control reactors possibly due to the variation of MWS and feeding mode in the bench-scale reactors.

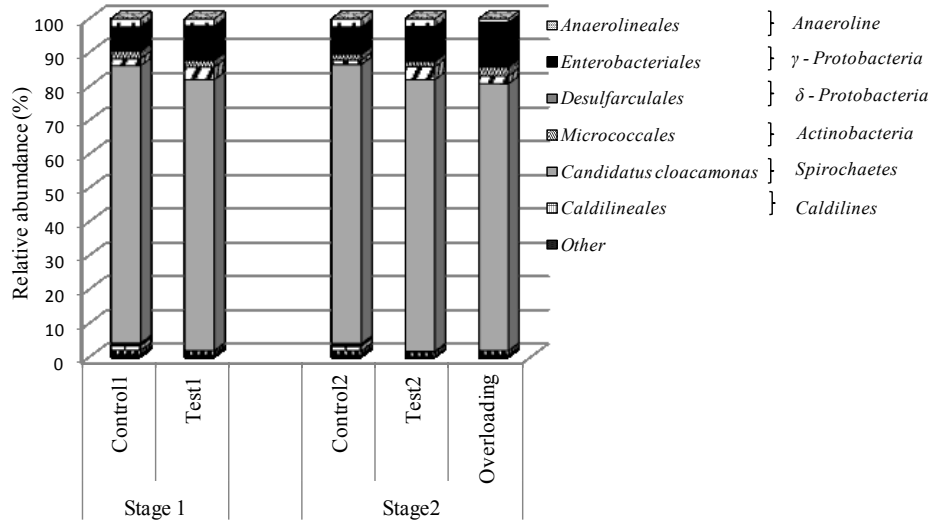


Figure 5.2. Distribution of order level of bacterial community categorized in brackets for class level

The total number of bacterial sequences was reduced by 33% in reactor T-1 at the 150% relative COD loading, compared to that of the C-1 reactor (see the Table C-1.1 in the Appendix) while the distribution of the bacterial community changed very little, as shown in Table 5.5. Sequences from four phyla were identified in the reactors as shown in Table 5.5. The dominant sequence identified in reactor T-1 was associated with the phylum *Spirochaetes* (80.4%), followed by the phyla *Proteobacteria* (12.1%), *Actinobacteria* (1.5%) and *Chloroflexi* (2.1%). While the genus *Candidatus Cloacamonas* remained the dominant community in reactor T-1, the sequence abundance of the genus *Esherichia* within the phylum *Proteobacteria* increased by 12% compared to the C-1 reactor (see Table C-1.4). In addition, although the phylum *Chloroflexi* was a minor population in the control reactor, C-1, with the addition of GTW, the sequence abundance of

phylum *Chloroflexi* decreased by 68% compared to the C-1 reactor and the affiliated genus *Caldilinea* was not measurable (see Table C-1.4).

Table 5.5. Relative abundance of phylogenetic groups of bacteria in reactors

Reactor		C-1	T-1	C-2	T-2	T-2'	
% Loading		100	150	100	190	400	
		^a % of total bacterial sequence reads					^b PF
Phylum	Genus (similarity %)	Stage 1		Stage 2			
<i>Spirochaetes</i>	<i>Spaerochaeta</i> (95)	0.4	0.4	0.3	0.3	0.0	U
	Candidatus <i>Cloacamonas</i> (99)	82.0	80.0	82.2	80.3	78.9	S
<i>Actinobacteria</i>	<i>Demequina</i> (99)	0.2	0.0	0.3	0.0	0.0	F
	<i>Dermatophilus</i> (92)	2.0	1.5	1.2	1.6	1.4	H
<i>Proteobacteria</i>	<i>Desulfarculus</i> (93)	2.2	2.0	1.7	1.5	2.6	A
	<i>Esherichia</i> (97)	7.2	12.1	8.1	12.5	14.2	A
<i>Chloroflexi</i>	<i>Anaerolinea</i> (95)	2.3	2.1	2.4	2.3	1.0	F
	<i>Caldilinea</i> (94)	2.1	0.0	2.3	0.0	0.0	F
<i>Other</i>		1.6	1.9	1.5	1.5	1.9	

^a The relative abundance of taxon defined as the number of sequences divided by the total number of sequence per sample; ^b Putative function; U: unknown, S: syntrophic, F: fermentative, H: hydrolysis, A: acidogenesis.

During Stage 2, the 190% relative COD loading to the T-2 reactor resulted in little change to the total sequence abundance of bacteria compared to the C-2 reactor (Table C-1.1). Despite the addition of GTW to reactor T-2, the relative

distribution of bacterial strains remained similar to that in the control reactor (Table 5.5) with the greatest changes in relative sequence abundance being within the genera *Esherichia* (+54%) and *Caldilinea* (-100%), which carry out acidogenesis and fermentation, respectively. As shown in Figure 5.2 and Table 5.5, the genus *Candidatus Cloacamonas* remained the prevailing bacterial community with a relative sequence abundance of 80.3% in the T-2 reactor at the 190% relative COD loading.

At the 400% relative COD loading, the total sequence abundance of bacterial populations decreased by approximately 18% in the T-2' reactor compared to the control reactor (C-2) and to reactor T-2 at the 190% relative COD loading (Table C-1.1). The larger changes in relative sequence abundances shown in Table 5.5 at the highest relative COD loading were in the genera *Esherichia* (+20%) and *Anaerolinea* (-57%), compared to those in reactor T-2. The genus *Caldilinea* remained undetectable in reactor T-2'. As shown in Figure 5.2, the genus *Candidatus Cloacamonas* within the phylum *Spirochaetes* constituted the dominant percentage of the total bacterial sequences under all loading conditions. The abundance and distribution of *Spirochaetes* in anaerobic digesters have been rarely investigated because of the inadequate knowledge of this phylum. The relative sequence abundance of phylum *Proteobacteria*, as the second largest population found in this study at all loadings, increased by 71% in reactor T-2' under the overloaded conditions compared to that in C-2. Chen et al. (2008) reported that even low concentrations of long chain fatty acids (LCFA) from the degradation of lipid-rich materials could be detrimental to anaerobes, particularly for the gram-positive bacteria. The phylum *Actinobacteria* was the only gram-positive bacteria community found in this study. However, the relative abundance of genera in this phylum was low in all reactors. The affiliated genus *Demequina* completely disappeared after the GTW was added even during the “safe” loadings of the T-1 and T-2 reactors. However, the response of the genus *Dermatophilus* was not as clear (Table 5.5). LCFA inhibition was not investigated in this study, however because GTW is converted to LCFA before the breakdown to VFA compounds, the decrease in the phylum *Actinobacteria* after the addition of GTW

could be attributed to the existence of such intermediate lipid-degradation products. It should be noted that, as Chen et al. (2008) indicated, because methanogens' cell wall resembles that of gram-positive bacteria they are more vulnerable to the LCFA concentration than is the bacterial community.

5.3.4. Correlation between environmental parameters and microbial dynamics

The correlation between the microbial (bacterial and archaeal) community and the reactor's performance and stability parameters was investigated by performing a Canonical Correspondence Analysis (CCA). The CCA evidenced significant correlations ($p < 0.0001$) between the microbial communities (major genera of bacterial and archaeal communities), and the environmental variables pH, alkalinity and VFA concentration. A triplot of the CCA results is shown in Figure 5.3, and a review of its interpretation is given in Appendix B. As shown in Figure 5.3, both ordination axes combined explained 96.7% of bacterial and archaeal community variations, indicating that these environmental variables were major factors shaping the microbial community dynamics. The significance analysis of the environmental variables revealed that VFA accounted for much of the difference in both bacterial and archaeal community distributions arising from the addition of GTW to the feed. The VFA variable was negatively associated with the pH and alkalinity variables, as would be expected.

The archaeal and bacterial genera shown in Figure 5.3 represent approximately 90% and 95% of total sequence abundance of archaea and bacteria listed in Tables 5.4 and 5.5, respectively. The genus *Candidatus Cloacamonas*, represented as B4 in Figure 5.3, is located near the origin of the plot. This location indicates that the number of *Candidatus Cloacamonas* sequences had little response to changes in the environmental variables during the experiment. This is possibly due to its syntrophic characteristics. The location of *Esherichia* (B2) indicates that this genus was more abundant in test digesters than in the controls and was somewhat more abundant at higher than average VFA concentration and lower than average pH and alkalinity. In fact the abundance of *Esherichia*

sequences had the lowest coefficient of variation of any bacterial genus and was present in greatest abundance at low to moderate VFA concentration. Therefore, the variation in *Esheria* sequence abundance may be due to random error or to an environmental variable not considered during the analysis. Additionally, Ter Braak and Verdonshot (1995) indicate that inferences drawn from a triplot are not always accurate because the plot represents multi-dimensional relationships in only two dimensions.

The sequence abundance of *Anaerolinea* (B1) was greater at low VFA concentrations and higher pH and alkalinity. The genus *Dermatophilus* (B3) represented at most 3% of the total sequences under any loading condition and showed very little response to any of the environmental factors considered (Tables 5.5 and C-1.4).

In terms of the reactor loading conditions (sites), Figure 5.3 shows that the environmental conditions in reactors T-1 and T-2 were similar, as were those in C-1 and C-2. However, the environmental conditions in reactor T-2' were characterized by higher than average VFA and lower than average pH and alkalinity. The number of genus *Esheria* (B2) sequences was highest during the moderate GTW loadings (T-1 and T-2), but this genus reached its greatest relative sequence abundance during the overloading condition (T-2').

As shown in Figure 5.3, it is apparent that the archaeal genera points are not as closely clustered around the origin as are those of the bacterial community, indicating a generally greater response to changes in environmental factors than was the case for the bacterial genera. This was expected because methanogenic communities are generally more sensitive to changes in environmental conditions, including pH, alkalinity and VFA concentration.

With respect to the archaeal community, *Methanomicrobium* (A1) and *Methanosaeta* (A3) were the dominant methanogens throughout the study, with the genus *Methanosaeta* being particularly abundant in reactors T-1 and T-2. As shown in Figure 5.3, the sequence abundance of *Methanosaeta* was greatest under average values of the environmental factors considered. This suggests that these acetoclastic methanogens were important populations during stable operation and

increased in sequence diversity with the addition of GTW at the 150% and 190% relative COD loadings. The numbers of sequences of genus *Methanosarcina* (A2) were greatest at high VFA concentration during the overload condition in T-2. This behavior could be attributed to the higher growth rates of *Methanosarcina* at high acetate concentrations and their ability to produce methane via either the acetoclastic or hydrogenotrophic pathway.

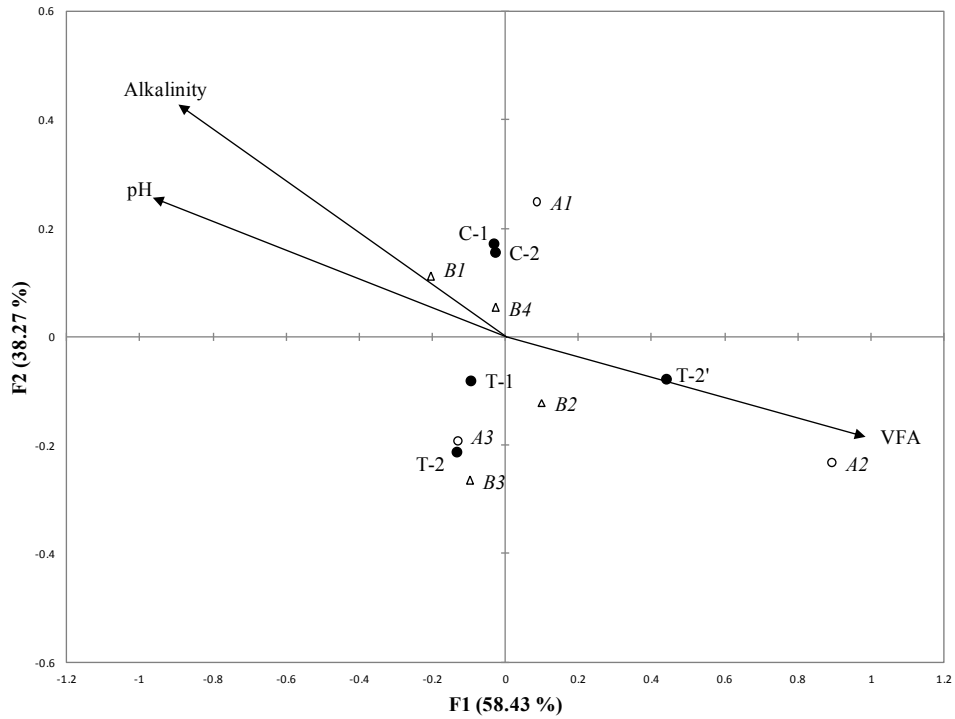


Figure 5.3. Canonical correspondence analysis (CCA) triplot showing the relationship between the relative sequence abundance of the major bacterial and archaeal communities and the environmental variables pH, alkalinity and VFA concentration in the different stages of GTW COD loadings (●). The environmental variables are shown as vectors in the plot. The open triangle symbols (Δ) represent the genera of bacterial populations that include B1: *Anaerolinea*; B2: *Esherichia*; B3: *Dermatophilus*; B4: *Candidatus Cloacamonas*. The open circle symbols (○) represent the genera of archaeal populations that include A1: *Methanomicrobium*; A2: *Methanosarcina*; A3: *Methanosaeta*.

The 50% reduction in *Methanosaeta* sequence abundance during the overload condition in reactor T-2' compared to that in the same reactor (T-2) at the 190% relative COD loading was accompanied with an 80% reduction in methane yield during the overloading condition compared to that at the 190% relative COD loading in T-2. Although the sequence abundance of *Methanosarcina* and *Methanomicrobium* increased considerably during overloading, these populations could not compensate for the loss of *Methanosaeta* sequences in methane production within the 21 days of reactor operation at the 400% relative COD loading. The triplot shown in Figure 5.3 indicates that the genus *Methanomicrobium* (A1) was most abundant under average environmental conditions and that sequence numbers were similar under all loading conditions.

Recently, a similar archaeal composition was reported during the mesophilic anaerobic co-digestion of organic wastes (Ike et al., 2010; Supaphol et al., 2011). This suggests that co-digestion of mixed organic wastes can promote a superior diversity of nutrients which can result in a broader diversity of microbial populations and greater reactor stability and performance. It should be noted that, understanding the role of syntrophic bacteria such as *Candidatus Cloacamonas* within the phylum *Spirochaetes* and their interactions with methanogens is key to the understanding of reactor performance and should be investigated further, particularly in the anaerobic co-digestion of mixed-substrates.

5.4. Conclusions

Mesophilic co-digestion of GTW with MWS under stable operating conditions led to enhanced biogas production and methane yield with acetoclastic methanogens (*Methanosaeta*) being the dominant population in terms of genus diversity. Increasing the proportion of GTW in digester feed to 300% COD loading relative to the MWS in the feed resulted in a decline in pH, alkalinity, biogas production and methane yield and an increase in VFA concentration. At this loading the absolute and relative sequence abundance of acetoclastic methanogens was reduced while the sequence abundance of hydrogenotrophic methanogens increased. The genus *Candidatus Cloacamonas* of the phylum

Spirochaetes remained dominant at all digester loadings throughout the study. The CCA triplot indicated that VFA concentration accounted for much of the major shifts in microbial sequence abundance.

CHAPTER 6. PILOT-SCALE ANAEROBIC CO-DIGESTION OF MUNICIPAL WASTEWATER SLUDGE WITH BIODIESEL WASTE GLYCERIN*

6.1. Introduction

Anaerobic digestion is a widely used process for the degradation and stabilization of organic waste due to its environmental and economical benefits. Direct anaerobic treatment of many industrial organic wastes is not practical because the wastes do not provide sufficient buffering capacity or nutrients to ensure stable operation, particularly at small scales. Conversely, municipal wastewater sludge is a reliable source of micro-nutrients and many municipal facilities do not employ all of the capacity available in on-site anaerobic sludge digesters (Schwarzenbeck et al. 2008). Therefore, co-digestion of industrial organic waste with municipal wastewater sludge allows beneficial use of materials that cannot be digested alone.

The biodiesel production industry generates a large amount of waste glycerin representing about 10% (wt) of the initial raw material (Chi et al., 2007). Annual waste glycerin generation increased rapidly after 2006 and is expected to reach 8.8 billion kg annually by 2015 (Ayoub and Abdullah, 2012). This has led to a surplus of waste glycerin and a dramatic decline in crude glycerin price (Yazdani and Gonzalez, 2007). The lack of an economical purification process for waste glycerin (Slinn et al., 2008), together with the variability of its quality have made the marketing of waste glycerin uneconomical (Robra et al., 2010). Therefore, beneficial disposal methods for waste glycerin have been investigated (Ayoub and Abdullah, 2012; Gu and Jerome, 2010).

Several studies have evaluated the benefits of co-digesting waste glycerin with organic wastes such as municipal solid waste (Fountoulakis et al., 2010), manure and energy crops (Holm-Nielsen et al., 2008) and pig manure (Amon et

* A version of this chapter has been published. Razaviarani et al. *Bioresource Technology*, 133(2013) 206-212.

al., 2006; Astals et al., 2012). Most studies have been conducted at lab-scale. Yet, pilot-scale studies which more closely resemble full scale operating conditions are required to assess several operational parameters.

The objective of this study was to identify the upper loading limit of biodiesel glycerin waste (BGW) during its co-digestion with municipal wastewater sludge (MWS) under mesophilic conditions at pilot scale. Volatile solids destruction, total COD reduction, biogas generation, and methane production were also measured at several organic loading rates.

6.2. Materials and Methods

6.2.1. Substrates

Municipal wastewater sludge (MWS) consisting of a 3:1 (v/v) mixture of primary treatment scum and sludge (PS) and thickened waste activated sludge (TWAS), was obtained from a Wastewater Treatment Plant (WWTP) in Edmonton, Alberta, Canada. Biodiesel waste glycerin from canola oil biodiesel production was collected from a biorefinery in Calgary, Alberta, Canada. Digested sludge from a full scale mesophilic anaerobic digester WWTP was used as the inoculum (seed) for the start-up of the digesters. The characteristics of MWS and BGW varied somewhat during the study as shown in Table 6.1. The BGW is an organic readily digestible material which had a high pH and alkalinity compared to the MWS. The SCOD/COD ratio indicates the level of the feed solubilization which directly affects the biogas production (Tang et al., 2010). This ratio was approximately 0.98 in the BGW which was almost 14 times higher than that of the MWS.

Table 6.1. Characteristics of municipal wastewater sludge (MWS) and biodiesel waste glycerin (BGW)

Feed	Parameters	Nominal COD loading (%)			
		100	130	150	180
MWS	COD (g/L)	34.1±4.5 ^a	37.83±2.32	31.06±1.06	31.50±1.35
	SCOD (g/L)	N/A ^b	2.75±0.25	2.29±0.60	1.60±0.07
	TS (g/L)	26.5±1.4	23.90±1.33	23.15±1.92	22.10±1.15
	VS (g/L)	20.5±1.3	18.05±1.12	16.18±1.06	16.33±0.87
	TA ^c (mg/L)	1520±8.5	1487±8.0	1506±9.2	1500±8.7
	pH	6.0±0.2	5.65±0.22	5.77±0.29	5.71±0.18
BGW	COD (g/L)	N/A	1830±21.21	1707±24.75	1707±24.75
	SCOD (g/L)	N/A	1790±6.36	1678±4.95	1678±4.95
	TS (g/L)	N/A	488±3.64	484±1.06	484±1.06
	VS (g/L)	N/A	426±2.56	442±5.65	442±5.65
	TA ^c (mg/L)	N/A	9454±11.5	9448±9.3	9448±9.3
	pH	N/A	8.39±0.02	8.33±.035	8.33±0.35

^a Standard deviation;

^b Not applicable;

^c Total alkalinity (TA) represented as mg/L CaCO₃.

6.2.2. Semi-continuous Pilot Digester

Two 1300 L (1200 L active volume) completely mixed digesters housed in a trailer were received from the King County Wastewater Treatment Division in Washington. The trailer pilot plant was transferred to and set up at the Gold Bar WWTP. The continuously stirred tank reactors (CSTR) were operated in the mesophilic temperature range (36±1°C) with a solids retention time (SRT) of 20 days. Each digester was initially fed 1200 L of seed sludge and then 60 L of

digested material was withdrawn and replaced with the same volume of feed each day (7 days/week) to provide a 20 day SRT. The control digester was fed only municipal wastewater sludge (MWS) while the test digester received the same MWS with BGW as a co-substrate. The organic loading rate was determined on the basis of total COD.

Each digester was heated via an external thermal jacket. The digesters' temperatures were monitored by type J thermocouples. A top-mounted three-bladed digester mixer was operated at a nominal shaft speed of 100 rpm in each digester. A data logger collected and logged the digesters' internal temperatures, volumes of biogas produced, and digester active volumes every 5 minutes.

6.2.3. Digester Feed and Organic Loading Rate Protocols

Initially, the digesters received the same amount and type of feed (MWS) in order to establish their baseline performance. This operating mode was continued for 30 days. Subsequently, the COD loading to the test digester was increased with the addition of BGW to the MWS feed to achieve the desired COD loading, while maintaining the 20-day SRT. Each COD loading to the test digester (expressed as a percentage of the control digester's COD loading) was maintained for at least 20 days (Table 6.2). The test digester loading rate was increased progressively by adding greater volumes of BGW to eventually reach the maximum nominal COD loading of 180% relative to the control digester COD loading.

Table 6.2. Organic loading rate (OLR) at various increments

Nominal COD loading (%)	OLR (kgVS/m ³ d)		OLR (kgCOD/m ³ d)	
	Control	Test	Control	Test
100	1.03±0.10 ^a	1.03±0.10	1.71±0.20	1.71±0.20
130	0.90±0.01	1.03±0.01	1.85±0.06	2.34±0.08
150	0.81±0.05	1.04±0.04	1.55±0.06	2.38±0.06
180	0.82±0.04	1.18±0.04	1.58±0.06	2.88±0.11

^a Standard deviation

Each day, a volume of MWS sufficient to meet the line flushing and feeding requirements for both digesters (approximately 70 L for each digester) was obtained from the on-site sludge blend tanks and transferred to a grinder tank where it was thoroughly mixed prior to being transferred to a feed tank (see Fig. 5.1). Before feeding, 60 L of digested sludge were drained from the control digester to its effluent tank. Samples were collected from the feed and the effluent tanks for subsequent analysis. The control digester feed line was flushed with the MWS and 60 L of MWS were then pumped from the feed tank to the control digester to return its active volume of 1200 L. Then, feed tank and control digester feed lines were emptied and flushed with clean water. The volume of MWS in the grinder tank was determined, and a quantity of BGW was added to the grinder tank in order to achieve the required total COD target (130%, 150% or 180% of the control digester feed COD). After thorough mixing, the feed was transferred to the feeding tank. 60 L of digested sludge were drained from the test digester to its effluent tank prior to start feeding. Samples were collected from the feed and effluent tanks for subsequent analysis. The test digester feed line was then flushed with the MWS-BGW mixture and 60 L of the mixture were pumped to the test digester to return its active volume to the 1200 L level. Finally, the test digester feed line and all tanks were emptied and flushed with clean water.

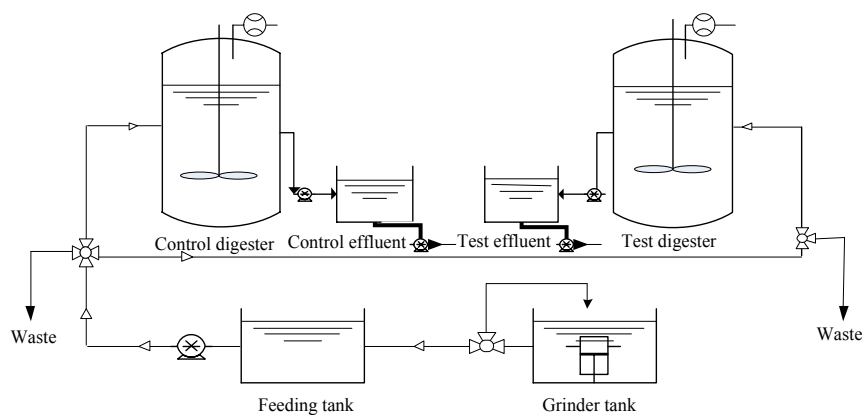


Figure 6.1. Schematic of the pilot scale anaerobic digester setup

6.2.4. Analytical Methods

A Hewlett Packard 5890 series II gas chromatograph (GC) was used to measure the CH₄ and CO₂ contents in the biogas. The GC was equipped by a Hayesep Q column and a thermal conductivity detector (TCD). Total and soluble chemical oxygen demand (COD, SCOD) in influents and effluents were measured with the closed reflux (5220C) method using HACH DR/4000U spectrophotometer and Orion COD125 thermo reactor. Total solids and volatile solids were measured according to standard methods 2540C and 2540E, respectively. Total alkalinity (TA), partial alkalinity (PA) and pH were measured using Thermix stirrer 120S and ACCUMET AB15 Plus pH meter. The titration end point for partial alkalinity was pH 5.75 and that for total alkalinity was pH 4.30 using the 2320B titration method. All the above measurements were quantified according to the standard methods in triplicate (APHA, 2005). Volatile fatty acids (acetate, propionate, iso-butyrate, n-butyrate, iso-valerate and n-valerate) in the digester effluents were quantified by a Dionex, ICS-2500 with N₂ as the carrier gas equipped with a self-regenerating suppressor (CSRS® ultra II, 4mm) and auto sampler AS50 with a 25µl injection volume. 10 mN NaOH solution was used as the eluent at the ambient temperature with a flow rate of 1.2 ml/min. Samples used for the VFA analysis were all centrifuged at 3030 rpm for 5 min and filtered through a 0.22 µm sterile syringe driven filter (Millex®-GV). Sulfate (SO₄²⁺) was measured with the Sulfa Ver 4 method using Sulfa Ver

reagent and HACH DR/4000U spectrophotometer based on an internally developed method.

6.3. Results and Discussions

6.3.1. Baseline Operation

Baseline operation was conducted to achieve steady state in the two digesters and assess the equivalence of their performance. The mean values and standard deviations of the six parameters monitored during this stage are listed in Table 6.3. Paired two tailed t-tests performed on the data indicated that the parameter means were not significantly different for the two digesters as shown by the *p*-values given in Table 6.3. This indicates that an equivalent baseline performance level had been established in the digesters.

Table 6.3. Comparison of digester performance during baseline operation

Parameter	Mean value \pm standard deviation			<i>p</i> -value
	Feed	Control effluent	Test effluent	
TCOD (g/L)	34.1 \pm 4.5 ^a	13.4 \pm 2.7	14.1 \pm 1.1	0.40
VS (g/L)	20.5 \pm 1.3	10.8 \pm 0.4	11.3 \pm 0.4	0.44
Methane production (m ³ /d)	N/A ^b	0.63 \pm 0.1	0.58 \pm 0.1	0.39
pH	6.0 \pm 0.2	7.2 \pm 0.1	7.2 \pm 0.1	0.34
PA (mg CaCO ₃ /L)	N/A	2577 \pm 92	2535 \pm 85	0.27
TA (mg CaCO ₃ /L)	1520 \pm 8.5	3656 \pm 139	3599 \pm 95	0.30

^a Standard deviation;

^b Not applicable.

6.3.2. Reactor Performance

Reactor performance was assessed in terms of COD and VS removal efficiencies and methane production.

6.3.2.1. COD Removal Efficiency

The COD removal efficiency is a measurement of organic waste stabilization. The %COD removals are shown in Fig. 5.2 as are the percentages of the test digester COD loadings due to BGW. At the baseline, the COD removal efficiencies of 61% and 59% were achieved in the control and test digesters, respectively. These values represent mean COD removal rates of 1.04 and 1.00 kg COD/(m³·d) in control and test digesters, respectively. When the test digester COD loading was increased to 130% of the control COD loading its COD removal efficiency increased to 115% of that of the control (Fig. 5.2). The COD removal rates during this loading period were 1.22 kg COD/(m³·d) and 1.88 kg COD/(m³·d) in the control and test digesters, respectively. Taking into account the mean COD loadings of 1.85 kg COD/(m³·d) and 2.34 kg COD/(m³·d) to the control and test digesters, respectively, the COD loading that was not removed and would appear in the effluent was 0.63 kg COD/(m³·d) and 0.46 kg COD/(m³·d) for the control and test digesters respectively, indicating a superior quality of test digester effluent in terms of COD stabilization.

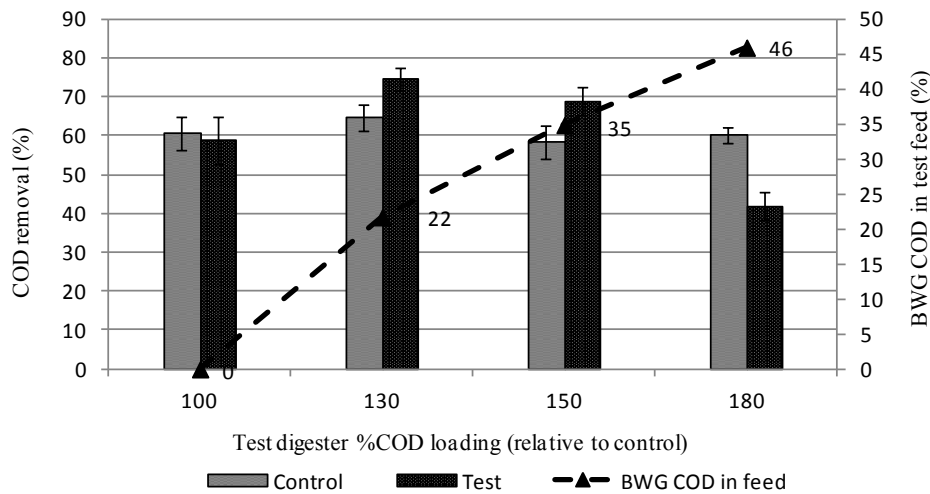


Figure 6.2. COD removal efficiency and BGW COD percentage at various loadings.

At the nominal 150% test digester COD loading relative to the control, COD from BGW represented 35% of its total COD loading (Fig. 5.2). The efficiency of COD removal in the test digester was 1.35 times that of the control digester at this loading. During this period, the COD removal rates in the control and test digesters were 0.93 kg COD/(m³·d) and 1.69 kg COD/(m³·d), respectively. The COD values in the control and test digester effluents were 0.62 kg COD/(m³·d) and 0.69 kg COD/(m³·d), respectively. These results indicate that the increased loading did not adversely affect the test digester effluent quality in terms of COD and used the digester treatment capacity more effectively. The observed improvement in the COD removal efficiency due to the BGW addition is similar to the results of previous studies. Astals et al. (2012) co-digested pig manure with crude glycerol under mesophilic conditions in a 4 L working-volume reactor. COD removal efficiency was reported to increase by 61% during the co-digestion of a mixture in which COD from BGW amounted to 65% of the total 3.56 kg COD/(m³·d) loading.

A reduction in COD removal efficiency was noted when the test digester loading was increased to 180% of the control digester's COD loading. Under this condition, the COD due to BGW represented 46% of the test digester's total COD loading (Fig. 5.2). COD removal efficiency in the test digester declined to only 70% of the control digester's COD removal efficiency. Clearly this loading was not sustainable as it allowed 58% of the applied COD to be released in the digester effluent.

6.3.2.2. Volatile Solids Removal Efficiency

Volatile solids removal is a major anaerobic digestion performance indicator as it relates to the mass of organic solids destroyed. VS removals as well as the percentages of total VS due to BGW in test digester feed are shown in Fig. 5.3. The VS removal efficiency in the control and test digesters was not significantly different at the baseline loading (100%) when they achieved average VS removals of 47% and 45%, respectively. These represent VS removal rates of 0.49 and 0.46 kg/(m³·d) in the control and test digesters, respectively. During the 130% COD

loading period when VS from BGW represented 13% of the total 1.03 kg VS/(m³·d) test digester loading, its VS removal efficiency was 12% greater than that of the control, as shown in Fig. 5.3. Given the higher test digester VS loading, this corresponds to a 45% greater VS removal rate being achieved in the test digester compared to the control. During this period, the actual VS removal rates were 0.38 and 0.55 kg VS/(m³·d) in the test and control, respectively. These loading and removal rates indicate that the amounts of VS loading that was not removed and would appear in the effluent were 0.52 and 0.48 kg VS/(m³·d) for the control and test digesters, respectively. At the test digester loading of 150 %COD, when VS from BGW accounted for 23% of the total 1.04 kg VS/(m³·d) loading, the VS removal rates in the control and test digesters were 0.32 and 0.52 kg/(m³·d), respectively. This corresponds to a 64% increase in VS removal rate in the test digester relative to the control. These loading and removal rates indicate that the amounts of VS loading that was not removed and would appear in the effluent were 0.49 and 0.52 kg VS/(m³·d) for the control and test digesters, respectively. Improvement in VS removal due to the addition of waste glycerin is in agreement with previous studies. Astals et al. (2012) reported that BGW addition amounting to 67% to the total 1.9 kg VS/(m³·d) loading increased the VS removal efficiency up to 107% compared to the digestion of pig manure alone.

Increasing the VS from BGW to 31% of the total 1.18 kg VS/(m³·d) test digester loading resulted in its VS removal efficiency being approximately 30% lower than that of the control digester (Fig 5.3). This indicates that a process upset had occurred in the test digester.

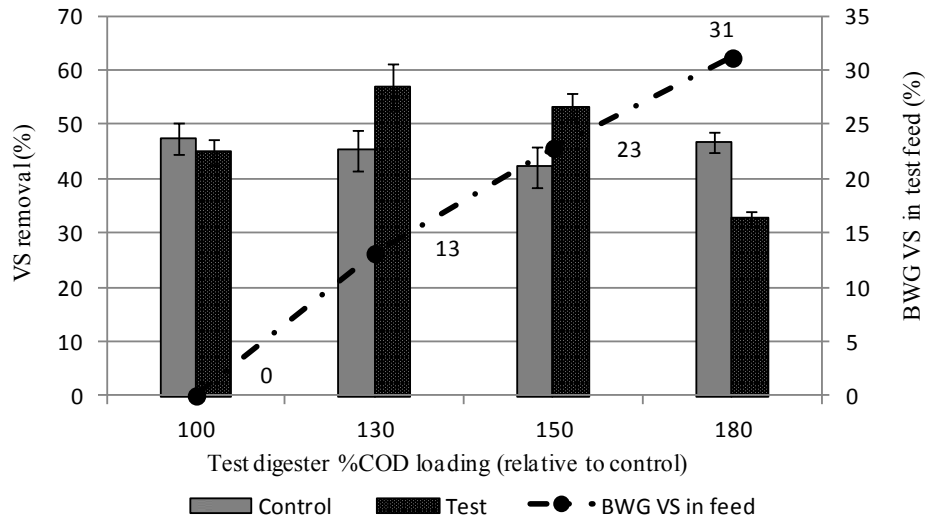


Figure 6.3. VS removal efficiency and BGW VS percentage at various loadings.

6.3.2.3. Biogas and Methane Production Rates

The gas production rate (GPR) and methane production rate (MPR) are two major performance indicators in the anaerobic process. The GPR and MPR, expressed as the volume of biogas or methane produced daily per unit reactor volume, are shown in Fig. 5.4. At the baseline, no statistically relevant difference was found for the mean GPR or MPR of the test and control digesters when only MWS was fed to both digesters (Table 6.3). Progressive addition of BGW to the test digester feed increased its GPR as well as MPR relative to the control (Fig. 4). The test digester GPR and MPR increased to 1.45 and 0.93 $\text{m}^3/(\text{m}^3 \cdot \text{d})$ at its 130% COD loading. These represented 39% and 48% increases in the GPR and MPR relative to the control digester, respectively. As the BGW addition was increased to the 150% COD level in test digester, its GPR and MPR were 65% and 83% greater than those of the control digester. The MPR values in the control and test digesters were 0.47 and 0.86 $\text{m}^3/(\text{m}^3 \cdot \text{d})$, respectively. Therefore, the addition of BGW enhanced the methane production by 0.39 $\text{m}^3/(\text{m}^3 \cdot \text{d})$. At this 150% loading, the test digester feed contained 1.1% (v/v) of BGW. Fountoulakis and Manios (2010) reported that the addition of 1% (v/v) BGW to sewage sludge increased the MPR in their 3 L anaerobic digester from 0.16 to 0.4 $\text{m}^3/(\text{m}^3 \cdot \text{d})$. As

shown in Fig. 5.4, when the test digester %COD loading was increased to 180% relative to the control, its GPR and MPR declined dramatically.

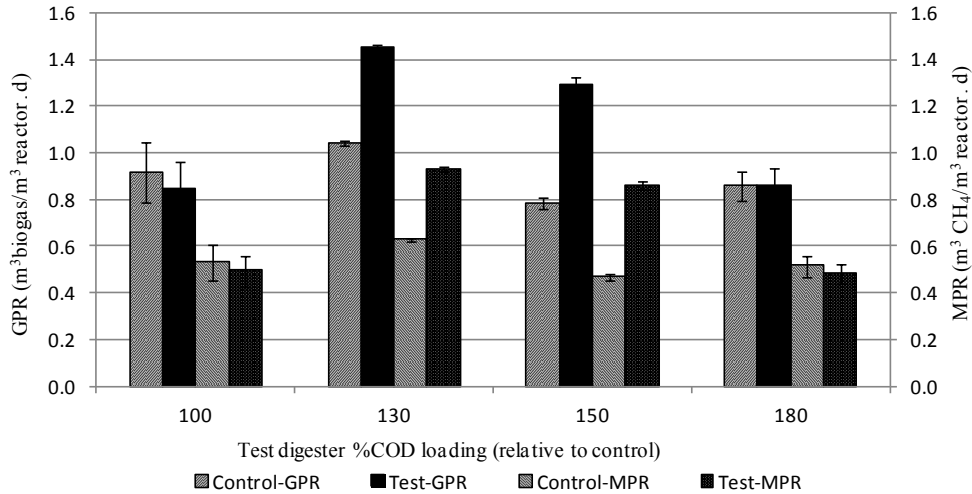


Figure 6.4. Gas production rate and methane production rate at various loadings

6.3.3. BGW Loading and Specific Methane Production

To express how effectively the BGW addition influences the methane production, the specific methane production (SMP) was determined in terms of COD and VS added as shown in Fig. 5.5. The SMP is defined here as the volume of methane produced daily per unit mass of COD or VS added to the reactor daily.

There was no significant difference between control and test digester SMP at the 100 %COD loading (Fig. 5.5). The SMP in terms of COD added to the test and control digesters were also not significantly different during the test digester nominal 130% and 150% COD loadings. However, the SMP in terms of VS added to each digester was 30% greater in the test digester relative to the control at the nominal 130% loading and 40% greater at the 150% loading. The composition of the biogas produced in the control digester remained relatively constant throughout the test period as shown in Table 6.4. The methane content of biogas produced in the test digester increased from approximately 58% at the 100% loading (no BGW) to a high of 66.5% at the nominal 150% test digester loading (Table 6.4). Dramatic declines in the test digester SMP values were

observed during the 180% loading period with 48% and 34% decreases in the test digester SMP in terms of COD and VS added compared to the control (Fig. 5.5).

Enhancements in biogas and methane production by addition of BGW to organic wastes have been reported by a number of researchers (Castrillon et al., 2011; Fountoulakis et al., 2010; Ma et al., 2008; Robra et al., 2010; Tokumoto and Tanaka, 2012). The improvement in methane production was linked to the increase in the overall degradation of the feed organics (in terms of VS) as solubilization of BGW is significantly higher than that of the MWS (Table 6.1) and the higher methane potential of BGW.

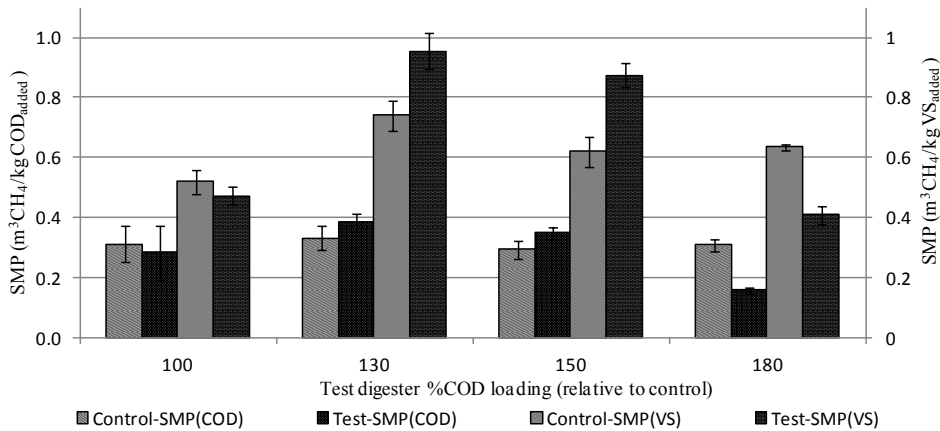


Figure 6.5. SMP in terms of COD and VS added in various loadings

6.3.4. Process Stability

The process stability was determined through the investigation of sensitive parameters such as pH, partial and total alkalinity, volatile fatty acids (VFA) and SO_4^{2+} . The mean value and standard deviation of the effluents from both reactors are presented in Table 6.4. The pH value as an indicator of acid-base balance in effluents remained in the optimum range of 6.6-7.8 as a stabilized anaerobic process (Ferrer et al., 2010). During co-digestion, PA and TA in the test digester were always lower than those of in the control digester and the VFA concentrations were generally greater in the test. The VFA/Alkalinity ratio remained below 0.03; 10 times lower than the maximum safe values of 0.3

reported by Siles et al. (2010). The ratio of intermediate alkalinity (IA) to partial alkalinity (PA) was reported by Astals et al. (2012) and Ferrer et al. (2010) as a highly sensitive parameter to assess the stability of an anaerobic process. This ratio should remain below 0.4 for stable operation. The IA/PA ratio did not exceed 0.4 in either of digesters until it reached 0.45 in the test digester at the 180% COD nominal loading. A reduction in alkalinity is typically caused by an increase in VFA and CO₂ generation. During the process, VFA and %CO₂ in both digesters remained at acceptable levels but increases were observed at the 180% loading in test (Table 6.4). These results suggest that a large reduction in PA (below 2500 mg CaCO₃/L) in the test digester beginning from the period of 180% loading resulted a considerable decline in the test digester's buffering capacity where the system was exhibiting signs of instability.

It is well-known that the anaerobic digestion process involves interactions and syntrophy among the several groups of bacteria and archaea. Syntrophy and competition between sulfur reducing bacteria (SRB) and methane producing bacteria (MPB) in the reactors is presented in terms of a COD/SO₄²⁺ ratio in Table 6.4. The predominance of either of SRB or MPB depends on a combination of factors involved in the anaerobic process. At the COD/SO₄²⁺ ratio of 2, while the MPB prevail over the SRB in acetate degradation, the SRB are more dominant in H₂ utilization (O'Reilly and Collieran, 2006). During co-digestion, the COD/SO₄²⁺ ratios were above approximately 4 in both the test and control digesters. O'Reilly and Collieran (2006) also indicated that at a COD/SO₄²⁺ ratio of 4 and above, the MPB are the main population involved in acetate degradation and H₂ utilization. Thus, the MPB were not hampered by SRB predominance during the process as the COD/SO₄²⁺ ratio were always above 4 in the test.

Table 6.4. Characteristics of reactor effluents and emissions

Parameter		Nominal COD loading (%)			
		100	130	150	180
Control	pH	7.22±0.06 ^c	7.28±0.07	7.18±0.03	7.21±0.01
	PA ^a (mg/L)	2577±79	2693±144	2436±98	2372±38
	TA (mg/L)	3656±139	3747±176	3377±135	3256±38
	VFA ^b (mg/L)	9.01±1.29	7.30±1.56	3.48±1.66	5.78±N/A ^d
	COD/SO ₄ ²⁺	5.98±N/A	4.72±N/A	4.73±N/A	3.98±N/A
	%CH ₄	58±0.75	60±0.84	60±0.74	60±0.63
	%CO ₂	41.72±0.89	39.67±0.92	39.36±0.10	38.93±0.80
Test	pH	7.20±0.07	7.25±0.07	7.18±0.05	7.09±0.05
	PA (mg/L)	2534±85	2492±94	2305±134	2041±123
	TA (mg/L)	3599±95	3522±116	3155±203	2970±150
	VFA (mg/L)	16.03±4.84	4.85±2.9	42.1±8.12	91.09±N/A
	COD/SO ₄ ²⁺	6.59±N/A	4.98±N/A	5.20±N/A	6.29±N/A
	%CH ₄	58±0.77	64±1.17	66.5±2.02	56±1.68
	%CO ₂	41.55±0.66	35.92±0.83	33.48±1.55	43.37±1.69

^a Partial alkalinity (PA) and total alkalinity (TA) represented as mg/L CaCO₃; ^b Volatile fatty acids (VFA) represented as mg/L acetic acid; ^c Standard deviation; ^d Not available.

The accelerated increase in VFA concentration in the test digester and decrease in the biogas CH₄ content suggest that methanogens inhibition occurred at the 180% COD loading. Consequently, as the proportion of the BGW in the feed was increased and reached 1.8% (v/v) of the feed, a reduction in methane

production was observed. In a similar study, Fountoulakis et al. (2010) reported that adding 3% (v/v) BGW to sewage sludge resulted in VFA accumulation and process instability. Robra et al. (2010) proposed another scenario for the methanogens inhibition due to the addition of BGW to the cattle slurry in a 4 L CSTR digester at mesophilic conditions. They observed that increasing the addition of BGW from 5% to 10% (wt) in the feed, no significant improvement in biogas production was achieved, although a greater amount of BGW had been fed. This observation was attributed to the high concentrations of methanol and KOH in their BGW which inhibited biocenosis and caused process instability.

6.3.5. Maximum Safe Loading Rate

The maximum safe loading limit for BGW during co-digestion depends on the characteristics of the primary substrate and the BGW itself. The limit established from the present research, as shown in Figs. 5.2 to 5.5, was found at the 150% nominal COD loading where the COD due to BGW was 35% of the 2.38 kg COD/(m³·d) loading and the VS from BGW was 23% of the 1.04 kgVS/(m³·d) loading. This amount of BGW represented 1.1% (v/v) of the feed material.

6.4. Conclusions

Co-digestion of BGW and MWS at the maximum feasible OLR of 1.1% BGW (v/v) increased the GPR and MPR in test by 65% and 83% compared to the control digester, respectively. At this loading, the test digester COD and VS removal rates were 82% and 63%, greater than those in the control digester, respectively. A considerable decline was observed in the test digester methane production, COD and VS removals when the proportion of COD and VS due to BGW in its feed was increased to 46% and 31% of the 2.38 kg COD/(m³·d) and 1.04 kg VS/(m³·d) loadings, respectively.

CHAPTER 7. ANAEROBIC CO-DIGESTION OF BIODEISEL WASTE GLYCERIN WITH MUNICIPAL WASTEWATER SLUDGE: MICROBIAL COMMUNITY DYNAMICS AND REACTOR PERFORMANCE*

7.1. Introduction

Over the past decades, the production of biodiesel fuels as alternatives to fossil fuels has drawn much attention because they are derived from renewable resources in a more sustainable manner which is potentially less harmful to the environment (Ito et al., 2005). The 2012 European annual combined biodiesel production capacity was estimated to be greater than 23 million metric tons (MMT) (EBB, 2013), where the biodiesel production in the US exceeded 63 MMT in 2013 (National Biodiesel Board, 2014). Production of 100 kg of biodiesel yields approximately 10 kg of glycerin waste as a co-product. Numerous industries such as pharmaceutical, cosmetics, and food processing, use refined glycerol as a raw input material. However, the crude glycerin generated as a co-product of biodiesel production requires purification before being suitable for use in these industries. Also, the generation of glycerin waste has exceeded the present market demands, which has caused a 10-fold decrease in the price of refined glycerol and consequently has resulted in the purification of the biodiesel glycerin waste becoming uneconomical (Slinn et al., 2008). Therefore, the crude glycerin is often considered a waste stream instead of a co-product, which makes its disposal a fundamental environmental concern (Leoneti et al., 2012).

Several approaches have been proposed to develop applications of biodiesel waste glycerin (BGW) in order to make biodiesel production more economical. Among the many approaches proposed to develop commercial applications for biodiesel waste glycerin (BGW) in order to make biodiesel production more economical, anaerobic co-digestion of BGW has shown great promise because it is based on a proven technology and both stabilizes the waste and produces

* A version of this chapter has been submitted for publication. Razaviarani and Buchanan, *Water Research* (July 2014).

biogas. BGW is a readily degradable material however; the mono digestion of this industrial waste is not practical due to the lack of sufficient nutrients such as nitrogen (Razaviarani et al., 2013b).

Disposal of municipal wastewater sludge (MWS) as a main by-product generated in wastewater treatment plants (WWTPs) is a major challenge which typically represents up to 50% of the overall operating costs of a WWTP. Anaerobic sludge digestion as a reliable technology employed worldwide to stabilize organics and reduce solids, destroy pathogens and produce biogas as the source of energy (Appels et al., 2008). It is broadly reported in many studies that anaerobic co-digestion of a mixture of organic wastes resulted in enhanced biogas production and organic matter removal rates (Hosseini Koupaie et al., 2014; Razaviarani et al., 2013a). Co-digestion of BGW with other organic wastes has been investigated in several studies and the benefits of the addition of BGW to improve the reactor's performance and efficiency were unanimously reported. Astals et al. (2011) investigated the potential of biodiesel waste glycerin as the major carbon source for methane production in its co-digestion with pig manure and reported a methane yield of 0.215 L/gCOD at the maximum BGW loading of 0.2 (w/w) of the feed.

The performance and stability of anaerobic digestion depend greatly on the microbial activities involved through the four major stages of digestion: hydrolysis, acidogenesis, acetogenesis and methanogenesis. Understanding of process performance and reactor stability is enhanced greatly by knowledge of the relationships between reactor environmental conditions and microbial community dynamics (Pervin et al., 2013). Yet, due to the complexity of the microbial interactions in such systems, the microbial dynamics and community structure has remained essentially a black box in anaerobic digestion systems (Supaphol et al., 2011).

Recently, pyrosequencing technology has been broadly used as a high-throughput sequencing technique in the field of microbial analysis based on the sequence-by-synthesis principle. This new technology has the potential

advantages of accuracy, flexibility and parallel processing over the current conventional methods (Fakruddin et al., 2012).

The objective of this study was to investigate the linkage between the reactors' performance and stability and microbial community dynamics of BGW co-digestion with MWS at various BGW loadings. To assess the effects of adding BGW to the MWS on the microbial community structure, the study was carried out at (1) steady-state, and (2) BGW overloading conditions. The 454-pyrosequencing analysis was applied to identify the methanogenic and the bacterial communities.

7.2. Materials and methods

7.2.1. Inoculum and wastes

The raw materials used as substrate were municipal wastewater sludge (MWS) and biodiesel waste glycerin (BGW). The MWS consisting of a 4:1 (v/v) blend of primary sludge (PS) and waste activated sludge (WAS), was collected from a Wastewater Treatment Plant (WWTP) in Edmonton, Alberta, Canada. The BGW was obtained from a canola oil biodiesel refinery in Calgary, Alberta. Following collection, substrates were stored at 4°C until their utilization. The inoculum (biomass) used for reactor start-up was digested sludge collected from a full-scale mesophilic anaerobic reactor at the Edmonton WWTP. The characteristics of substrates and inoculum are shown in Table 7.1.

Table 7.1. Characteristics of substrates and inoculum

Parameter	Phase 1		Phase 2		Inoculum
	MWS ₁	BGW	MWS ₂	BGW	
Density (kg/L)	0.9	1.10	0.92	1.10	0.98
COD (g/L)	75.3	1631	40.9	1486	22.9
TS (g/L)	63.9	277.0	22.9	275.0	22.3
VS (g/L)	35.7	240.2	18.3	236.0	12.2
TSS (g/L)	61.5	33.5	19.2	31.5	20.9
VSS (g/L)	34.8	28.3	15.6	26.0	11.3
VFA (mg/L)	2982.8	^d nm	1639.9	^b nm	7.9
TKN (mgN/L)	804	nm	794	nm	2140
TAN (mgN/L)	346	nm	332	nm	755
^a Alkalinity (mg/L)	1850	nm	2000	nm	nm
pH	5.8	9.0	5.7	10.2	7.3

^a Alkalinity represented as mg/L CaCO₃; ^b Non-measured.

7.2.2. Reactor setup and operation

The study was conducted in two separate phases based on the collection of MWS at different times from the WWTP. Digestion was carried out in two identical 10 L (8 L working volume) reactors, mixed by magnetic stirrers and operated under mesophilic conditions (37°C) with a solids retention time (SRT) of 20 days. Reactor contents were maintained at 37±1 °C using heating tape wrapped around the reactors and the temperatures were monitored and controlled by Type K thermocouples and digital temperature controllers. An insulating jacket was applied around each reactor to minimize heat loss.

Initially, each reactor was filled with 8 L of inoculum and the reactors' headspace was purged with nitrogen gas. Every day, 400 mL of digested material

was withdrawn from each reactor and replaced with the same volume of substrate to provide a 20 day SRT. During the entire experiment one reactor served as control (C1) and received only MWS while the other was operated as the test reactor (T1) and was fed with a mixture of MWS and an amount of BGW based on a percentage of the control reactor COD loading. During the first phase of the experiment, reactors C1 and T1 received the equal amount of MWS_1 to establish their baseline performance for a period of 30 days (1.5 SRT). When the equivalence of the reactors' performance was established, the COD loading of T1 was increased with the addition of a known volume of BGW to the MWS_1 to obtain the desired COD loading of 130% relative to the control reactor. This operating mode was continued for 3 SRT (60 days) to reach the steady-state conditions and then sampling was conducted daily for 10 days. Similarly, for the second phase, the control reactor, C2, and test reactor, T2, were fed with same volume of MWS_2 for 30 days to establish the baseline performance. Then the T2 reactor was with fed a mixture of BGW and MWS_2 to reach the COD loading of 150% relative to the C2 reactor. The steady state conditions were achieved after 3 SRTs when coefficients of variation of effluent COD, VSS and methane daily measurements were less than 5%. Thereafter, for a period of 10 days, samples were collected for the subsequent analyses. Following this 10-day sampling period, the loading to T2 was increased to 200% of the control COD loading by increasing the proportion of BGW in its feed. This loading was continued for 3 weeks and steady state performance was not attained. Reactor loadings and substrate mixture ratios during the experiment are shown in Table 7.2.

Table 7.2. Substrate loading characteristics

Parameters	Unit	Phase 1		Phase 2		
		C 1	T 1	C 2	T 2	
Reactor						
^a COD loading	%	100	130	100	150	200
BGW in feed	% by volume	0.00	1.25	0.00	1.35	2.72
Organic loading rate	g COD/L·d	3.77	4.82	2.05	3.02	4.01

^a COD loading percentages to the Test reactors were relative to the Control reactors in each phase

7.2.3. Analytical methods

Total and soluble chemical oxygen demands (COD, SCOD) of substrates and effluents were measured with the close reflux (5220C) method using HACH COD reactor and GENESYS20 spectrophotometer. Total solids (TS), volatile solids (VS), total suspended solids (TSS) and volatile suspended solids (VSS) were quantified using methods 2540G and 2540D, respectively. Total alkalinity (TA), partial alkalinity (PA) and pH were determined using Thermix stirrer 120S and ACCUMET AB15 Plus pH meter. The titration end points for PA and TA were pH 5.75 and 4.3, respectively according to Standard Method 2320B. All the above analyses were performed according to the standard methods in triplicate (APHA, 2005). For the VFA analysis, all samples were centrifuged at 5000 g for 10 min and then the supernatants were filtered through the 0.45 μ m and 0.2 μ m nylon syringes. Individual volatile fatty acids (acetate, propionate, iso-butyrate, n-butyrate, iso-valerate and n-valerate in the substrates and digested effluents were quantified by a Varian 430 gas chromatograph (GC) equipped by Stabilwax-DA capillary column and a flame ionization detector (FID). Total ammonia and TKN were measured by the Biochemical Analytical Service Laboratory (BASL) staff in the University of Alberta according to the standard methods.

The biogas flow rate from each reactor was quantified by a digital gas flow meter and logged to a lab computer. Agilent 7890A gas chromatograph (GC) was used to measure the CH₄ content in the biogas. The GC was equipped by Agilent

GS-Q column and a flame ionization detector (FID). The CO₂ percentage in biogas was intermittently measured using a Fyrite gas analyzer according to the method specified by the manufacturer (Bacharach Inc., 2010).

7.2.4. Microbial community analysis

7.2.4.1. Sludge sampling and DNA extraction

Well-homogenized effluent sludge samples were collected from the reactors during the last 10 days of steady-state period operation at each COD loading. Total genomic DNA was extracted from approximately 500 µL of sample using Fast DNA® Spin kit for soil (Biomedical, USA) according to the manufacturer's instructions. The samples were initially centrifuged at 10,000g for 20min, and the supernatant was removed carefully to obtain the settled biomass for DNA extraction. NanoDrop® 2000C spectrophotometer was used to determine the concentrations, quality and integrity of the extracted DNA (Thakuria et al., 2008). Extracted DNAs were stored at -20°C until submitted to the microbiology lab for the pyrosequencing analysis.

7.2.4.2. Pyrosequencing analysis

The 16S rRNA genes were amplified using bar-coded universal bacterial and archaeal primers for each sample. The sequence of the forward and reverse primers for bacterial universal were; (27F: AGR GTT TGA TCM TGG CTC AG, 519r: GTN TTA CNG CGG CKG CTG) and for archaeal universal were (349F: GYG CAS CAG KCG MGA AW, 806r: GGA CTA CVS GGG TAT CTA AT). The PCR reactions were conducted in a single step 30 cycle PCR using HotStarTaq Plus Master Mix Kit (Qiagen, Valencia, CA) under following conditions: initial denaturation at 94°C for 3 min, followed by 28 cycles of 94°C for 30s; annealing at 53°C for 40s and elongation at 72°C for 1 min; after which a final elongation step at 72°C for 5 min was performed. All the amplified 16S rRNA from different samples was mixed in equal concentrations and purified

using Agencourt Ampure beads (Agencourt Bioscience Corporation, MA, USA). All samples were subjected to pyrosequencing using Roche 454 FLX Titanium instruments and reagents according to the manufacture's guidelines. Raw nucleotide sequence reads were sorted out using a proprietary analysis pipeline. Initially, the barcode sequences shorter than 200bp, non-16S rRNA sequences and sequences with homo-polymer runs exceeding 6bp were removed from barcode sorted sequences. Then, sequences were de-noised and chimera sequences of selected reads were also removed. Operational taxonomic units (OTUs) of each sequence were identified after removal of singleton sequences, clustering at 3% divergence (97% similarity). Final OTUs were taxonomically classified using BLAST and database derived from GreenGenes, RDP11 and NCBI (DeSantis et al., 2006) and compiled into each taxonomic level into both "count" and "percentage" datasets. The count dataset contains the actual number of sequences while the percentage dataset defined as the ratio of number of assigned sequence reads of specific taxon divided by the number of total sequence reads.

7.2.5. Statistical analysis

Canonical correspondence analysis (CCA) was performed using XLSTAT software version 2014 (Addin-soft) to determine the correlation between microbial communities (bacteria and archaea) and reactors' performance and stability variables.

7.3. Results and discussion

7.3.1. Reactors' stability

The stability of the reactors during different phases was assessed with the evolution of pH, volatile fatty acids, alkalinity and the VFA/Alkalinity and Propionate/Acetate ratios throughout the experiment. As shown in Table 7.3, the pH value in effluent for the different loads remained almost constant in the range of 7.3-7.45 throughout the entire experiment excluding in the overloading period. These values stayed within the optimum range for methanogens as indicates a

stabilized anaerobic reactor (Ferrer et al., 2010). At 200% COD loading, pH decreased markedly to the value of 6.2 where the system was exhibiting signs of instability. The VFA/alkalinity ratio always remained well below the critical value of 0.3 reported by Siles et al., (2010), thus indicating that process operated fairly stable during the safe loading of BGW. However, at 200% COD loading (overloading), a dramatic increase in VFA was typically resulted a reduction in buffer capacity in the reactor where the VFA/Alk ratio jumped considerably to 0.7 which is well above the maximum safe value. Similar behavior was reported by Razaviarani et al. (2013), who observed signs of instability in the BGW co-digestion with MWS under mesophilic conditions due to the accumulation of VFA and a reduction in the pH values as consequences of the BGW overloading. The same authors reported that the increase in BGW from 1.1% to 1.8% (v/v) in the feed reduced the buffer capacity and resulted signs of instability in the system. Fountoulakis et al., (2010) also observed an accelerated increase in VFA when the addition of BGW to the sewage sludge increased from 1% to 3% (v/v) and resulted process instability. In this study, the signs of reactors' instability were observed when the BGW of 2.72% (v/v) of the feed was introduced to the reactor.

As shown in Table 7.3, the main VFA component during the addition of the BGW was propionate mostly at phase 2. In T1 and T2 reactors, although the total VFA concentration remained low enough according to the low VFA/Alkalinity ratio, the portion of propionate in the VFA was notably high compared to the other VFA components. Interestingly, 70% and 60% of the total VFA concentration detected in T2 and Overloading (OL) reactors were propionate with the values of 20.9 and 1380 mg/L, respectively. Increase in propionate level after addition of BGW to the sewage sludge was also observed by Fountoulakis et al. (2010) and was attributed to the high value of maximum specific utilization rate (μ_{\max}) of glycerol compared to that of propionate. Fountoulakis et al. (2010) reported the glycerin μ_{\max} of 3.6 d⁻¹ while the μ_{\max} for the propionate was reported 0.49 d⁻¹ by Angelidaki et al. (1999) in anaerobic systems. The ratio of propionate to acetate (Pr/Ac) was reported by Nuchdang and Phalakornkule (2012) as a sensitive parameter to assess the stability of anaerobic process. This ratio should

remain below 1.4 as indicates that reactor is working under stabilized condition. As shown in Table 7.3, the Pr/Ac ratio remained well below the critical value during the entire experiment until it reached 2.1 in the reactor at the 200% COD loading. In addition, propionate as a major end product of glycerol degradation can be optimally utilized in anaerobic digestion when the pH is kept between 6.8 and 7.3 (Fukuzaki et al., 1990). These results suggest that the overloading of BGW causes the propionate accumulation in the reactors and can finally establish the reactor instability. The results of this study support the assumption of propionate accumulation as the major cause of reactor instability at the overloading BGW addition.

Table 7.3. Reactors' stability and performance parameters at different phases of organic loadings.

Parameters	Phase 1		Phase 2		
	C 1	T 1	C 2	T 2	
Reactor					
% COD loading	100	130	100	150	200
pH	7.3	7.45	7.33	7.30	6.2
Alkalinity (mg/L)	4060	4909	4180	4193	2820
VFA (mg/L)	39.5	109.9	54.1	29.7	2333.3
Acetic ac.(mg/L)	21.7	56.5	33.8	13.8	661.1
Propionic ac.(mg/L)	7.0	41.8	4.4	15.9	1380.4
Butyric ac.(mg/L)	22.2	7.0	6.4	^b nd	116.8
Valeric ac.(mg/L)	4.5	4.8	9.5	nd	175.0
Pr/Ac	0.3	0.7	0.1	1.1	2.1
^a VFA : Alkalinity	0.01	0.03	0.003	0.006	0.7
Biogas production (L/d)	8.2	12.2	4.5	9.0	4.8
Methane yield (LCH ₄ /gVS _{added})	0.34	0.53	0.33	0.70	0.25

^a Alkalinity represented as mg/L CaCO₃; ^b VFA represented as mg/L acetic acid.

7.3.2. Reactors' performance

Biogas production and methane yield are two major performance indicators that are to be enhanced in co-digestion systems. As shown in Table 7.3, addition of BGW to the test reactors' feed increased the biogas production and methane yield relative to the control reactors in each phase. In phase 1, the biogas production and methane yield increased to 12.2 L/d and 0.53 L/gVS_{added} at the 130% COD loading to reactor T1. These represented 48% and 56% increases in biogas production and methane yield compared to the C1 reactor, respectively. At this COD loading, the T1 reactor feed contained 1.25% (v/v) of BGW. At 150% relative COD loading in Phase 2, the addition of 1.35% (v/v) BGW to the T2 feed resulted 100% and 121% increases in biogas production and methane yield relative to the C2 reactor, respectively. Progressive addition of 2.72% (v/v) BGW added to the reactor T2 feed resulted in a substantial reduction in biogas production and methane yield. These results indicated that addition of BGW in a safe loading range as a co-substrate can enhance biogas production and methane yield.

The COD and VS removal efficiencies in anaerobic reactor are two essential stabilization indicators as they are related to the amount of destroyed organic material. The COD and VS removal percentages at two different phases are shown in Figure 7.1. In phase 1, when the T1 reactor relative COD loading was increased to 130% of the C1 reactor COD loading, the COD and VS removal percentages in T1 increased by 23% and 27% relative to the C1 reactor, respectively. The COD and VS removal rates at this loading were 2.52 g COD/L.d and 1.2 g VS/L.d in the T1 reactor, respectively. These represented 58% and 34% increases in COD and VS removal rates after addition of 1.25% (v/v) BGW to the feed of reactor T1 compared to the C1 reactor. The efficiency of COD and VS removals at 150% COD loading in T2 reactor were 1.46 and 1.38 times that of the C2 reactor, respectively. These represent the COD removal rates of 0.85 and 1.82 g COD/L.d, and VS removal rates of 0.4 and 0.6 g VS/L.d in the C2 and T2 reactors, respectively. Improvement in COD and VS removals arising from the addition of BGW is in agreement with previous studies. Razaviarani et al., (2013)

observed increases of 81% and 64% of COD and VS removal rates when they added 1.1% (v/v) BGW to the feed. Astals et al., (2011) also reported the increases of 61% and 107% of COD and VS removal efficiencies when BGW amounted to 65% of the total 3.56 kg COD/m³.d organic loading.

As shown in Figure 7.1, further increase in the addition of BGW at 200% COD loading resulted in reductions of COD and VS removal efficiencies. This loading with 2.72% (v/v) BGW in the feed resulted in the COD and VS removal efficiencies being 40% and 38% lower than those of the C2 reactor, respectively. Therefore, this BGW loading was not sustainable as the process upset was observed in the T2 reactor.

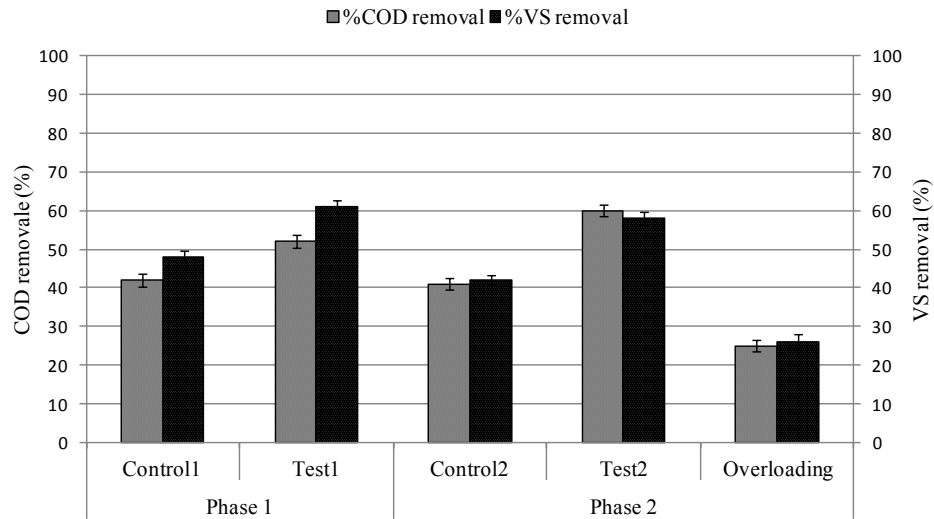


Figure 7.1. COD and VS removal percentages at different phases.

7.3.2. Methanogenic community dynamics

The archaeal 16S rRNA gene sequences at different taxonomic levels and the percentage of major phylotypes in each phase are summarized in Table 7.4 (genus level) and Figure 7.2 (order and family levels). As shown in Table 7.4, throughout the experiment, eight methanogenic genus sequences were identified in the archaeal sequence reads that all belong to the phylum *Euryarchaeota*. The orders *Methanomicrobiales* and *Methanosarcinales* were found to be the dominant

archaeal communities in both phases, while the number of sequences from the *Methanobacteriales* order were much fewer than those of the two former orders (Figure 7.2). The numbers of archaeal phylogenetic groups during each operating condition are presented in the Appendix, Table C-2.1.

The methanogenic community distribution between acetoclastic and hydrogenotrophic methanogens remained almost identical despite the different batches of MWS being fed to the control reactors in phases 1 and 2. The genus *Methanomicrobium* (hydrogenotrophic methanogens) and the genus *Methanosaeta* (acetoclastic methanogens) were the main methanogenic populations and were detected in approximately equal sequence abundance in the control reactors (Tables 7.4 and C-2.2). This suggests that both groups of methanogens were responsible for the methane production in the control reactors which were fed only MWS. This result is in agreement with a previous study that reported the genus *Methanosaeta* as the main acetoclastic methanogens when municipal wastewater sludge was fed to the digester (Demirel and Scherer, 2008). Kim et al., (2014) reported that an even distribution of hydrogenotrophic and acetotrophic methanogen populations in an anaerobic reactor indicates that the reactor is operating under stable conditions.

Table 7.4. Relative abundance of phylogenetic groups of archaeal in reactors

Rank and Taxon		^a Abundance (%) in the relevant genus				
Class	Genus (^b PF)	Phase 1		Phase 2		
Reactor		C 1	T 1	C 2	T 2	T 2
% COD loading		100	130	100	150	200
<i>Methanomicrobia</i>	<i>Methanomicrobium</i> (^c H)	42.0	1.6	41.1	69.9	95.7
	<i>Methanospirillum</i> (H)	2.1	3.8	1.4	0.7	0.0
	<i>Methanoculleus</i> (H)	3.5	0.0	3.2	1.6	0.3
	<i>Methanosarcina</i> (^d A/H)	4.7	5.4	3.7	2.5	0.2
	<i>Methanosaeta</i> (A)	43.9	85.9	47.8	23.7	3.4
<i>Methanobacteria</i>	<i>Methanobacterium</i> (H)	1.5	2.3	1.4	1.6	0.1
	<i>Methanosphaera</i> (H)	2.1	0.0	0.0	0.0	0.0
	<i>Methanobrevibacter</i> (H)	0.2	0.0	1.4	0.0	0.0
Other		0.0	0.9	0.0	0.0	0.3

Phylum; *Euryarchaeota*; ^a the relative abundance of taxon defined as the number of sequences divided by the total number of sequence per sample; ^b Putative function; ^c Hydrogenotrophic methanogens; ^d Acetoclastic methanogens.

During the 130% relative COD loading period, the total number of archaeal community sequences remained almost unchanged in reactor T1 relative to the C1 reactor (see Table C-2.1). However, at this loading with the addition of 1.25% (v/v) BGW to the feed, more than 85% of the archaeal sequence reads were assigned to the genus *Methanosaeta* within the order *Methanosarcinales* (Table 7.4). In comparison to reactor C1, the sequence abundance of genus *Methanosaeta* (acetoclastic methanogens) more than doubled while that of the

genus *Methanomicrobium* (hydrogenotrophic methanogens) decreased by a 96% in the T1 reactor (Table C-2.3). These methanogenic population dynamics were accompanied by 48% and 56% increases in biogas production and methane yield, respectively, in T1 reactor compared to C1. Typically, two-thirds of the methane is produced through the pathway of acetate in anaerobic processes (Kundu et al., 2014). Leclerc et al. (2004) reported that only one acetoclastic methanogen group, either *Methanosarcina* or *Methanosaeta*, dominates in an anaerobic digester with the dominance being based partly on the type of substrate and reactor loading. *Methanosaeta* have a lower half-saturation constant and maximum growth rate when utilizing acetate, while *Methanosarcina* have a higher half-saturation constant and maximum growth rate when using acetate (Conklin et al., 2006). Thus, *Methanosaeta* tend to dominate at low acetate concentrations and *Methanosarcina* generally dominate at higher acetate concentrations. As shown in Table 7.3, it is evident that during this loading, the concentration of acetic acid stayed well below (<1mM) and *Methanosaeta* were observed to be most abundant sequences. McMahon et al. (2001) investigated the microbial population in the mesophilic anaerobic co-digestion of municipal solid waste with the MWS and observed that *Methanosarcina* were the predominant acetoclastic methanogens in an unstable co-digester when the acetate concentration was high. The low acetate concentration and predominance of *Methanosaeta* suggest that the T2 reactor was operating under stable conditions.

In Phase 2, the 150% relative COD loading to the T2 reactor resulted in approximately a 168% increase in the total sequence abundance of archaea compared to the C2 reactor (see Table C-2.1). The biogas production and methane yield in reactor T2 at this loading were 2.0 and 2.2 times that of the C2 reactor, respectively (Table 7.3). At this loading, with the addition of 1.35 % (v/v) BGW to the feed, the sequence abundances of the genera *Methanomicrobium* and *Methanosaeta* increased 4.6 and 1.3 fold compared to those of the control reactor (C2), respectively (Table C-2.2). Degradation of propionic acid, as the main product of glycerol degradation, is accelerated in the present of H₂-utilizing methanogens (Fukuzaki et al., 1990). The same authors reported that the

production of methane from propionate degradation is thermodynamically feasible only when the H₂ partial pressure is kept low enough (0.1 to 10.1 Pa) by H₂-utilizing methanogens. During 150% relative COD loading, the pH value and VFA/Alkalinity ratio in reactor T2 remained in the optimum ranges (Table 7.3) indicating stable reactor operation. Moreover, the reduction of CO₂ by H₂ via the hydrogenotrophic pathway is more energetically favorable than acetoclastic reactions (Leclerc et al., 2004), this may have resulted in the development of many more hydrogenotrophic populations than acetoclastic methanogens in reactor T2. These findings suggested that much of the CH₄ was produced from the H₂/CO₂ pathway and that a greater number of hydrogenotrophic methanogens was present in the T2 reactor compared to the C2 reactor (Figure 7.2 and Table 7.4). Yang et al. (2008) also reported that hydrogenotrophic methanogens were the essential dominant archaeal group during the digestion of glycerol-containing synthetic wastes.

At the 200% relative COD loading, the total sequence abundance of methanogens increased by approximately 45% in reactor T2 compared to the same reactor at the 150% relative COD loading (See Table C-2.1). However, the 50% increase in BGW COD loading resulted in an 80% reduction of acetoclastic methanogen total sequence abundance and an 89% increase in hydrogenotrophic methanogen total sequence abundance compared to those measured at the 150% relative COD loading (Table C-2.3). Acetic acid and propionic acid accumulated in T2 when it received 2.72% (v/v) BGW in its feed at the 200% relative loading (Table 7.3). Ziganshin et al. (2010) reported that accumulation of acetic acid and propionic acid could be attributed to the inhibition of syntrophic propionate-oxidizers as well as inefficient acetate utilization by acetoclastic methanogens which resulted in a reduction of methane yield and as a result an increase in hydrogenotrophic methanogens. Karakashev et al. (2006) indicated that in the presence of inhibitors such as high VFA concentrations, acetate is metabolized by syntrophic acetate oxidation to H₂ and CO₂ with methane formation occurring via the hydrogenotrophic pathway. This occurs mostly in the absence of a *Methanosaeta* community. The similar results obtained from the BGW

overloading in this study support the involvement of the syntrophic acetate oxidation pathway at the 200% relative COD loading.

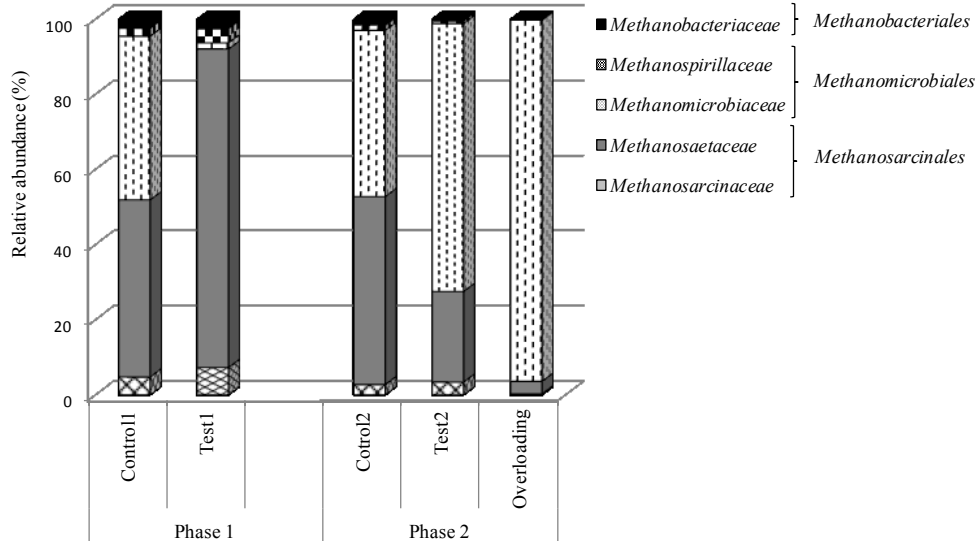


Figure 7.2. Distribution of *family* level of archaeal community categorized in brackets for *order* level.

7.3.3. Bacterial community dynamics

The 16S rRNA gene sequences of the bacterial community in each reactor during the first and second phases of operation are presented in Figure 7.3 and Table 7.5. In both phases, the inoculum contained three times more bacterial sequences than archaeal sequences (see Table C-2.1). Bacterial phyla *Spirochaetes* and *Proteobacteria* were found dominant in the inoculum bacterial community with relative abundance of 87% and 9.4%, respectively (see Table C-1.2). The genus *Candidatus Cloacamonas* affiliated within phylum *Spirochaetes* was present in the greatest number of sequences in all reactors during the experiment could be attributed to the inoculum, in which the genus *Candidatus Cloacamonas* was dominant. Yet, the presence and abundance of *Spirochaetes* in anaerobic digesters have rarely been investigated, possibly because the importance of this phylum in anaerobic digestion has not been fully appreciated

(Lee et al., 2013). The genus *Candidatus Cloacamonas* branching from the *Spirochaetes* was previously found to be hydrogen-producing syntrophs that are involved in the oxidation of propionate into acetate and CO₂ (Pelletier et al., 2008). This reaction is thermodynamically favorable only when the H₂ partial pressure remains low by coupling the propionate-oxidizing reaction with the hydrogen-utilizing reaction mediated by hydrogenotrophic methanogens. Thus, the prevalence of *Spirochaetes* and its affiliated genus *Candidatus Cloacamonas* throughout this study could be attributed to these interesting characteristics and roles in anaerobic systems.

As shown in Figure 7.3, the bacterial distributions in control reactors during the study remained quite stable despite the different batches of MWS being fed. However, the total number of bacterial sequences in C1 and C2 decreased by 10% and 47% compared to the inoculum, respectively. This alteration could have arisen from various factors such as changing substrate characteristics in the feed. The phylum *Spirochaetes* was dominant in C1 and C2 reactors with relative sequence abundances of 82.0% and 82.2%, respectively. The phyla *Proteobacteria*, *Chloroflexi* and *Actinobacteria* were also identified as the other three major populations in the reactors.

The relative sequence abundance of *Spirochaetes* and *Actinobacteria* increased in reactor T1 at the 130% relative COD loading compared to reactor C2 (Table 7.5). In contrast, the relative abundances of *Proteobacteria* and *Chloroflexi* were diminished considerably in T1 at this loading compared to C1. As shown in Table 7.5, about 93% of the total bacterial sequence abundance in T1 belonged to the genus *Candidatus Cloacamonas* which is a 13% increase relative to C1.

Table 7.5. Relative abundance of phylogenetic groups of bacteria in reactors

Taxon		^a Genus % of total bacterial sequence reads				
Phylum	Genus (^b PF)	Phase 1		Phase 2		
Reactor		C 1	T 1	C 2	T 2	
% COD loading		100	130	100	150	200
<i>Spirochaetes</i>	<i>Spaerochaeta</i> (U)	0.4	0.5	0.3	0.2	0.0
	<i>Candidatus Cloacamonas</i> (S)	82.0	92.9	82.2	90.0	95.7
<i>Actinobacteria</i>	<i>Demequina</i> (F)	0.2	0.4	0.3	0.0	0.0
	<i>Dermatophilus</i> (H)	2.0	2.9	1.2	7.8	1.8
<i>Proteobacteria</i>	<i>Desulfarculus</i> (A)	2.2	0.0	1.7	0.0	0.0
	<i>Esherichia</i> (A)	7.2	0.0	8.0	0.0	0.0
<i>Chloroflexi</i>	<i>Anaerolinea</i> (F)	2.3	1.8	2.4	0.0	0.0
	<i>Caldilinea</i> (F)	2.1	0.0	2.3	0.0	0.0
Other		1.6	1.5	1.6	2.0	2.5

^a The relative abundance of taxon defined as the number of sequences divided by the total number of sequence per sample; ^b Putative function; U: unknown, S: syntrophic, F: fermentative, H: hydrolysis, A: acidogenesis.

In Phase 2, with the addition of 1.35% (v/v) BGW to the feed, the total number of bacterial sequences increased from 4841 in C2 to 6056 in T2 reactor. This represents a 25% increase in total bacterial sequences in T2 compared to that of the C2 reactor. As shown in Figure 7.3, 90% of the total sequence abundance belonged to the *Candidatus Cloacamonas* affiliated within phylum *Spirochaetes*. Despite the increased loading, the propionic acid concentration remained relatively low (Table 7.3) suggesting that the increased numbers of hydrogenotrophic methanogen sequences also detected in reactor T2 (Table C-

2.3) maintained H₂ concentrations low enough to prevent inhibition of propionic acid oxidizing bacteria. These findings suggested that both microbial populations, syntrophic bacteria and H₂-utilizing methanogens, contributed to accelerate the degradation of VFAs. These results indicate that a stable and resilient bacterial community was established at this loading.

At the 200% relative COD loading, the total bacterial sequence abundance diminished to 3076 which was 37% lower than that in C2 and 49% lower than of T2 at its 150% loading. These reductions in bacterial sequence abundance occurred simultaneously with the drastic decline of acetoclastic methanogens and the reactor exhibiting signs of instability.

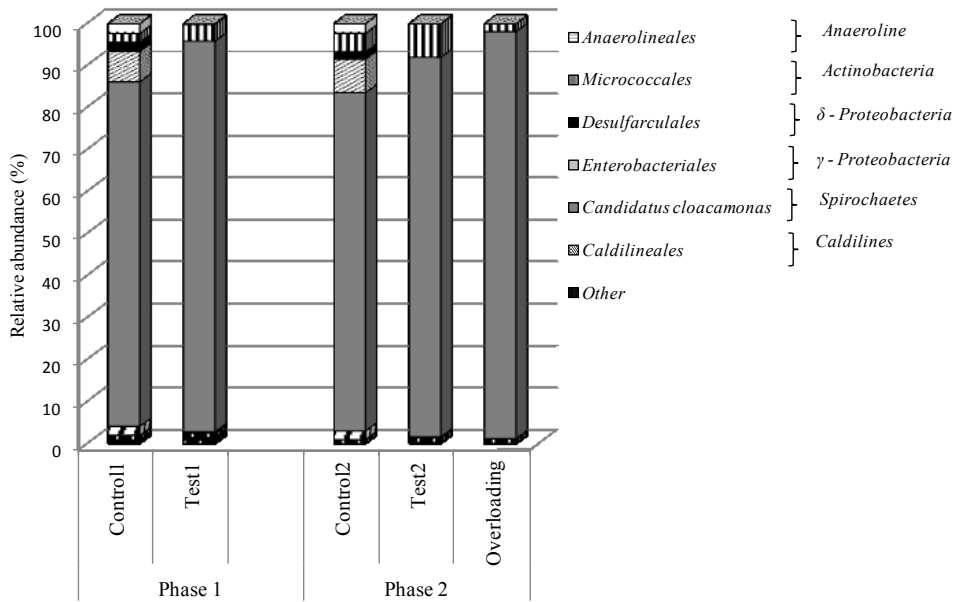


Figure 7.3. Distribution of *family* level of bacterial community categorized in brackets for *order* level.

7.3.4. Correlation between environmental variables and microbial dynamics

A multivariate canonical correspondence analysis (CCA) was performed using XLSTAT software to illustrate potential correlations between the sequence reads of bacteria and archaea and the environmental variables pH, alkalinity and VFA throughout the experiment. A triplot of the CCA results is shown in Figure

7.4 and a review of its interpretation is given in the Appendix B. In the triplot, the ordination axes combine to explain 97.48% of total bacterial and archaeal community variations, indicating that these environmental variables were major factors shaping the microbial community dynamics. Significant correlations ($p < 0.05$) were observed between microbial communities (bacterial and archaeal communities) and the environmental variables pH, alkalinity and VFA. As shown in Figure 7.4, the VFA variable was negatively associated with the pH and alkalinity variables, as would be expected.

As shown in Figure 7.4, genus *Candidatus Cloacamonas* (B7) is located near the origin of the plot, indicating that this genus was affected only slightly by changes in the environmental conditions considered. *Candidatus Cloacamonas* remained predominant for all reactor loadings, possibly because of being syntrophic bacteria. In general, this genus was more abundant at lower than average VFA concentrations and higher than average pH and alkalinity. Lee et al. (2013) found that the abundance of *Spirochaetes* is negatively correlated to the alkalinity variable and that this phylum is likely to be dominant under the weekly alkaline conditions.

The location of *Dermatophilus* (B6) indicates that the response of this genus to the environmental variables resembled that of *Candidatus Cloacamonas* (B7), as the two genera are grouped close together in the plot. The location of genus *Demequina* (B5) indicates that this genus was more abundant in the test reactors than in controls and was somewhat more abundant at lower than average VFA concentration and higher than average pH and alkalinity.

The sequence numbers of genera *Anaerolinea* (B1), *Caldilinea* (B2), *Esherichia* (B3) and *Desulfarculus* (B4) were more abundant in control reactors than in tests and all these genera were more abundant at lower than average VFA concentration and higher than average pH and alkalinity. In fact, none of these genera were detected at COD loadings above 130% relative to the control reactor loadings, and the genera *Esherichia* (B3) and *Desulfarculus* (B4) affiliated within phylum *Proteobacteria* were absent at all test digester loadings.

As shown in Figure 7.4, the reactors' locations indicate that the environmental conditions in reactors T1 and T2 were similar, as were those in C1 and C2. However, the environmental conditions during the overload condition of reactor T2 (shown as OL in the figure) were characterized by much higher than average VFA and much lower than average pH and alkalinity.

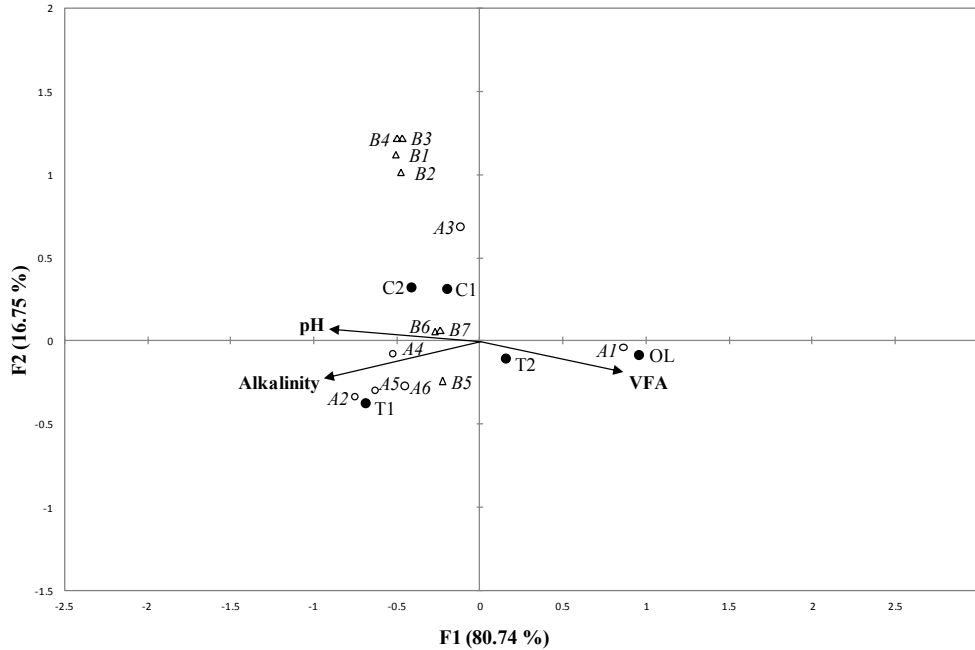


Figure 7.4. Canonical correspondence analysis (CCA) triplot showing the correlation between the sequence abundance of microbial communities and the environmental variables [pH, Alkalinity and VFAs] in the various COD loadings (●). The environmental variables represented in CCA are shown as vectors in the plot. The triangle symbol (Δ) represents the sequence genus of bacterial communities that include: B1: *Anaerolinea*; B2: *Caldilinea*; B3: *Escherichia*; B4: *Desulfarculus*; B5: *Demequina*; B6: *Dermatophilus*; B7: *Candidatus Cloacamonas*. The open circle symbols (○) represent the genus of archaeal populations that include A1: *Methanomicrobium*; A2: *Methanospirillum*; A3: *Methanoculleus*; A4: *Methanosarcina*; A5: *Methanosaeta*; A6: *Methanobacterium*.

The sequences of *Methanomicrobium* (A1) and *Methanosaeta* (A5) were generally present in greatest abundance throughout the study with sequences of the genus *Methanosaeta* being most abundant in reactor T1 (the 130% relative COD loading). The hydrogenotrophic genus *Methanomicrobium* (A1) sequences were more abundant at higher than average BGW loadings in reactor T2 and particularly during the overloaded condition (OL in Figure 7.4). These findings suggest that the hydrogenotrophic methanogens were important populations during higher BGW loadings and increased in sequence abundance with the addition of BGW at the 150% and 200% relative COD loadings. The dominance of hydrogenotrophic populations in digesters in which inhibitory conditions prevail has been reported in literature (Demirel and Scherer, 2008). The 89% increase in hydrogenotrophic methanogens sequences (A1) during the BGW overloading compared to that in the same reactor (T2) at the 150% relative COD loading was accompanied with 80% reduction in the number of acetoclastic methanogen sequences. The CCA triplot shown in Figure 7.4 indicates that genera *Methanosarcina* (A4) and *Methanosaeta* (A5) were more abundant at higher than average pH and alkalinity and lower than average VFA concentration. The methanogenic population changes during the overload condition was accompanied by 47% and 64% reductions in biogas production and methane yield compared to those in T2 at the 150% relative COD loading. This, together with the increase in propionate and the decline in the number of bacterial sequences, suggests that H₂ had built-up in the system and inhibited propionic acid oxidizing bacteria. Despite the large increase in the number of hydrogenotrophic methanogen sequences sufficient population numbers were not achieved within the 21 days of reactor operation at the 200% relative COD loading to restore stability to the reactor and methane production declined.

The location of *Methanoculleus* (A3) indicates that this genus was more abundant in control reactors. In fact *Methanoculleus* sequences were present in the lowest abundance at low and high BGW loadings (130% and 200% relative COD loadings). The response of this genus to the environmental conditions was not monotonic and the variation in its sequence abundance may be due to random

error or to an environmental variable not considered during the analysis. The genera *Methanospirillum* (A2) and *Methanobacterium* (A6) were present in each reactor during stable operation (not present during overloading conditions) and their sequences were more abundant at higher than average pH and alkalinity and lower than average VFA concentration.

These microbial dynamics results suggest that co-digestion of mixed organic wastes under stable operating conditions can support a broader diversity of microbial populations, and particularly of methanogenic populations compared to mono-digestion of MWS. This may be due to the availability of greater variety and concentrations of nutrients. It should be noted that, understanding the role of syntrophic bacteria such as *Candidatus Cloacamonas* within the phylum *Spirochaetes* and their interactions with methanogens is key to the understanding of reactor performance and should be investigated further, particularly in the anaerobic co-digestion of mixed-substrates.

7.4. Conclusions

Co-digestion of BGW with MWS under stable mesophilic operating conditions resulted in faster and greater reductions of VS and COD, as well as in enhanced biogas production and methane yield. Stable operating conditions were achieved at BGW loadings that represented 50% of the MWS feed COD, which for the BGW used in the study represented 1.35% of the feed by volume. These higher loadings correlating were associated with increased numbers of methanogen sequences. The acetoclastic methanogens (mostly *Methanosaeta*) sequences were dominant at moderate BGW loading (30% of the MWS feed COD), while hydrogenotrophic (mostly *Methanomicrobium*) populations prevailed at higher BGW loadings (50% and 100% of the MWS feed COD). Reductions in pH, alkalinity, biogas production and methane yield at the highest BGW loading (100% of MWS feed COD) were accompanied with a dramatic increase in VFA concentrations, mainly propionic acid. The genus *Candidatus Cloacamonas* was the predominant bacterial genus in all reactors throughout the study.

CHAPTER 8. GENERAL CONCLUSIONS AND RECOMMENDATIONS

8.1. Thesis Overview

Anaerobic digestion (AD) is a complex biological process performed in the absence of oxygen to produce biogas, mainly CH_4 and CO_2 , and stabilize organic matter. This process is a robust technology that has been applied at municipal wastewater treatment plants (WWTPs) for decades to treat the sewage sludge. However, the mono-digestion of a single substrate can possess some weakness and disadvantages related to the type and source of the substrate. The lack of enough buffer capacity and source of micro-nutrients, producing inhibitor by-products and compounds are some of the drawbacks in the AD of individual substrate. Most of these issues can be overcome by the simultaneous AD of two or more substrates in a process called anaerobic co-digestion (ACD). Generally, ACD focuses on mixing different substrates to benefit from positive interactions including nutrient balance and dilution of inhibitory compounds. Under such circumstances, reactor performance and stability is enhanced which has mainly a consequence of improvement in biogas and methane production. Despite these benefits of ACD, selection of appropriate co-substrates with an optimal blend ratio to provide the best synergisms is a key in such systems. Therefore, ACD of different organic waste and the decisions on their ratios require more attention to the critical parameters such as, buffer capacity, pH, and micro-nutrient balance.

Municipal wastewater sludge (MWS) is one of the most highly ranked co-substrates used in anaerobic co-digesters mainly because of its special characteristics such as relatively low C/N ratio and high buffer capacity. Moreover, the AD capacity in WWTPs is not fully utilized by MWS mono-digestion and this surplus is a major driving force behind the MWS co-digestion.

Restaurant grease trap waste (GTW) and biodiesel glycerin waste (BGW) are two of the major commercial and industrial organic waste streams produced in large quantities in the world. The restaurant GTW characteristics can vary mostly depending on the sources and the collection devices. The restaurant GTW has a high biochemical oxygen demand with a high content in fat, oil and grease (FOG)

which make it a reliable source of energy. Depending on the portion of FOG, the dewatered GTW contains high methane production potential. However, the mono-digestion of GTW is not practical because of a number of issues such as, inhibition of methanogens, clogging in the liquid or gas systems, foaming and biomass floatation. The BGW is a readily digestible substrate with the potential of complete COD degradation. But, anaerobic mono-digestion of BGW is not viable due to the lack of important micronutrients such as nitrogen.

Therefore, ACD of MWS with GTW or BGW allows beneficial use of these organic wastes that cannot be digested alone. The advantages of co-digestion of MWS with these organic wastes were investigated in the literature. Yet, there was a lack of a thorough investigation on the reactor's behaviors during the ACD of MWS with these organic wastes.

This work focused on assessing the reactor's behaviors during ACD of MWS with GTW and BGW in two separate trials at three different phases; (1) the maximum feasible loading of each co-substrate, (2) modeling the GTW co-digestion system at steady state condition, and (3) correlations between reactor performance and stability and microbial community dynamics during steady state and overloading conditions. The objectives of this research were achieved through accomplishing these steps in different phases.

In order to achieve these objectives, in the first phase, pilot-scale study was performed to investigate the reactor performance and stability during the ACD of MWS with GTW and BGW in two separate trials. The maximum feasible organic loading of both co-substrates based on COD were determined through the pilot study in two 1300 L reactors. In the second phase, two 10 L reactors were used to calibrate the Anaerobic Digestion Model No.1 (ADM1) for steady state anaerobic co-digestion of MWS with GTW. At this phase, the anaerobic respirometry test was also carried out for 10 days period for the calibration of kinetic parameters. Given that anaerobic digestion comprises multiple biological reactions mediated by microbial activities, the reactor performance and stability is strongly correlated to the microbial community structures during addition of co-substrate to the feed. In the third phase, two 10 L reactors were used to investigate this relationship at

steady state and overloading of co-substrate (GTW or BGW) in two separate trials. Pyrosequencing analysis was applied to determine the sequence abundance of microbial (bacterial & archaeal) community and canonical correspondence analysis (CCA) was used to determine the correlations between the microbial community dynamics and reactor performance in each trial. The reactors in all three phases were operating under mesophilic condition at a 20 day SRT.

8.2. Conclusions

Based on the experimental results and analyses obtained from all three phases in this research, the following conclusions were drawn:

1. At the pilot scale GTW co-digestion, the test digester loading was increased incrementally to a maximum of 280% of the control digester COD loading. The highest feasible GTW loading was determined to be 23% and 58% in terms of its total 1.58 kg VS/(m³.d) and 3.99 kg COD/(m³.d) loadings, respectively. This test digester COD loading represented 240% of the control digester COD loading. At this loading, test digester biogas production was 67% greater than that of the control. During the test digester quasi steady state loading period when VS from GTW represented 19% of its total VS loading, the test digester COD and VS removal rates were 2.5 and 1.5 fold those of the control digester, respectively. The test digester biogas production declined markedly when the percentage of VS from GTW in its feed was increased to 30% of its total VS loading. Causes of the reduced biogas production were investigated and attributed to inhibition due to long chain fatty acid accumulation.
2. At the pilot scale BGW co-digestion, the highest proportion of BGW that did not cause a process upset was determined to be 23% and 35% of the total 1.04 kg VS/ (m³.d) and 2.38 kg COD/ (m³.d) loadings, respectively. At this loading, the biogas and methane production rates in the test

digester were 1.65 and 1.83 times greater than of those in the control digester which received only MWS, respectively. The COD and VS removal rates at this loading in the test digester were 1.82 and 1.63-fold those of the control digester, respectively. Process instability was observed when the proportion of BGW in the test digester feed was 31% and 46% of the 1.18 kg VS/ (m³·d) and 2.88 kg COD/ (m³·d) loadings, respectively.

3. The Anaerobic Digestion Model No.1, implemented in the GPS-X computational simulator, was calibrated to simulate the steady state anaerobic co-digestion of municipal wastewater sludge and restaurant grease trap waste (GTW). Substrate characterizations combined with anaerobic respirometric analysis were applied for model calibration. Initial biomass concentrations and distributions were estimated using methane production rate curves together with effluent values from full-scale anaerobic digesters. Two separate datasets obtained from steady state mesophilic lab-scale experiments were used to calibrate and validate the model. The modified model was able to predict reasonably well the steady-state results of biogas production, CH₄ and CO₂ contents, pH, alkalinity, COD and VSS observed within the evaluated GTW loading. Finally, the calibrated model was validated using pilot-scale co-digestion results obtained during the study reported in Chapter 2. The model output was in good agreement with measured values of methane production, pH, ammonia, alkalinity and COD.
4. Linkage between reactor performance and microbial community dynamics was investigated during mesophilic anaerobic co-digestion of restaurant grease waste (GTW) with municipal wastewater sludge (MWS) using 10 L completely mixed reactors and a 20 day SRT. Addition of GTW to the test reactors enhanced the biogas production and methane yield by up to 65% and 120%, respectively. Pyrosequencing revealed that *Methanosaeta* and *Methanomicrobium* were the dominant acetoclastic and hydrogenotrophic

methanogen genera, respectively, during stable reactor operation. The number of *Methanosarcina* and *Methanomicrobium* sequences increased and that of *Methanosaeta* declined when the proportion of GTW in the feed was increased to cause an overload condition. Under this overload condition, the pH, alkalinity and methane production decreased and VFA concentrations increased dramatically. Candidatus *Cloacamonas*, affiliated within phylum *Spirochaetes*, were the dominant bacterial genus at all reactor loadings. The CCA triplot indicated that among the studied environmental variables, VFA concentration accounted for much of the major shifts in microbial sequence abundance during GTW co-digestion.

5. Two 10 L completely mixed reactors operating at 37°C and 20 days SRT were used to evaluate the relationships between reactor performance and microbial community dynamics during anaerobic co-digestion of biodiesel waste glycerin (BGW) with municipal wastewater sludge (MWS). The addition of up to 1.35% (v/v) BGW to reactor feeds yielded increased VS and COD removal rates together with enhanced the biogas production and methane yield. This proportion of BGW represented 50% of the MWS feed COD. Pyrosequencing analysis showed *Methanosaeta* (acetoclastic) and *Methanomicrobium* (hydrogenotrophic) to be the methanogenic genera present in greatest diversity during stable reactor operation. *Methanosaeta* sequences predominated at the lowest BGW loading while those of *Methanomicrobium* were present in greatest abundance at the higher BGW loadings. Genus Candidatus *Cloacamonas* was present in the greatest number of bacterial sequences at all loadings. Alkalinity, pH, biogas production and methane yield declined and VFA concentrations (especially propionate) increased during the highest BGW loading.

8.3. Future Research and Recommendations

1. In the pilot-scale study, the safe upper limit on co-substrate (GTW and BGW) loadings were identified after incremental increases in the proportions of co-substrate to the test digester feed. This feeding mode continued until the signs of inhibition or instability were observed. However, the ability of the digester to recover was not investigated after the process distress was observed. Further research is required for investigation of the possible process recovery during the incrementally addition of GTW or BGW to the MWS at mesophilic anaerobic co-digestion.
2. During the research, in the pilot and bench scale experiments, the required inoculum (biomass) to start up the reactors was the effluent collected from a full-scale mesophilic anaerobic digester which was fed by municipal wastewater sludge. The effects of inoculum adaptation under the certain conditions in terms of feeding mode and type of substrate on the process efficiency and performance have been reported in literature. Using the acclimatized biomass collected from a reactor effluent working with the similar feeding components (GTW and BGW) can improve the performance of co-digestion of MWS with either of GTW or BGW. Having the acclimated inoculum under similar conditions can increase the degradation rate and reduce the inhibitory effects of by-products such as LCFA, VFA, ammonia, and others. Therefore, finding the effects of using acclimated biomass on the reactor performance, recovery duration and increasing the maximum loading level for anaerobic co-digestion of MWS with GTW and BGW in different trails is suggested for the future research.
3. In the bench-scale study, although the bacterial and archaeal community dynamics (sequences) were identified by pyrosequencing analysis, the numbers of bacterial and archaeal species during the co-digestion of MWS

with GTW or BGW remained unknown. For the future research, available microbial techniques such as qPCR (the copies number of gene) can be applied following the DNA extraction and PCR. Determination of numbers of each identified species can elucidate the contribution of the target individual sequences to the biodegradation of mixed substrates during the anaerobic co-digestion of MWS with GTW or BGW.

4. In this research, the Anaerobic Digestion Model no.1 (ADM1) was calibrated to simulate and predict the behavior of steady state anaerobic co-digestion of MWS and GTW. Anaerobic respirometric analysis with substrate characterizations were applied for the model calibration. For the future research, it is suggested to apply a similar method for the calibration of ADM1 to simulate the steady state anaerobic BGW co-digestion with MWS. Several calibrations and modifications of ADM1 are available in the literature, but a very limited number of studies have focused on the modeling co-digestion systems and none has addressed modeling the co-digestion of MWS with BGW.

REFERENCES

- Ağdağ, O., N., Sponza, D., T., 2007. Co-digestion of mixed industrial sludge with municipal solid wastes in anaerobic simulated landfilling bioreactors. *J. Hazard. Mater.* , 140, 75-85.
- Àlvarez, J.A., Otero, L., Lema, J.M., 2010. A methodology for optimising feed composition for anaerobic co-digestion of agro-industrial wastes. *Bioresour. Technol.*, 101, 1153-1158.
- Amon, T., Amon, B., Kryvoruchko, V., Bodiroza, V., Patsch, E., Zollitsch, W., 2006. Optimising methane yield from anaerobic digestion of manure: Effects of dairy systems and of glycerine supplementation. *Int. Cong. Ser.*, 1293, 217-220.
- Angelidaki, I., Ellegaard, L., Ahring, B.K., 1999. A comprehensive model of anaerobic bioconversion of complex substrates to biogas. *Biotechnol. Bioeng.* , 63, 363-372.
- APHA, 2005. Standard Methods for the Examination of Water and Wastewater. 21st ed. American Public Health Association Washington DC, USA.
- Appels, L., Baeyens, J., Degrève, J., Dewil, R., 2008. Principles and potential of the anaerobic digestion of waste-activated sludge. *Progr. Energ. Combust.* , 34, 755-781.
- Appels, L., Lauwers, J., Degrève, J., Helsen, L., Lievens, B., Willems, K., Van Impe, J., Dewil, R., 2011. Anaerobic digestion in global bio-energy production: Potential and research challenges. *Renew. Sust. Energ. Rev.*, 15, 4295-4301.
- Ariesyady, H.D., Ito, T., Okabe, S., 2007. Functional bacterial and archaeal community structures of major trophic groups in a full-scale anaerobic sludge digester. *Water Res.*, 41, 1554-1568.
- Astals, S., Esteban-Gutiérrez, M., Fernández-Arévalo, T., Aymerich, E., García-Heras, J.L., Mata-Alvarez, J., 2013. Anaerobic digestion of seven different sewage sludges: A biodegradability and modelling study. *Water Res.*, 47, 6033-6043.
- Astals, S., Nolla-Ardèvol, V., Mata-Alvarez, J., 2012. Anaerobic co-digestion of pig manure and crude glycerol at mesophilic conditions: Biogas and digestate. *Bioresour. Technol.*, 110, 63-70.
- Ayoub, M., Abdullah, A.Z., 2012. Critical review on the current scenario and significance of crude glycerol resulting from biodiesel industry towards more sustainable renewable energy industry. *Renew. Sust. Energ. Rev.*, 16, 2671-2686.

Bapteste, É., Brochier, C., Boucher, Y., 2005. Higher-level classification of the Archaea: evolution of methanogenesis and methanogens. *Archaea*, 1, 353-363.

Batstone, D., Keller J, Angelidaki I, Kalyuzhnyi SV, Pavlostathis SG, Rozzi A, Sanders WT, Siegrist H, VA., V., 2002a. The IWA Anaerobic Digestion Model No 1 (ADM1). *Water Sci. Technol.*, 45, 65-73.

Batstone, D.J., Keller, J., Angelidaki, I., Kalyuzhny, S., Pavlostathis, S., Rozzi, A., Sanders, W., Siegrist, H., Vavilin, V., 2002b. Anaerobic digestion model no. 1 (ADM1). IWA publishing.

Bernard, O., Hadj-Sadok, Z., Dochain, D., Genovesi, A., Steyer, J.-P., 2001. Dynamical model development and parameter identification for an anaerobic wastewater treatment process. *Biotechnol. Bioeng.*, 75, 424-438.

Blumensaat, F., Keller, J., 2005. Modelling of two-stage anaerobic digestion using the IWA Anaerobic Digestion Model No. 1 (ADM1). *Water Res.*, 39, 171-183.

Bond, T., Brouckaert, C.J., Foxon, K.M., Buckley, C.A., 2012. A critical review of experimental and predicted methane generation from anaerobic codigestion. *Water Sci. Technol.*, 65, 183-189.

Borowski, S., Doman'ski, J., Weatherley, L., 2014. Anaerobic co-digestion of swine and poultry manure with municipal sewage sludge. *Waste Manage*, 34, 513-521.

Bouallagui, H., Lahdheb, H., Ben Romdan, E., Rachdi, B., Hamdi, M., 2009. Improvement of fruit and vegetable waste anaerobic digestion performance and stability with co-substrates addition. *J. Environ. Manage.*, 90, 1844-1849.

Boubaker, F., Ridha, B.C., 2008. Modelling of the mesophilic anaerobic co-digestion of olive mill wastewater with olive mill solid waste using anaerobic digestion model No. 1 (ADM1). *Bioresour. Technol.*, 99, 6565-6577.

Breznak, J.A., 2002. Phylogenetic diversity and physiology of termite gut spirochetes. *Integr. Comp. Biol.*, 42, 313-318.

Castrillon, L., Fernandez-Nava, Y., Ormaechea, P., Maranon, E., 2011. Optimization of biogas production from cattle manure by pre-treatment with ultrasound and co-digestion with crude glycerin. *Bioresour. Technol.*, 102, 7845-7849.

Chen, Y., Cheng, J.J., Creamer, K.S., 2008. Inhibition of anaerobic digestion process: A review. *Bioresour. Technol.*, 99, 4044-4064.

Chen, Z., Hu, D., Zhang, Z., Ren, N., Zhu, H., 2009. Modeling of two-phase anaerobic process treating traditional Chinese medicine wastewater with the IWA Anaerobic Digestion Model No. 1. *Bioresour. Technol.*, 100, 4623-4631.

Chi, Z., Pyle, D., Wen, Z., Frear, C., Chen, S., 2007. A laboratory study of producing docosahexaenoic acid from biodiesel-waste glycerol by microalgal fermentation. *Process Biochem.*, 42, 1537-1545.

Chong, M.-L., Sabaratnam, V., Shirai, Y., Hassan, M.A., 2009. Biohydrogen production from biomass and industrial wastes by dark fermentation. *Int. J. Hydrogen Energ.*, 34, 3277-3287.

Cirne, D.G., Paloumet, X., Björnsson, L., Alves, M.M., Mattiasson, B., 2007. Anaerobic digestion of lipid-rich waste - Effects of lipid concentration. *Renew. Energ.*, 32, 965-975.

Conklin, A., Stensel, H.D., Ferguson, J., 2006. Growth kinetics and competition between *Methanosarcina* and *Methanosaeta* in mesophilic anaerobic digestion. *Water Environ. Res.*, 78, 486-496.

Davidsson, A., Lavstedt, C., la Cour Jansen, J., Gruvberger, C., Aspegren, H., 2008. Co-digestion of grease trap sludge and sewage sludge. *Waste Manage.*, 28, 986-992.

De Gracia, M., Grau, P., Huete, E., Gomez, J., Garcia-Heras, J., Ayesa, E., 2009. New generic mathematical model for WWTP sludge digesters operating under aerobic and anaerobic conditions: Model building and experimental verification. *Water Res.*, 43, 4626-4642.

De Gracia, M., Huete, E., Beltrán, S., Grau, P., Ayesa, E., 2011. Automatic characterisation of primary, secondary and mixed sludge inflow in terms of the mathematical generalised sludge digester model. *Water Sci. Technol.*, 64, 557-567.

De Meester, S., Demeyer, J., Velghe, F., Peene, A., Van Langenhove, H., Dewulf, J., 2012. The environmental sustainability of anaerobic digestion as a biomass valorization technology. *Bioresour. Technol.*, 121, 396-403.

Delbes, C., Moletta, R., Godon, J.J., 2000. Monitoring of activity dynamics of an anaerobic digester bacterial community using 16S rRNA polymerase chain reaction "single strand" conformation polymorphism analysis. *Environ. Microbiol.*, 2, 506-515.

Demirel, B., Scherer, P., 2008. The roles of acetotrophic and hydrogenotrophic methanogens during anaerobic conversion of biomass to methane: a review. *Rev. Environ. Sci. Bio/Technol.*, 7, 173-190.

Demirel, B., Yenigun, O., 2002. Two-phase anaerobic digestion processes: a review. *J. Chem. Technol. Biot.*, 77, 743-755.

Derbal, K., Bencheikh-lehocine, M., Cecchi, F., Meniai, A.H., Pavan, P., 2009. Application of the IWA ADM1 model to simulate anaerobic co-digestion of organic waste with waste activated sludge in mesophilic condition. *Bioresour. Technol.*, 100, 1539-1543.

Derek R. Lovley, Daryl F. Dwyer, and Klung, a. M. J. 1982. Kinetic Analysis of Competition between Sulfate Reducers and Methanogens for Hydrogen in sediments. *Appl. Environ. Microbiol.*, 43(6), 1373-1379.

DeSantis, T.Z., Hugenholtz, P., Larsen, N., Rojas, M., Brodie, E.L., Keller, K., Huber, T., Dalevi, D., Hu, P., Andersen, G.L., 2006. Greengenes, a chimera-checked 16S rRNA gene database and workbench compatible with ARB. *Appl. Environ. Microbiol.*, 72, 5069-5072.

Dworkin, M., Falkow, S., Rosenberg, E., Schleifer, K.-H., Stackebrandt, E., Schmitz, R., Daniel, R., Deppenmeier, U., Gottschalk, G., 2006. *The Anaerobic Way of Life: The Prokaryotes*. Springer, New York, pp. 86-101.

EBB, 2010. European Biodiesel Board, The EU biodiesel industry. Available from: <http://www.ebb-eu.org/stats.php>. Accessed in July 2014.

Elbeshbishy, E., Nakhla, G., 2012. Batch anaerobic co-digestion of proteins and carbohydrates. *Bioresour. Technol.*, 116, 170-178.

Fakruddin, M., Chowdhury, A., Nur Hossain, M., Mannan, K., Mazumdar, R.M., 2012. Pyrosequencing-principles and applications. *Int J Life Sci Pharm Res*, 2, 65-76.

Fernández, A., Huang, S., Seston, S., Xing, J., Hickey, R., Criddle, C., Tiedje, J., 1999. How stable is stable? Function versus community composition. *Appl. Environ. Microbiol.*, 65, 3697-3704.

Fernandez, J.M., Omil, F., Mendez, R., Lema, J.M., 2001. Anaerobic treatment of fibreboard manufacturing wastewaters in a pilot scale hybrid USBF reactor. *Water Res.*, 35, 4150-4158.

Ferrer, I., Vázquez, F., Font, X., 2010. Long term operation of a thermophilic anaerobic reactor: Process stability and efficiency at decreasing sludge retention time. *Bioresour. Technol.*, 101, 2972-2980.

Fezzani, B., Cheikh, R.B., 2009. Extension of the anaerobic digestion model No. 1 (ADM1) to include phenolic compounds biodegradation processes for the simulation of anaerobic co-digestion of olive mill wastes at thermophilic temperature. *J. Hazard. Mater.*, 162, 1563-1570.

Folch, J., Lees, M., Sloane-Stanley, G., 1957. A simple method for the isolation and purification of total lipids from animal tissues. *J Biol Chem*, 226, 497-509.

Forster, C., 1991. Anaerobic upflow sludge blanket reactors: aspects of their microbiology and their chemistry. *J. Biotechnol.*, 17, 221-231.

Fountoulakis, M.S., Petousi, I., Manios, T., 2010. Co-digestion of sewage sludge with glycerol to boost biogas production. *Waste Manage.*, 30, 1849-1853.

Fukuzaki, S., Nishio, N., Shobayashi, M., Nagai, S., 1990. Inhibition of the fermentation of propionate to methane by hydrogen, acetate, and propionate. *Appl. Environ. Microbiol.*, 56, 719-723.

Galí, A., Benabdallah, T., Astals, S., Mata-Alvarez, J., 2009. Modified version of ADM1 model for agro-waste application. *Bioresour. Technol.*, 100, 2783-2790.

Gallert, C., Bauer, S., Winter, J., 1998. Effect of ammonia on the anaerobic degradation of protein by a mesophilic and thermophilic biowaste population. *Appl. Microbiol. Biotechnol.*, 50, 495-501.

Gerardi, M.H., 2006. Wastewater Bacteria. John Wiley & Sons, New Jersey.

Girault, R., Bridoux, G., Nauleau, F., Poullain, C., Buffet, J., Peu, P., Sadowski, A.G., Béline, F., 2012. Anaerobic co-digestion of waste activated sludge and greasy sludge from flotation process: Batch versus CSTR experiments to investigate optimal design. *Bioresour. Technol.*, 105, 1-8.

Girault, R., Bridoux, G., Nauleau, F., Poullain, C., Buffet, J., Steyer, J.P., Sadowski, A.G., Béline, F., 2012. A waste characterisation procedure for ADM1 implementation based on degradation kinetics. *Water Res.*, 46, 4099-4110.

Girault, R., Rousseau, P., Steyer, J., Bernet, N., Béline, F., 2011. Combination of batch experiments with continuous reactor data for ADM1 calibration: application to anaerobic digestion of pig slurry. *Water Sci. Technol.*, 63, 2575-2582.

Girault, R., Steyer, J., Zaher, U., Sadowski, A., Nopens, I., Béline, F., Zak, A., Kujawski, O., Holm, N., Rönner-Holm, S., 2010. Influent Fractionation and Parameter Calibration for ADM1: Lab-Scale and Full-scale Experiments. 2nd IWA/WEF Wastewater Treatment Modelling Seminar, Quebec, Canada, pp. 171-18.

Gomez, X., Cuetos, M.J., Cara, J., Moran, A., Garcia, A.I., 2006. Anaerobic co-digestion of primary sludge and the fruit and vegetable fraction of the municipal solid wastes: Conditions for mixing and evaluation of the organic loading rate. *Renew. Energ.*, 31, 2017-2024.

Gregor D., Z., Natasa, U.-z., Milenko, R., 2008. Full-scale anaerobic co-digestion of organic waste and municipal sludge. *Biomass Bioenerg.*, 32, 162-167.

- Griffin, M.E., McMahon, K.D., Mackie, R.I., Raskin, L., 1998. Methanogenic population dynamics during start-up of anaerobic digesters treating municipal solid waste and biosolids. *Biotechnol. Bioeng.*, 57, 342-355.
- Gu, Y., Jerome, F., 2010. ChemInform Abstract: Glycerol as a Sustainable Solvent for Green Chemistry. *ChemInform*, 41.
- Hansen, A.C., Zhang, Q., Lyne, P.W.L., 2005. Ethanol-diesel fuel blends-a review. *Bioresour. Technol.*, 96, 277-285.
- Hartmann, H., Ahring, B.K., 2005. Anaerobic digestion of the organic fraction of municipal solid waste: Influence of co-digestion with manure. *Water Res.*, 39, 1543-1552.
- Hattori, S., 2007. Syntrophic acetate-oxidizing microbes in methanogenic environments. *Microbes Environ.*, 23, 118-127.
- Henze, M., Gujer, W., Mino, T., Loosdrecht, M.V., 2000. Activated Sludge Models ASM1,ASM2,ASM2d and ASM3. IWA.
- Hill, D.T., Barth, C.L., 1977. A Dynamic Model for Simulation of Animal Waste Digestion. *J. Water Pollut. Con. F.*, 49, 2129-2143.
- Holm-Nielsen, J.B., Lomborg, C.J., Oleskowicz-Popiel, P., Esbensen, K.H., 2008. On-line near infrared monitoring of glycerol-boosted anaerobic digestion processes: Evaluation of process analytical technologies. *Biotechnol. Bioeng.*, 99, 302-313.
- Hori, T., Haruta, S., Ueno, Y., Ishii, M., Igarashi, Y., 2006. Dynamic transition of a methanogenic population in response to the concentration of volatile fatty acids in a thermophilic anaerobic digester. *Appl. Environ. Microbiol.*, 72, 1623-1630.
- Hosseini Koupaie, E., Barrantes Leiva, M., Eskicioglu, C., Dutil, C., 2014. Mesophilic batch anaerobic co-digestion of fruit-juice industrial waste and municipal waste sludge: Process and cost-benefit analysis. *Bioresour. Technol.*, 152, 66-73.
- Husain, A., 1998. Mathematical models of the kinetics of anaerobic digestion-a selected review. *Biomass Bioenerg.*, 14, 561-571.
- Iacovidou, E., Ohandja, D.-G., Voulvoulis, N., 2012. Food waste co-digestion with sewage sludge-Realising its potential in the UK. *J. Environ. Manage.*, 112, 267-274.
- Ike, M., Inoue, D., Miyano, T., Liu, T.T., Sei, K., Soda, S., Kadoshin, S., 2010. Microbial population dynamics during startup of a full-scale anaerobic digester treating industrial food waste in Kyoto eco-energy project. *Bioresour. Technol.*, 101, 3952-3957.

Ito, T., Nakashimada, Y., Senba, K., Matsui, T., Nishio, N., 2005. Hydrogen and ethanol production from glycerol-containing wastes discharged after biodiesel manufacturing process. *J. Biosci. Bioeng.*, 100, 260-265.

Jackson, B. E., and McInerney, M. J. 2002. "Anaerobic microbial metabolism can proceed close to thermodynamic limits." *Nature*, 415(6870), 454-456.

Johnson, T., Shea, T., Gabel, D., Forbes, B., 2011. Introducing FOG to solids, *Water Environ. Technol. Magaz.*

Kabouris, J.C., Tezel, U., Pavlostathis, S.G., Engelmann, M., Dulaney, J.A., Todd, A.C., Gillette, R.A., 2009. Mesophilic and Thermophilic Anaerobic Digestion of Municipal Sludge and Fat, Oil, and Grease. *Water Environ. Res.*, 81, 476-485.

Kabouris, J.C., Tezel, U., Pavlostathis, S.G., Engelmann, M., Todd, A.C., Gillette, R.A., 2008. The anaerobic biodegradability of municipal sludge and fat, oil, and grease at mesophilic conditions. *Water Environ. Res.*, 80, 212-221.

Kalloum, S., Bouabdessalem, H., Touzi, A., Iddou, A., Ouali, M.S., 2011. Biogas production from the sludge of the municipal wastewater treatment plant of Adrar city (southwest of Algeria). *Biomass Bioenerg.*, 35, 2554-2560.

Karakashev, D., Batstone, D.J., Angelidaki, I., 2005. Influence of environmental conditions on methanogenic compositions in anaerobic biogas reactors. *Appl. Environ. Microbiol.*, 71, 331-338.

Karakashev, D., Batstone, D.J., Trably, E., Angelidaki, I., 2006. Acetate oxidation is the dominant methanogenic pathway from acetate in the absence of Methanosaetaceae. *Appl. Environ. Microbiol.*, 72, 5138-5141.

Kiepper, B., Governo, J., Zacharias, H., 2001. Characterization of the Generation, Handling and Treatment of Spent Fat, Oil, and Grease (FOG) from Georgia's Food Service Industry Trans. G. The Pollution Prevention Assistance Division Department of Natural Resources Atlanta. The University of Georgia.

Kim, S., Bae, J., Choi, O., Ju, D., Lee, J., Sung, H., Park, S., Sang, B.-I., Um, Y., 2014. A pilot scale two-stage anaerobic digester treating food waste leachate (FWL): Performance and microbial structure analysis using pyrosequencing. *Process Biochem.*, 49, 301-308.

Kleerebezem, R., Van Loosdrecht, M., 2006. Waste characterization for implementation in ADM1. *Water Sci. Technol.*, 54, 167-174

Knezevic, Z., Mavinic, D.S., Anderson, B.C., 1995. Pilot Scale Evaluation of Anaerobic Codigestion of Primary and Pretreated Waste Activated Sludge. *Water Environ. Res.*, 67, 835-841.

- Komemoto, K., Lim, Y., Nagao, N., Onoue, Y., Niwa, C., Toda, T., 2009. Effect of temperature on VFAs and biogas production in anaerobic solubilization of food waste. *Waste Manage.*, 29, 2950-2955.
- Kotsopoulos, T., Karamanlis, X., Dotas, D., Martzopoulos, G., 2008. The impact of different natural zeolite concentrations on the methane production in thermophilic anaerobic digestion of pig waste. *Biosystems Engineer.*, 99, 105-111.
- Kundu, K., Bergmann, I., Klocke, M., Sharma, S., Sreekrishnan, T.R., 2014. Impact of abrupt temperature increase on the performance of an anaerobic hybrid bioreactor and its intrinsic microbial community. *Bioresour. Technol.*, 47.
- Lawrence, A.W., McCarty, P.L., 1969. Kinetics of Methane Fermentation in Anaerobic Treatment. *Water Pollution Control Federation*, 41, R1-R17.
- Leclerc, M., Delgènes, J.-P., Godon, J.-J., 2004. Diversity of the archaeal community in 44 anaerobic digesters as determined by single strand conformation polymorphism analysis and 16S rDNA sequencing. *Environ. Microb.*, 6, 809-819.
- Lee, C., Kim, J., Shin, S.G., OFlaherty, V., Hwang, S., 2010. Quantitative and qualitative transitions of methanogen community structure during the batch anaerobic digestion of cheese-processing wastewater. *Appl. Microb Biotechnol.*, 87, 1963-1973.
- Lee, S.-H., Park, J.-H., Kang, H.-J., Lee, Y.H., Lee, T.J., Park, H.-D., 2013. Distribution and abundance of Spirochaetes in full-scale anaerobic digesters. *Bioresour. Technol.*, 145, 25-32.
- Leoneti, A.B., Aragao-Leoneti, V., De Oliveira, S.V.W.B., 2012. Glycerol as a by-product of biodiesel production in Brazil: Alternatives for the use of unrefined glycerol. *Renew. Energ.*, 45, 138-145.
- Li, C., Champagne, P., Anderson, B.C., 2011. Evaluating and modeling biogas production from municipal fat, oil, and grease and synthetic kitchen waste in anaerobic co-digestions. *Bioresour. Technol.*, 102, 9471-9480.
- Lin, J., Zuo, J., Ji, R., Chen, X., Liu, F., Wang, K., Yang, Y., 2012. Methanogenic community dynamics in anaerobic co-digestion of fruit and vegetable waste and food waste. *J. Environ. Sci.*, 24, 1288-1294.
- Liu, X., Gao, X., Wang, W., Zheng, L., Zhou, Y., Sun, Y., 2012. Pilot-scale anaerobic co-digestion of municipal biomass waste: Focusing on biogas production and GHG reduction. *Renew Energ.*, 44, 463-468.

Liu, X., Liu, H., Chen, Y., Du, G., Chen, J., 2008. Effects of organic matter and initial carbon-nitrogen ratio on the bioconversion of volatile fatty acids from sewage sludge. *J.Chem. Technol. Biot.*, 83, 1049-1055.

Long, J.H., Aziz, T.N., Reyes Iii, F.L.d.l., Ducoste, J.J., 2012. Anaerobic co-digestion of fat, oil, and grease (FOG): A review of gas production and process limitations. *Process Saf. Environ.*, 90, 231-245.

Luostarinen, S., Luste, S., Sillanpää, M., 2009. Increased biogas production at wastewater treatment plants through co-digestion of sewage sludge with grease trap sludge from a meat processing plant. *Bioresour. Technol.*, 100, 79-85.

Lyberatos, G., Skiadas, I.V., 1999. Modeling of Anaerobic Digestion- A Review. *Global Nest: the Int. J.*, 1, 63-76.

Ma, J., Van Wambeke, M., Carballa, M., Verstraete, W., 2008. Improvement of the anaerobic treatment of potato processing wastewater in a UASB reactor by co-digestion with glycerol. *Biotechnol. Lett.*, 30, 861-867.

Macias-Corral, M., Samani, Z., Hanson, A., Smith, G., Funk, P., Yu, H., Longworth, J., 2008. Anaerobic digestion of municipal solid waste and agricultural waste and the effect of co-digestion with dairy cow manure. *Bioresour. Technol.*, 99, 8288-8293.

Mairet, F., Bernard, O., Ras, M., Lardon, L., Steyer, J.-P., Modeling anaerobic digestion of microalgae using ADM1. *Bioresour. Technol.*, 102, 6823-6829.

Marsh, S., 2007. Pyrosequencing applications. *Methods Mol Biol*, 373: 15-24.

Martín-González, L., Castro, R., Pereira, M.A., Alves, M.M., Font, X., Vicent, T., 2011. Thermophilic co-digestion of organic fraction of municipal solid wastes with FOG wastes from a sewage treatment plant: Reactor performance and microbial community monitoring. *Bioresour. Technol.*, 102, 4734-4741.

Martínez, E.J., Fierro, J., Sánchez, M.E., Gómez, X., 2012. Anaerobic co-digestion of FOG and sewage sludge: Study of the process by Fourier transform infrared spectroscopy. *Int. Biodeteri. Biodegr.*, 75, 1-6.

Mata-Alvarez, J., Dosta, J., Romero-Güiza, M.S., Fonoll, X., Peces, M., Astals, S., 2014. A critical review on anaerobic co-digestion achievements between 2010 and 2013. *Renewable and Sustainable Energy Reviews*, 36, 412-427.

McMahon, K.D., Stroot, P.G., Mackie, R.I., Raskin, L., 2001. Anaerobic codigestion of municipal solid waste and biosolids under various mixing conditionsII: microbial population dynamics. *Water Res.*, 35, 1817-1827.

- McMahon, K.D., Zheng, D., Stams, A.J., Mackie, R.I., Raskin, L., 2004. Microbial population dynamics during start-up and overload conditions of anaerobic digesters treating municipal solid waste and sewage sludge. *Biotechnol. Bioeng.*, 87, 823-834.
- Megonigal, J., Mines, M., Visscher, P., 2005. Linkages to Trace Gases and Aerobic Processes. *Biogeochem.*, 8, 317.
- Megonigal, J.P., Hines, M.E., Visscher, P.T., 2004. Anaerobic Metabolism: Linkages to Trace Gases and Aerobic Processes. in: S.W. H. (Ed.) *Biogeochem.*. Elsevier-Pergamon, Oxford, pp. p.317-424.
- Meta-Alvarez, J., 2003. Biomethanization of the Organic Fraction of Municipal Solid Wastes. IWA Publishing, London.
- National Biodiesel Board, 2014. <http://www.biodiesel.org/production/production-statistics>. Accessed in July 2014.
- Neves, L., Oliveira, R., Alves, M.M., 2009. Fate of LCFA in the co-digestion of cow manure, food waste and discontinuous addition of oil. *Water Res.*, 43, 5142-5150.
- Nuchdang, S., Phalakornkule, C., 2012. Anaerobic digestion of glycerol and co-digestion of glycerol and pig manure. *J. Environ. Manage.*, 101, 164-172.
- O'Reilly, C., Colleran, E., 2006. Effect of influent COD/SO₄(²⁻) ratios on mesophilic anaerobic reactor biomass populations: physico-chemical and microbiological properties. *FEMS Microbiol Ecol.*, 56, 141-153.
- Padmasiri, S.I., Zhang, J., Fitch, M., Norddahl, B., Morgenroth, E., Raskin, L., 2007. Methanogenic population dynamics and performance of an anaerobic membrane bioreactor (AnMBR) treating swine manure under high shear conditions. *Water Res.*, 41, 134-144.
- Page, D., Hickey, K., Narula, R., Main, A., Grimberg, S., 2008. Modeling anaerobic digestion of dairy manure using the IWA Anaerobic Digestion Model no. 1 (ADM1). *Water Sci. Technol.*, 58, 689-695.
- Palatsi, J., Illa, J., Prenafeta-Boldú, F.X., Laureni, M., Fernandez, B., Angelidaki, I., Flotats, X., 2010. Long-chain fatty acids inhibition and adaptation process in anaerobic thermophilic digestion: Batch tests, microbial community structure and mathematical modelling. *Bioresour. Technol.*, 101, 2243-2251.
- Pelletier, E., Kreimeyer, A., Bocs, S., Rouy, Z., Gyapay, G., Chouari, R., Rivière, D., Ganesan, A., Daegelen, P., Sghir, A., 2008. "Candidatus Cloacamonas acidaminovorans": genome sequence reconstruction provides a first glimpse of a new bacterial division. *J. Bacteriol.*, 190, 2572-2579.

- Pereira, M.A., Pires, O.C., Mota, M., Alves, M.M., 2005. Anaerobic biodegradation of oleic and palmitic acids: Evidence of mass transfer limitations caused by long chain fatty acid accumulation onto the anaerobic sludge. *Biotechnol. Bioeng.*, 92, 15-23.
- Pereira, M.A., Roest, K., Stams, A.J., Mota, M., Alves, M., Akkermans, A.D., 2002. Molecular monitoring of microbial diversity in expanded granular sludge bed (EGSB) reactors treating oleic acid. *FEMS Microbiol. Ecol.*, 41, 95-103.
- Pereira, M.A., Sousa, D.Z., Mota, M., Alves, M.M., 2004. Mineralization of LCFA associated with anaerobic sludge: Kinetics, enhancement of methanogenic activity, and effect of VFA. *Biotechnol. Bioeng.*, 88, 502-511.
- Pervin, H.M., Dennis, P.G., Lim, H.J., Tyson, G.W., Batstone, D.J., Bond, P.L., 2013. Drivers of microbial community composition in mesophilic and thermophilic temperature-phased anaerobic digestion pre-treatment reactors. *Water Res.*, 47, 7098-7108.
- Ponsa', S., Gea, T., Sa'nchez, A., 2011. Anaerobic co-digestion of the organic fraction of municipal solid waste with several pure organic co-substrates. *Biosystems Engin.*, 108, 352-360.
- Quispe, C.A., Coronado, C.J., Carvalho Jr, J.o.A., 2013. Glycerol: Production, consumption, prices, characterization and new trends in combustion. *Renewable and Sustainable Energy Reviews*, 27, 475-493.
- Ramirez, I., Mottet, A., Carrère, H., Déléris, S., Vedrenne, F., and Steyer, J.-P. 2009a. Modified ADM1 disintegration/hydrolysis structures for modeling batch thermophilic anaerobic digestion of thermally pretreated waste activated sludge. *Water Research*, 43: 3479-3492.
- Ramirez, I., Volcke, E.I.P., Rajinikanth, R., Steyer, J.-P., 2009b. Modeling microbial diversity in anaerobic digestion through an extended ADM1 model. *Water Res.*, 43, 2787-2800.
- Raskin, L., Poulsen, L.K., Noguera, D.R., Rittmann, B.E., Stahl, D.A., 1994. Quantification of methanogenic groups in anaerobic biological reactors by oligonucleotide probe hybridization. *Appl. and Environ. Microb.*, 60, 1241-1248.
- Razaviarani, V., Buchanan, I.D., Malik, S., Katalambula, H., 2013a. Pilot-scale anaerobic co-digestion of municipal wastewater sludge with restaurant grease trap waste. *J. Environ. Manage.*, 123, 26-33.
- Razaviarani, V., Buchanan, I.D., Malik, S., Katalambula, H., 2013b. Pilot scale anaerobic co-digestion of municipal wastewater sludge with biodiesel waste glycerin. *Bioresour. Technol.*, 133, 206-212.

Rincón, B., Borja, R., González, J.M., Portillo, M.C., Sáiz-Jiménez, C., 2008. Influence of organic loading rate and hydraulic retention time on the performance, stability and microbial communities of one-stage anaerobic digestion of two-phase olive mill solid residue. *Biochem. Eng. J.*, 40, 253-261.

Robra, S., Serpa da Cruz, R., de Oliveira, A.M., Neto, J.A.A., Santos, J.V., 2010. Generation of biogas using crude glycerin from biodiesel production as a supplement to cattle slurry. *Biomass and Bioenerg.*, 34, 1330-1335.

Salerno, M., and Parry, D. 2009. "Waste Characterization Technical Memorandum-PhaseII."

Schwarzenbeck, N., Bomball, E., Pfeiffer, W., 2008. Can a wastewater treatment plant be a powerplant? A case study. *Water Sci. Technol.*, 57, 1555-1561.

Serrano, A., Siles, J.A., Chica, A.F., Martín, M.A., 2014. Improvement of mesophilic anaerobic co-digestion of agri-food waste by addition of glycerol. *J. Environ. Manage.*, 140, 76-82.

Siegrist, H., Vogt, D., Garcia-Heras, J.L., Gujer, W., 2002. Mathematical model for meso- and thermophilic anaerobic sewage sludge digestion. *Environ. Sci. Technol.*, 36, 1113-1123.

Siles, J.A., Martín, M.A., Chica, A.F., Martín, A., 2010. Anaerobic co-digestion of glycerol and wastewater derived from biodiesel manufacturing. *Bioresour. Technol.*, 101, 6315-6321.

Siles López, J.Á., Martín Santos, M.d.l.Á., Chica Pérez, A.F., Martín Martín, A., 2009. Anaerobic digestion of glycerol derived from biodiesel manufacturing. *Bioresour. Technol.*, 100, 5609-5615.

Silvestre, G., Rodríguez-Abalde, A., Fernández, B., Flotats, X., Bonmatí, A., 2011. Biomass adaptation over anaerobic co-digestion of sewage sludge and trapped grease waste. *Bioresour. Technol.*, 102, 6830-6836.

Slinn, M., Kendall, K., Mallon, C., Andrews, J., 2008. Steam reforming of biodiesel by-product to make renewable hydrogen. *Bioresour. Technol.*, 99, 5851-5858.

Sun, L., Müller, B., Westerholm, M., Schnürer, A., 2014. Syntrophic acetate oxidation in industrial CSTR biogas digesters. *J. Biotechnol.*, 171, 39-44.

Supaphol, S., Jenkins, S.N., Intomo, P., Waite, I.S., O'Donnell, A.G., 2011. Microbial community dynamics in mesophilic anaerobic co-digestion of mixed waste. *Bioresour. Technol.*, 102, 4021-4027.

Tang, B., Yu, L., Huang, S., Luo, J., Zhuo, Y., 2010. Energy efficiency of pre-treating excess sewage sludge with microwave irradiation. *Bioresour. Technol.*, 101, 5092-5097.

Tang, Y., Shigematsu, T., Morimura, S., Kida, K., 2005. Microbials Community Analysis of Mesophilic Anaerobic Protein Degradation Process Using Bovine Serum Albumin (BSA)-Fed Continuous Cultivation. *Biosci. Bioengineer.*, 99, 150-164.

Tenchov, B., Vescio, E.M., Sprott, G.D., Zeidel, M.L., Mathai, J.C., 2006. Salt tolerance of archaeal extremely halophilic lipid membranes. *J. Biol. Chem.*, 281, 10016-10023.

Thakuria, D., Schmidt, O., Mac Siáirtín, M., Egan, D., Doohan, F.M., 2008. Importance of DNA quality in comparative soil microbial community structure analyses. *Soil Biolog. Biochem.*, 40, 1390-1403.

Tokumoto, H., Tanaka, M., 2012. Novel anaerobic digestion induced by bacterial components for value-added byproducts from high-loading glycerol. *Bioresour. Technol.*, 107, 327-332.

Tost, J., and Gut, I.G., 2007. DNA methylation analysis by pyrosequencing. *Nat. Protocols*, 2: 2265-2275.

Wan, C., Zhou, Q., Fu, G., Li, Y., 2011. Semi-continuous anaerobic co-digestion of thickened waste activated sludge and fat, oil and grease. *Waste Manage.*, 31, 1752-1758.

Ward, A.J., Hobbs, P.J., Holliman, P.J., Jones, D.L., 2008. Optimisation of the anaerobic digestion of agricultural resources. *Bioresour. Technol.*, 99, 7928-7940.

Watanabe, R., Tada, C., Baba, Y., Fukuda, Y., Nakai, Y., 2013. Enhancing methane production during the anaerobic digestion of crude glycerol using Japanese cedar charcoal. *Bioresour. Technol.*, 150, 387-392.

Weiss, M.S., Abele, U., Weckesser, J., Welte, W., Schiltz, E., Schulz, G.E., 1991. Molecular Architecture and Electrostatic Properties of a Bacterial Porin. *Science* 254, 1627-1630.

Wu, X.L., Chin, K.J., Stubner, S., Conrad, R., 2001. Functional patterns and temperature response of cellulose-fermenting microbial cultures containing different methanogenic communities. *Appl. Microbiol Biotechnol.*, 56, 212-219.

Yang, Y., Tsukahara, K., Sawayama, S., 2008. Biodegradation and methane production from glycerol-containing synthetic wastes with fixed-bed bioreactor under mesophilic and thermophilic anaerobic conditions. *Process Biochem.*, 43, 362-367.

Yasui, H., Goel, R., Li, Y., Noike, T., 2008. Modified ADM1 structure for modelling municipal primary sludge hydrolysis. *Water Res.*, 42, 249-259.

Yazdani, S.S., Gonzalez, R., 2007. Anaerobic fermentation of glycerol: a path to economic viability for the biofuels industry. *Curr. Opin. Biotechnol.*, 18, 213-219.

Yuan, Q., Sparling, R., Oleszkiewicz, J.A., 2011. VFA generation from waste activated sludge: Effect of temperature and mixing. *Chemosphere*, 82, 603-607.

Zhu, Z., Hsueh, M.K., He, Q., 2011. Enhancing biomethanation of municipal waste sludge with grease trap waste as a co-substrate. *Renew. Energ.*, 36, 1802-1807.

Ziganshin, A.M., Schmidt, T., Scholwin, F., Il'inskaya, O.N., Harms, H., Kleinsteuber, S., 2010. Bacteria and archaea involved in anaerobic digestion of distillers grains with solubles. *Appl. Microbiol. Biotechnol.*, 89, 2039-2052.

Ziganshin, A.M., Liebetrau, J., Pröter, J., Kleinsteuber, S., 2013. Microbial community structure and dynamics during anaerobic digestion of various agricultural waste materials. *Appl. Microbiol. Biotechnol.*, 97, 5161-5174.

Wang, H., Tolvanen, K., Lehtomäki, A., Puhakka, J., Rintala, J., 2010. Microbial community structure in anaerobic co-digestion of grass silage and cow manure in a laboratory continuously stirred tank reactor. *Biodegrad.*, 21, 135-146.

APENDIX A: Pilot-Scale Supplementary Data

Pilot-Scale setup:



Figure A1. The Pilot Trailer



Figure A2. Pilot Anaerobic Digesters



Figure A3. Mixing and Feeding Tanks

A.1. GTW Co-digestion

The daily biogas production per unit digester active volume of the test and control digesters is shown in Figure A1.1 throughout the study period.

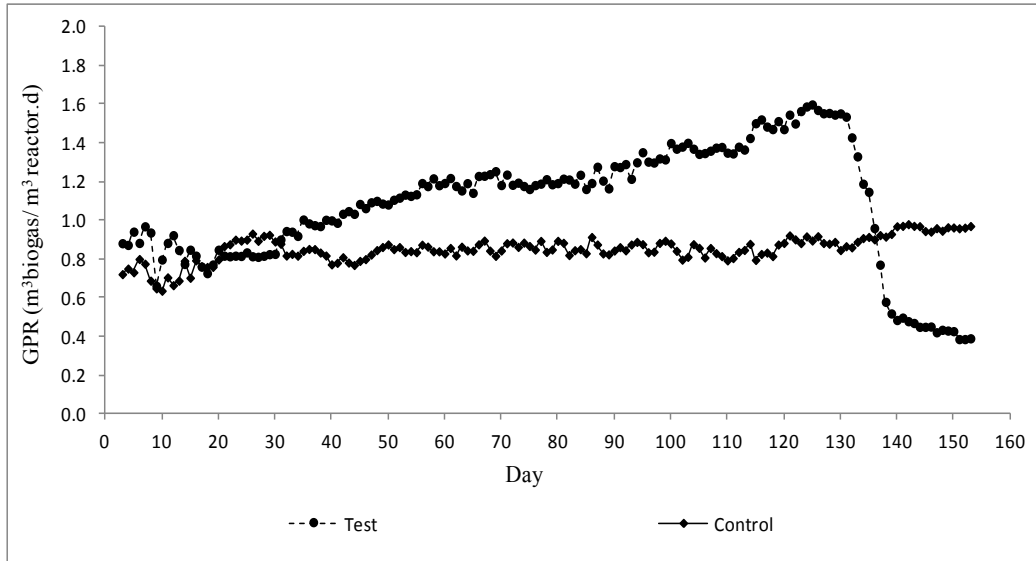


Figure A1.1. Daily biogas production per unit reactor volume of control and test digesters.

The control and test digesters received blended sludge during the first 30 days. The control digester continued to receive the blended sludge throughout the test period. However, the test digester received restaurant grease in addition to the blended sludge beginning at day 30. Data collected during the final 10 days at each loading level was used to calculate digester performance.

True steady state could not be achieved because of the changes in the influent sludge characteristics. Unlike bench-scale studies, which involve smaller feed volumes that can be stored under conditions that preserve their characteristics, the larger volumes of sludge required in the pilot-scale study (approximately 150 L per day including the piping hold-up) required that fresh samples be obtained daily from the on-site sludge blend tank. The control digester was operated throughout the 155 day study at the same loading rate and with the same type of feed (blended sludge from the full-scale plant). Because of the varying

characteristics of the blended sludge, comparisons are made between the test and control digester on an on-going basis. Quasi steady state was deemed to prevail when coefficient of variation of effluent COD and VS daily measurements was less than 5%. The variability of the test and control digester effluents in terms of COD and VS are shown graphically and statistically in the tables and figures.

The variation in effluent COD concentrations of the test and control digesters during the final 10 days of the nominal 100% loading period is illustrated in Figures A1.2 and A1.3, respectively.

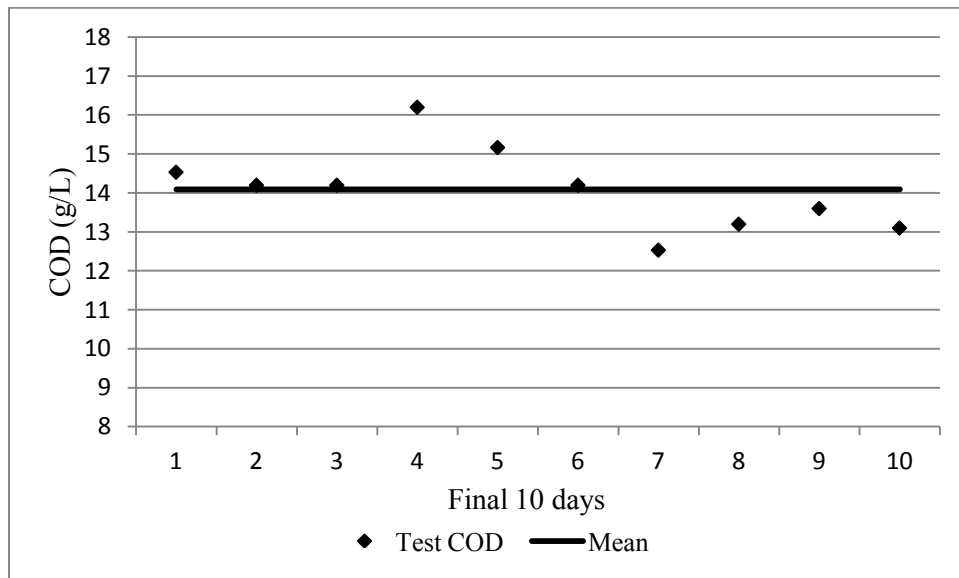


Figure A1.2. Deviation of test digester effluent COD from its mean value during the final 10 days of the 100% loading.

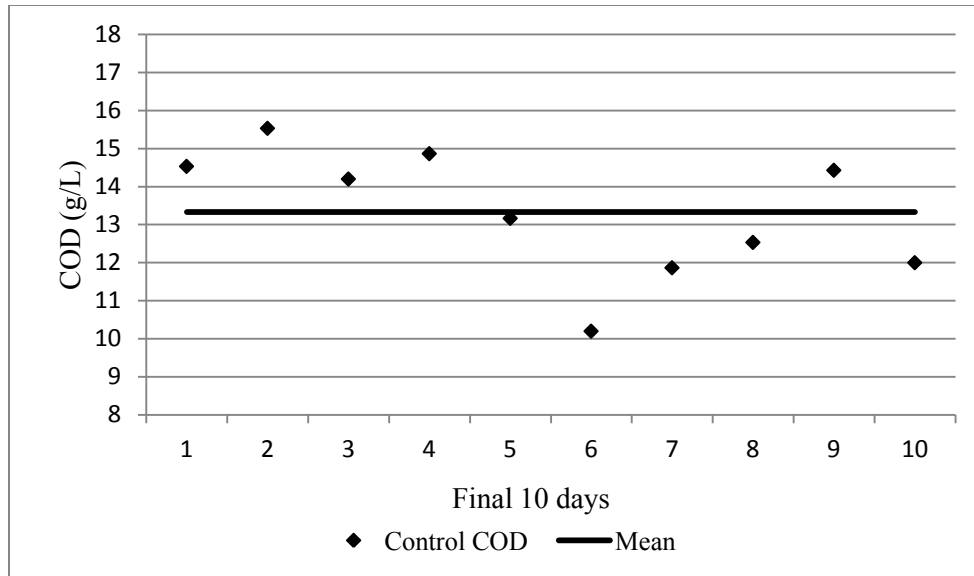


Figure A1.3: Deviation of control digester effluent COD from its mean value during the final 10 days of the 100% loading.

The mean value of effluent COD, its standard deviation and coefficient of variation for the test and control digesters during the final 10 days of the 100% loading period are shown in Table A1.1.

Table A1.1. Statistical measures of effluent COD variability during the final 10 days of the nominal 100% loading period.

Effluent	Mean	Std. Dev	COV
COD	(g/L)	(g/L)	(%)
Control	13.3	1.67	12.5
Test	14.1	1.07	7.6

The VS concentrations in the test and control digester effluents during the final 10 days of the nominal 100% loading period are shown in Figures A1.4 and A5.

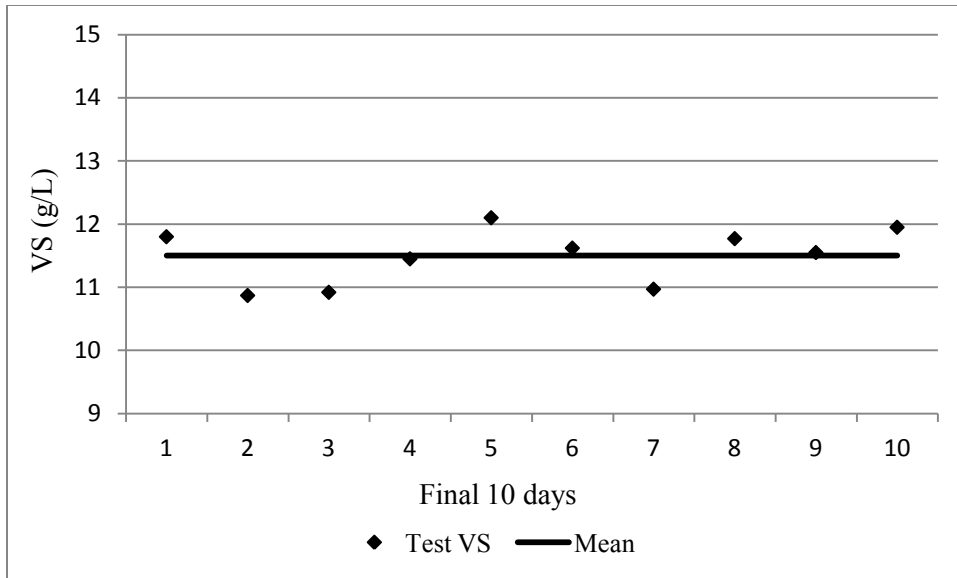


Figure A1.4. Deviation of test digester effluent VS from its mean value during the final 10 days of the 100% loading.

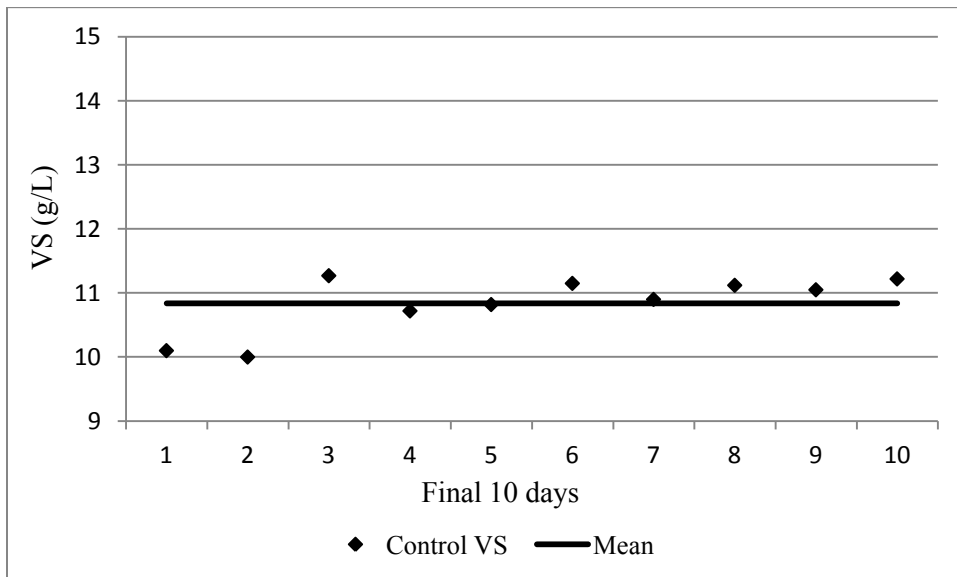


Figure A1.5. Deviation of control digester effluent VS from its mean value during the final 10 days of the 100% loading.

The mean value of effluent VS, its standard deviation and coefficient of variation for the test and control digesters during the final 10 days of the nominal 100% loading period are shown in Table A1.2.

Table A1.2. Statistical measures of effluent VS variability during the final 10 days of the nominal 100% loading period.

Effluent	Mean	Std. Dev	COV
VS	(g/L)	(g/L)	(%)
Control	10.8	0.4	4.1
Test	11.5	0.4	3.8

The variation in effluent COD concentrations of the test and control digesters during the final 10 days of the nominal 190% loading period is illustrated in Figures A1.6 and A1.7, respectively.

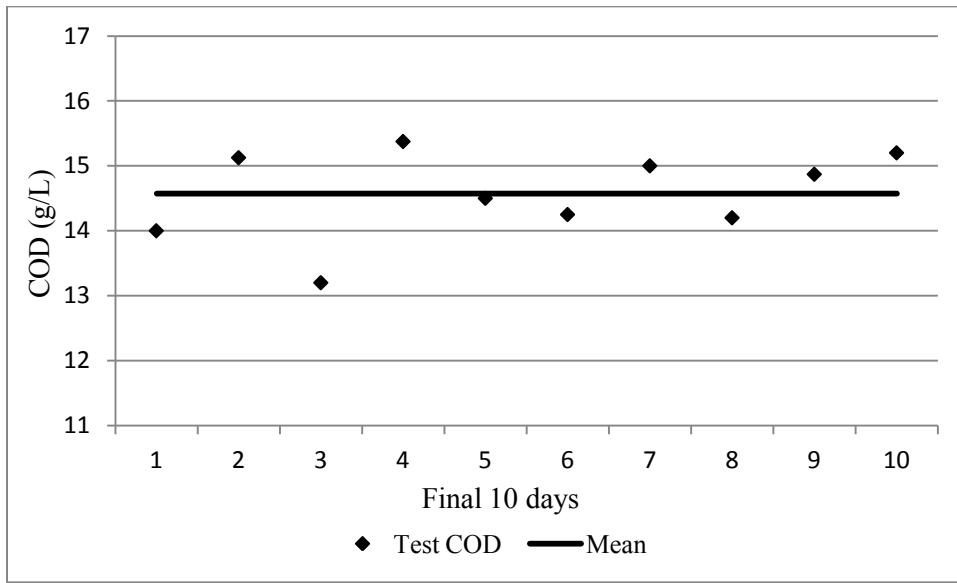


Figure A1.6. Deviation of test digester effluent COD from its mean value during the final 10 days of the 190% loading.

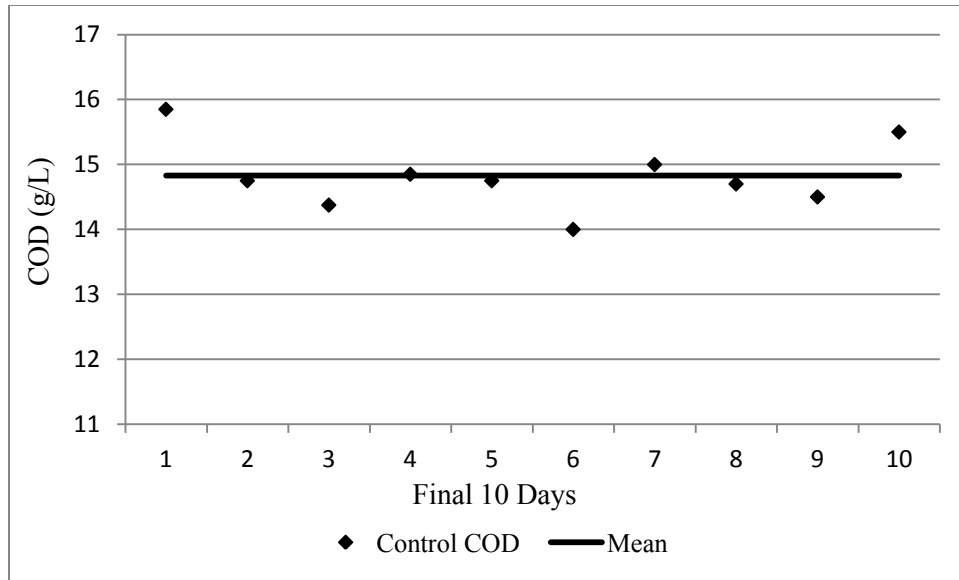


Figure A1.7. Deviation of control digester effluent COD from its mean value during the final 10 days of the 190% loading.

The mean value of effluent COD, its standard deviation and coefficient of variation for the test and control digesters during the final 10 days of the nominal 190% loading period are shown in Table A1.3.

Table A1.3. Statistical measures of effluent COD variability during the final 10 days of the nominal 190% loading period.

Effluent	Mean	Std. Dev	COV
COD	(g/L)	(g/L)	(%)
Control	14.8	0.5	3.6
Test	14.6	0.7	4.6

The VS concentrations in the test and control digester effluents during the final 10 days of the nominal 190% loading period are shown in Figures A1.8 and A1.9.

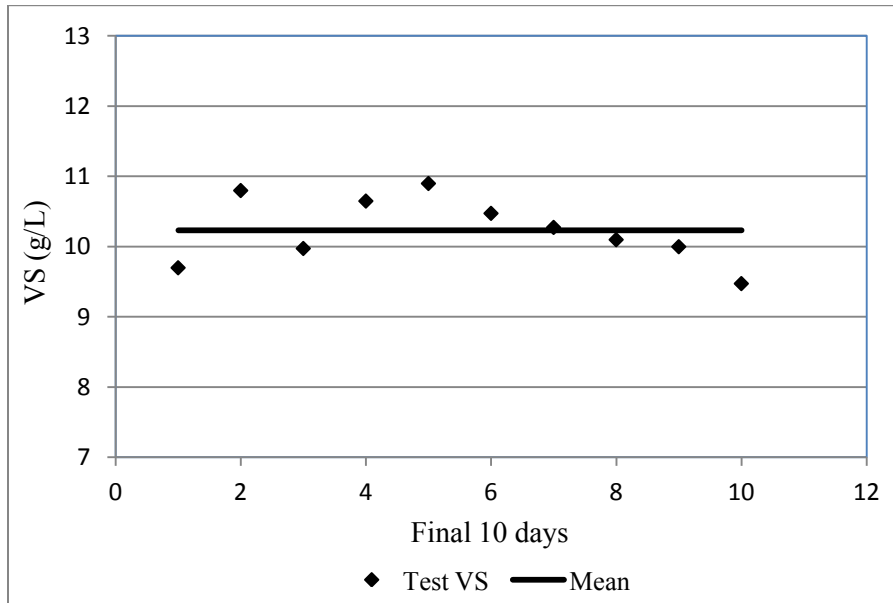


Figure A1.8. Deviation of test digester effluent VS from its mean value during the final 10 days of the 190% loading

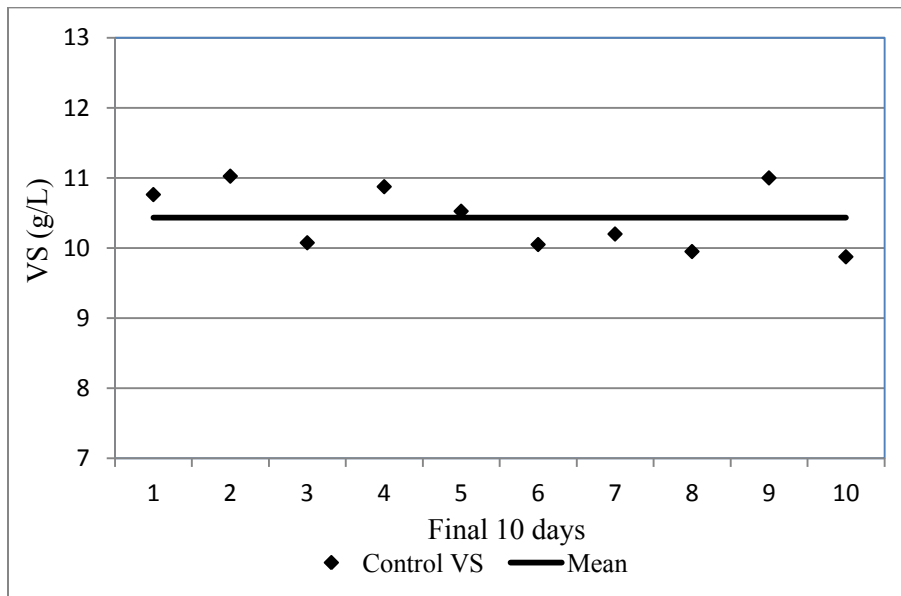


Figure A1.9. Deviation of control digester effluent VS from its mean value during the final 10 days of the 190% loading.

The mean value of effluent VS, its standard deviation and coefficient of variation for the test and control digesters during the final 10 days of the nominal 190% loading period are shown in Table A1.4.

Table A1.4. Statistical measures of effluent VS variability during the final 10 days of the nominal 190% loading period.

Effluent	Mean	Std. Dev	COV
VS	(g/L)	(g/L)	(%)
Control	10.4	0.5	4.4
Test	10.2	0.5	4.6

A.2. BGW Co-digestion

The control and test digesters received blended sludge during the first 30 days. The control digester continued to receive the blended sludge throughout the test period. However, the test digester received biodiesel waste glycerin in addition to the blended sludge beginning at day 30. Data collected during the final 10 days at each loading level was used to calculate digester performance. The daily measurements of influent and effluent COD concentrations throughout the study period are shown in Figure A2.1.

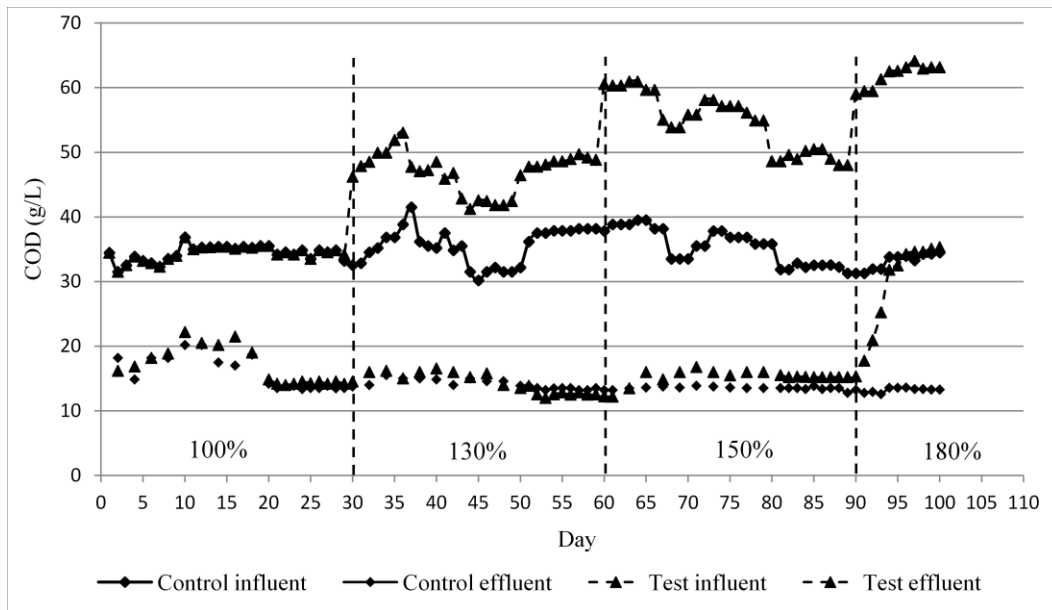


Figure A2.1. Influent and effluent COD concentrations throughout the study period.

Methane production in the control and test digesters was measured during the final 10 days of each test digester loading level and is shown in Figure A2.2. Other measurements that were made during the final 10 days of each test digester loading level are: the volatile solids concentrations in the influent and effluent of each digester (Figure A2.3); the total and partial alkalinity of each digester effluent (Figure A2.4); and the pH of each digester effluent (Figure A2.5).

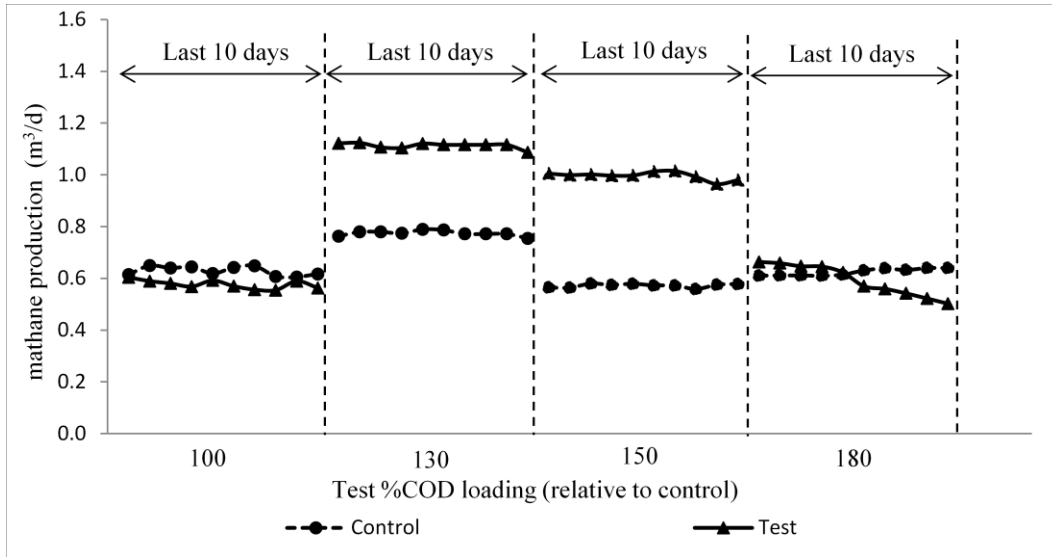


Figure A2.2. Daily methane production during the final 10 days of each loading level.

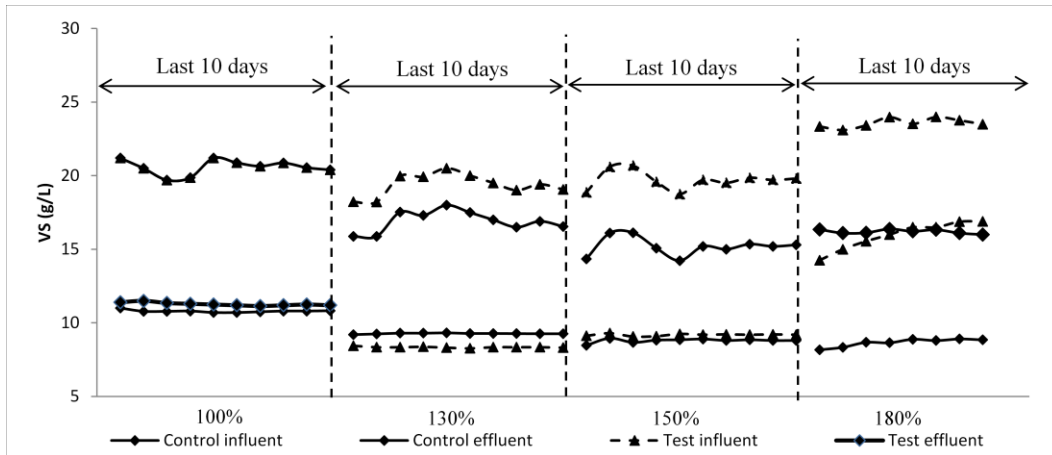


Figure A2.3. Daily influent and effluent volatile solids concentrations during the final 10 days of each loading level.

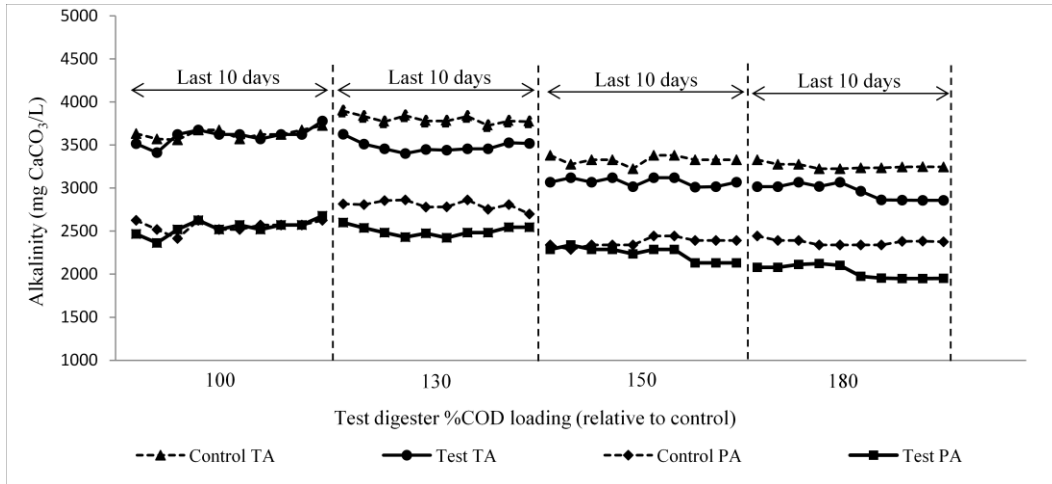


Figure A2.4. Total (TA) and partial (PA) alkalinity in each digester during the final 10 days of each test digester loading level.

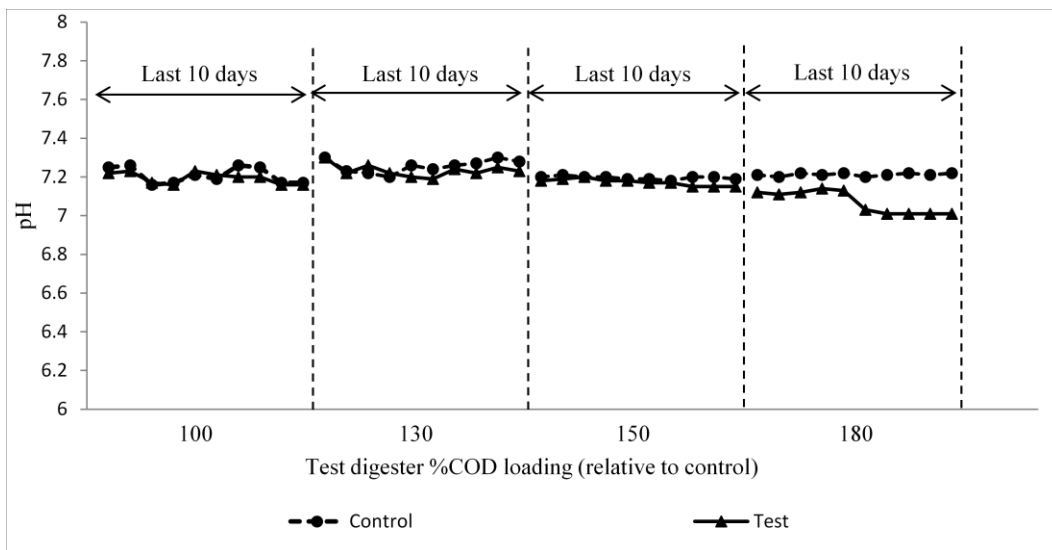


Figure A2.5. pH in each digester during the final 10 days of each test digester loading level.

APENDIX B: GTW Modeling Supplementary Data

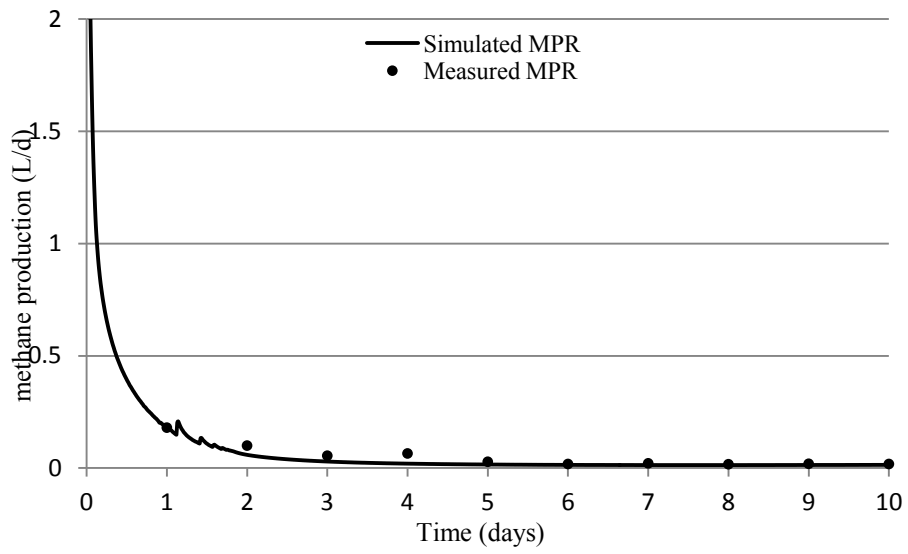
B.1. GTW Calibration Model

The initial concentration parameters represent the inoculum characteristics used in ADM1. These parameters have been adjusted through the simulation of full-scale anaerobic digester where the inoculum was sampled. The parameters which were adjusted in this study are listed in Table B1. The MPR curves obtained from the respirometry analysis and used throughout the study are also presented here in Figure B1.

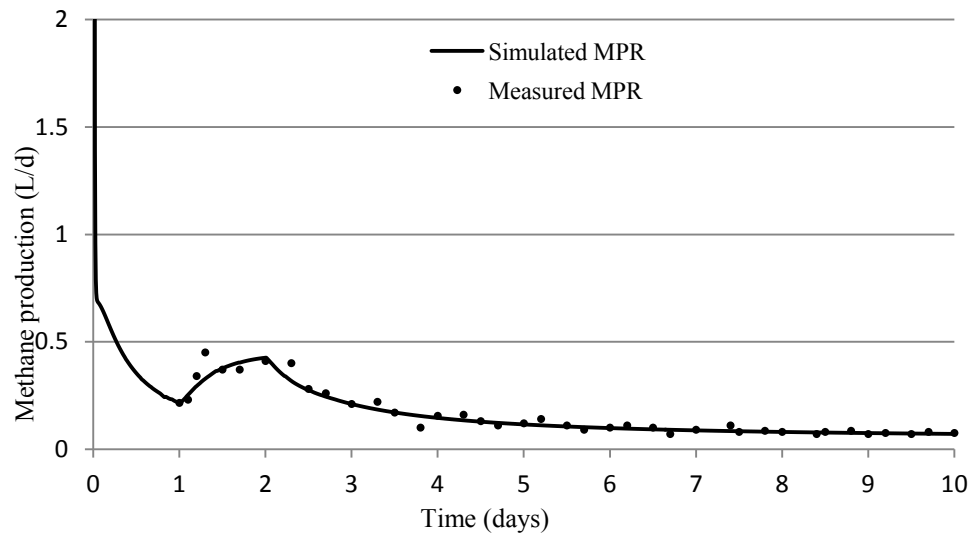
Table B1. Initial concentrations values in ADM1

Parameters	Symbol	Unit	Adjusted	Default
Initial methane	iS_{CH_4}	[mg COD/L]	51.0	50.0
Initial inorganic carbon	iS_{IC}	[mole C/m ³]	84.3	100
Initial inorganic nitrogen	iS_{IN}	[mgN/L]	929	3200
Initial total acetate	iS_{ac}	[mg COD/L]	5.54	180
Initial total propionate	iS_{pro}	[mg COD/L]	0.92	15
Initial total butyrate	iS_{bu}	[mg COD/L]	3.94	15
Initial total valerate	iS_{va}	[mg COD/L]	0.0	10
Initial monosaccharide	iS_{su}	[mg COD/L]	28.5	10
Initial amino acids	iS_{aa}	[mg COD/L]	6.22	5.0
Initial long chain fatty acids	iS_{fa}	[mg COD/L]	125	100
Initial soluble inerts	iS_i	[mg COD/L]	2710	5500
Initial composites	iX_c	[mg COD/L]	3080	5500
Initial carbohydrates	iX_{ch}	[mg COD/L]	50.6	50.0
Initial proteins	iX_{pr}	[mg COD/L]	34.0	50.0
Initial lipids	iX_{li}	[mg COD/L]	56.9	80.0
Initial sugar degraders	iX_{su}	[mg COD/L]	675	850
Initial amino acids degraders	iX_{aa}	[mg COD/L]	345	600
Initial LCFA degraders	iX_{fa}	[mg COD/L]	420	700
Initial valerate and butyrate degraders	iX_{C4}	[mg COD/L]	171	300
Initial propionate degraders	iX_{pro}	[mg COD/L]	100	135
Initial acetate degraders	iX_{ac}	[mg COD/L]	594	900
Initial hydrogen degraders	iX_{H_2}	[mg COD/L]	294	435

(a)



(b)



(c)

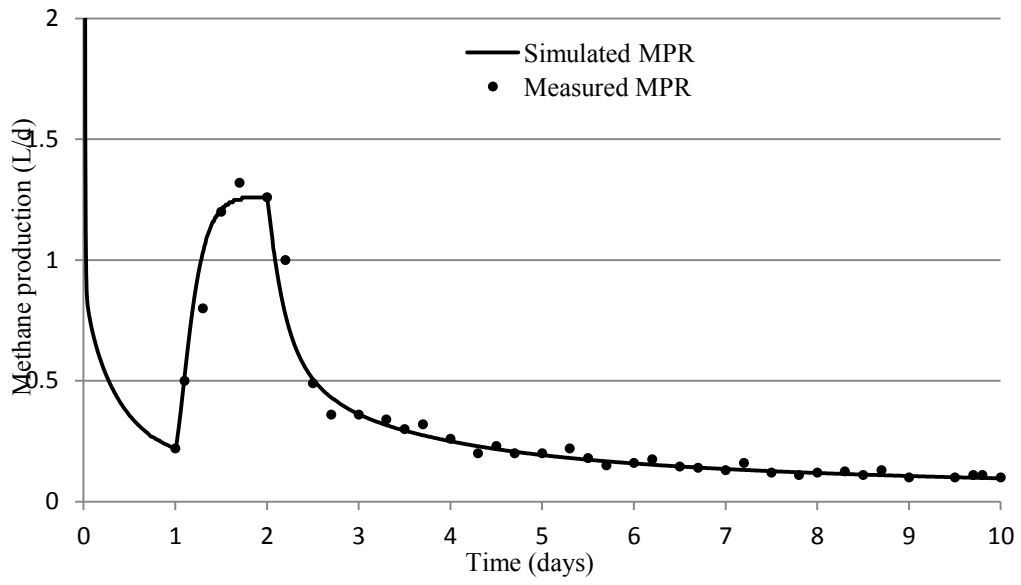


Figure B1. Methane production rates in respirometric batch experiments of (a) inoculum, (b) MSW, and (c) GTW+MWS.

APENDIX C: Microbial Supplementary Data

1- GTW co-digestion with MWS in bench-scale:

Table C-1.1. Total sequence abundance of bacteria and archaea in reactors

Total Sequence	Stage 1		Stage 2			Inoculum
	C 1	T 1	C 2	T 2	T 2'	
Bacteria	8224	5494	4841	4833	3990	9139
Archaea	5263	5103	2330	3592	3337	3309

Table C-1.2. Sequence numbers of archaeal phylogenetic groups in reactors.

Reactor		C-1	T-1	C-2	T-2	T-2'
% Loading		100	150	100	190	400
Number of sequences in the relevant genus						
Class	Genus (similarity %)	Stage 1		Stage 2		
<i>Methanomicrobia</i>	<i>Methanomicrobium (97)</i>	2210	1245	958	647	944
	<i>Methanospirillum (99)</i>	111	77	33	154	177
	<i>Methanoculleus (99)</i>	184	0	75	104	33
	<i>Methanosarcina (99)</i>	247	388	86	104	737
	<i>Methanosaeta (99)</i>	2310	3041	1114	2461	1161
<i>Methanobacteria</i>	<i>Methanobacterium (97)</i>	79	128	33	65	73
	<i>Methanosphaera (99)</i>	111	66	0	54	87
	<i>Methanobrevibacter (99)</i>	11	148	33	0	80
<i>Other</i>		0	10	0	4	43

Table C-1.3. Sequence numbers of phylogenetic groups of bacteria in the inoculum.

Phylum	Genus (similarity %)	Number of bacterial sequence reads
<i>Spirochaetes</i>	<i>Spaerochaeta</i> (95)	92
	<i>Candidatus Cloacamonas</i> (99)	7951
<i>Actinobacteria</i>	<i>Demequina</i> (99)	196
	<i>Dermatophilus</i> (92)	262
<i>Proteobacteria</i>	<i>Desulfarculus</i> (93)	151
	<i>Esherichia</i> (97)	292
<i>Chloroflexi</i>	<i>Anaerolinea</i> (95)	2
	<i>Caldilinea</i> (94)	10
<i>Other</i>		184

Table C-1.4. Sequence numbers of phylogenetic groups of bacteria in reactors.

Reactor		C-1	T-1	C-2	T-2	T-2'
% Loading		100	150	100	190	400
		Number of bacterial sequence reads				
Phylum	Genus (similarity %)	Stage 1		Stage 2		
<i>Spirochaetes</i>	<i>Spaerochaeta</i> (95)	33	22	15	14	0
	Candidatus <i>Cloacamonas</i> (99)	6744	4395	3979	3881	3148
<i>Actinobacteria</i>	<i>Demequina</i> (99)	16	0	15	0	0
	<i>Dermatophilus</i> (92)	164	82	58	77	56
<i>Proteobacteria</i>	<i>Desulfarculus</i> (93)	181	110	82	72	104
	<i>Esherichia</i> (97)	592	665	392	604	567
<i>Chloroflexi</i>	<i>Anaerolinea</i> (95)	189	115	116	111	40
	<i>Caldilinea</i> (94)	173	0	111	0	0
<i>Other</i>		132	104	73	72	76

Interpretation of the Canonical Correspondence Analysis Triplot

The outcome of the bacterial and archaeal CCA is represented in a triplot that displays environmental factors as arrows while genus and reactor (site) scores are shown as points. In the triplot shown in Figure 3, bacterial genera are shown as open triangles, archaeal genera as open circle and reactors as closed circles. The genera intend to be dominant in the sites (reactors) that are located near them and also be positioned close to the other genera which have distributional similarity to each other. For instance, reactors whose points are close to each other are environmentally similar. The proximity of a genus point to a reactor point is related to the relative abundance of that genus in that reactor environment compared to the genus relative abundance in other reactors. A genus located near a reactor tends to have a higher relative abundance of sequences in that reactor than it has in more distant reactors. The relative locations of genera indicate their distributional similarity to each other.

Environmental factor arrows radiate from the origin. The length of an environmental factor arrow indicates its importance to the ordination axis by which the microbial distribution can be explained, while the arrow direction indicates its correlation with each of the axes. The tail of an arrow can be extended through the origin away from its head. This is useful when estimating the degree of negative correlations. A small angle between the heads of arrows indicates the two environmental factors have a high degree of positive correlation. A small angle between the tails of two environmental factors (tails extended through the origin) means the two environmental variables have a high degree of negative correlation. The distance of a genus to an arrow indicates the approximate ranking of genus response to that environmental factor. A genus point that lies close to the origin is interpreted as the genus very little response to changes in environmental factors. The approximate ranking of a genus response to an environmental factor is higher than average when a perpendicular drawn from the species to the arrow lies on the same side of the origin as the head of the arrow, and is lower than average when the origin lies between the perpendicular drawn line and the head of the arrow.

2- BGW co-digestion with MWS in bench-scale:

Table C-2.1. Total sequence abundance of bacteria and archaea in reactors

Total Sequence	Phase 1		Phase 2			
	C 1	T 1	C 2	T 2	Inoculum	
Bacteria	8224	6343	4841	6056	3076	9139
Archaea	5263	5447	2390	6409	9258	3309

Table C-2.2. Sequence numbers of archaeal phylogenetic groups in reactors.

Reactor		C 1	T 1	C 2	T 2	T 2
% Loading		100	130	100	150	200
Number of sequences in the relevant genus						
Class	Genus (similarity %)	Phase 1		Phase 2		
<i>Methanomicrobia</i>	<i>Methanomicrobium (97)</i>	2210	89	983	4481	8861
	<i>Methanospirillum (99)</i>	111	209	33	44	0
	<i>Methanoculleus (99)</i>	183	0	76	102	28
	<i>Methanosarcina (99)</i>	248	296	88	159	18
	<i>Methanosaeta (99)</i>	2310	4679	1143	1517	314
<i>Methanobacteria</i>	<i>Methanobacterium (97)</i>	80	124	33	102	9
	<i>Methanosphaera (99)</i>	110	0	0	0	0
	<i>Methanobrevibacter (99)</i>	10	0	34	0	0
<i>Other</i>		0	50	0	4	28

Table C-2.3. Sequence numbers of phylogenetic groups of bacteria in reactors.

Reactor		C 1	T 1	C 2	T 2	T 2
% Loading		100	150	100	190	400
		Number of bacterial sequence reads				
Phylum	Genus (similarity %)	Phase 1		Phase 2		
<i>Spirochaetes</i>	<i>Spaerochaeta</i> (95)	33	22	15	10	0
	Candidatus <i>Cloacamonas</i> (99)	6744	5895	3979	5452	2944
<i>Actinobacteria</i>	<i>Demequina</i> (99)	16	25	15	5	0
	<i>Dermatophilus</i> (92)	164	182	58	477	57
<i>Proteobacteria</i>	<i>Desulfarculus</i> (93)	181	0	82	0	0
	<i>Esherichia</i> (97)	592	0	392	0	0
<i>Chloroflexi</i>	<i>Anaerolinea</i> (95)	189	115	116	0	0
	<i>Caldilinea</i> (94)	173	0	111	5	0
Other		132	104	73	106	75